T.C.

İSTANBUL KÜLTÜR UNIVERSITY

INSTITUTE OF GRADUATE STUDIES

SEISMIC RESPONSE OF LIQUID STORAGE TANKS ON BASE ISOLATED STRUCTURES WITH TRIPLE FRICTION PENDULUM SYSTEM

Master of Applied Science Thesis

HAMZA HASSAN NUH

1800005586

Department: Civil Engineering

Programme: Structural Engineering

Supervisor: Assist. Prof Dr. Gökhan YAZICI

January 2022

T.C.
İSTANBUL KÜLTÜR UNIVERSITY
INSTITUTE OF GRADUATE STUDIES

SEISMIC RESPONSE OF LIQUID STORAGE TANKS ON BASE ISOLATED STRUCTURES WITH TRIPLE FRICTION PENDULUM SYSTEM

Master of Applied Science Thesis

HAMZA HASSAN NUH

1800005586

Department: Civil Engineering

Program: Structural Engineering

Supervisor and Chairperson:
Assist. Prof Dr. Gökhan YAZICI

Members of Examining Committee:
Assist. Prof Dr. Erdal COŞKUN

Assist. Prof Dr. Cenk ÜSTÜNDAĞ

January 2022

ACKNOWLEDGEMENT

In the name of Allah, the most compassionate and merciful. Alhamdulillah. All praise and thanks to Allah for his strength and blessing in allowing me to complete this thesis.

I am immensely thankful to my supervisor, Assist. Prof. Dr. Gökhan YAZICI, for his great guidance and, at times, tremendous patience throughout my studies and thesis at Istanbul Kultur University. I am really grateful to him for the knowledge and advice he has shared with me. Without his help and guidance, this work would not have been completed.

From the bottom of my heart, I would like to extend my profound thanks to my family, without whom my education journey would be impossible to achieve. To my sisters, who motivated me to pursue my dreams, I will always be sincerely grateful for their everlasting love and support. To my mother, Sado Mohamud Ige, for her unwavering hope in me and her prayers. I am extremely thankful to my brother, Abdiaziz Nuh, for his hard work, which enabled him to provide me the opportunity to achieve the kind of education I aspired to.

University: **İstanbul Kültür University**

Institute: **Institute of Graduate Studies**

Department: **Civil Engineering**

Program: **Structural Engineering**

Supervisor: **Assist. Prof. Dr. Gökhan YAZICI**

ABSTRACT

The use of base isolation systems is a common and effective method of reducing the seismic response of structures. This thesis investigates the seismic response of liquid storage tanks in a base isolated structure isolated with Triple Friction Pendulum bearings subjected to six unidirectional near-field ground motions. The time history analysis of the structure was conducted with the Sap2000 structural analysis program. The seismic response of liquid storage tanks with different aspect ratios located in different floors was investigated for both the fixed base and the isolated structure using the floor accelerations obtained from the time history analysis of the building model. Seismic response of the contained liquid has been modelled using a mechanical analogue model which considers the flexibility of the tank wall. The variation of tank design parameters namely, the base shear, overturning moment, and liquid sloshing displacement were investigated for the fixed base and isolated structure using a MATLAB script. The analysis results indicate that base isolation can significantly reduce the dynamic response of tanks during earthquake ground motion events, especially for the tanks located on the upper floors of the structure.

Keywords: Liquid storage tanks; seismic isolation; triple friction pendulum; sloshing.

Üniversite: İstanbul Kültür Üniversitesi

Enstitüsü: Lisansüstü Eğitim Enstitüsü

Anabilim Dalı: İnşaat Mühendisliği

Programı: Yapı (İngilizce)

Tez Danışmanı: Dr. Öğretim Üyesi Gökhan YAZICI

ÖZET

Sismik izolasyon sistemlerinin kullanımı, yapıların sismik tepkisini azaltmak için yaygın ve etkili bir yöntemdir. Bu tez, altı tek yönlü yakın alan yer hareketine maruz kalan Üçlü Sürtünmeli Sarkaç mesnetleri ile izole edilmiş, sismik izolasyonlu bir yapıdaki sıvı depolama tanklarının sismik davranışını araştırmaktadır. Yapının zaman tanım alanı analizi Sap2000 yapısal analiz programı ile yapılmıştır. Bina modelinin zaman tanım alanı analizinden elde edilen kat ivmeleri kullanılarak, farklı katlarda bulunan farklı en boy oranlarına sahip sıvı depolama tanklarının sismik davranışı hem sabit taban hem de sismik izolayonlu yapı için incelenmiştir. Depolanan sıvının sismik davranışı, tank duvarının esnekliğini dikkate alan mekanik bir analog model kullanılarak modellenmiştir. Tank tasarım parametrelerinin değişimi, yani taban kesmesi, devrilme momenti ve sıvı çalkantı yer değiştirmesi, bir Matlab betiği kullanılarak sabit taban ve sismik izolasyonlu yapı modelleri için araştırılmıştır. Analiz sonuçları, sismik izolasyonun, özellikle yapının üst katlarında bulunan tanklar için, deprem yer hareketi etkisi altında tanklarda oluşan dinamik etkileri önemli ölçüde azaltabileceğini göstermektedir.

Anahtar Kelimeler: Sıvı depolama tankları; Sismik İzolasyon; Üçlü Sürtünme Sarkaç sistemi; Çalkalanma

TABLE OF CONTENT

LIST OF FIGURES

LIST OF TABLES

LIST OF ABBREVIATIONS

ERB : Elastomeric Rubber Bearing

LRB : Lead Rubber Bearing

PTFE : Polytetrafluoroethylene

FP : Friction Pendulum

FPS : Friction Pendulum System

RC : Reinforced Concrete

NRB : Natural Rubber Bearing

LDRB : Low Damped Rubber Bearing

HDRB : High Damped Rubber Bearing

FNA : Fast Nonlinear Analaysis

LST1 : Liquid Storage Tank 1

LST2 : Liquid Storage Tank 2

LST3 : Liquid Storage Tank 3

LIST OF SYMBOLS

R1 **:** R adius of The Outer Bottom Concave Surface of the Triple Friction Pendulum

R2 **:** Radius of The Inner Bottom Concave Surface of the Triple Friction Pendulum

R3 **:** Radius of The Inner Top Concave Surface of the Triple Friction Pendulum

R4 **:** Radius of The Outer Top Concave Surface of the Triple Friction Pendulum

d1 **:** Displacement Capacity of The Outer Bottom Surface of The Triple Friction Pendulum

d2 **:** Displacement Capacity of The Inner Bottom Surface of The Triple Friction Pendulum

d3 **:** Displacement Capacity of The Inner Top Surface of The Triple Friction Pendulum

d4 **:** Displacement Capacity of The Outer Top Surface of The Triple Friction Pendulum

h1 **:** Height of The Outer Bottom Surface of The Triple Friction Pendulum

h2 **:** Height of The Inner Bottom Surface of The Triple Friction Pendulum

h3 **:** Height of The Inner Top Surface of The Triple Friction Pendulum

h4 **:** Height of The Outer Top Surface of The Triple Friction Pendulum

µ1 **:** Friction Coefficient of The Outer Bottom Surface of The Triple Friction Pendulum

µ2 **:** Friction Coefficient of The Inner Bottom Surface of The Triple Friction Pendulum

µ3 **:** Friction Coefficient of The Inner Top Surface of The Triple Friction Pendulum

µ4 **:** Friction Coefficient of The Outer Top Surface of The Triple Friction Pendulum

h **:** uniform thickness of the tank wall

ρ **:** liquid density (mass)

E **:** modulus of elasticity.

C_i **:** Impulsive Coefficient

C_c **:** Convective coefficient

m_w **:** mass of tank wall

m_r **:** mass of tank roof

S_e (T_{imp}) : impulsive spectral acceleration

S_e (T_{con}) : convective spectral acceleration

h_i : heights of the centroids of impulsive hydrodynamic pressure wall

h_c : heights of the centroids of convective hydrodynamic pressure walls

h_w : height center of gravity of the tank wall

h_r : height of the center of gravity of the roof

Q : Total base shear

M : overturning moment

M' : overturning moment below base

d : liquid displacement

g : gravity due to acceleration

T_{imp} : impulsive period

T_{con} : compulsive period

K : stiffness

C : damping coefficient

M : mass of the structure

R(t) : External Load Vector

u(t) : displacement

$\dot{u}(t)$: velocity

$\ddot{u}(t)$: acceleration

CHAPTER 1

INTRODUCTION

1.1 Introduction

Conventional seismic-resistant design of structures aims to increase the capacity of the structure to withstand the expected lateral inertial forces. However, in terms of cost and performance, this method may not be the most efficient. Compared to conventional approach, seismic isolation aims to decrease the seismic demand on the superstructure. Furthermore, base isolation allows the designer to use a greater variety of architectural forms and structural components.

Base isolation aims to decouple the structure from the damaging effects of earthquake ground motions. If the superstructure is isolated from the ground during an earthquake, the ground will move, but the structure will only undergo a little movement. The main purpose of base isolation is to limit the transfer of earthquake-caused forces to the superstructure. Base isolation was first developed in the early 1900s. Base isolation works by using isolation bearings with low lateral stiffness, such that in a seismic event, when the ground moves strongly, the structure only moves moderately. Base isolation reduces the earthquake response of the structure by changing the effective fundamental frequency of the system out of the range wherein seismic activity would cause the largest inertia forces. In this case, resonance is reduced, and the earthquake acceleration response is minimized because the period has been increased well beyond the period limit of the seismically induced ground motion [1]. The target fundamental period of the isolated structure can be achieved by adjusting the lateral stiffness of the isolation system. Base isolation bearings with hysteric force-displacement properties have been shown to provide the needed high lateral flexibility and damping while also having enough lateral stiffness to resist wind-induced horizontal forces [2]. Over time, various base isolation systems have been proposed including, elastomeric rubber bearings (ERB), lead rubber bearings (LDB), and PTFE sliding bearings.

The practice of base isolation has gained prominence in recent decades to provide earthquake protection to structures and their components. Today seismic isolation is widely used for the seismic protection of structures with motion-sensitive equipment (such as computer systems centers), high-risk buildings (such as nuclear power plants), and structures of particular significance immediately following earthquakes (healthcare centers, disaster management facilities), and storage tanks and vessels.

This thesis investigates the seismic response of small-scale liquid storage tanks in isolated structures. Various types of liquid storage tanks are available, including those that are supported on the ground, elevated, and partially buried. The volume, scale, and importance of these structures have increased over the years, enabling an understanding of their seismic response and the development of appropriate and efficient methodologies for their analysis and design to resist seismic ground motion.

The Friction Pendulum System (FPS) is a remarkably efficient and commonly used seismic isolation system of the sliding type. While the volume of filling liquid in a storage tank and the weight of the structure are not precisely determined at the time of the earthquake, it appears that the FPS performs better since the period of the isolation device is not dependent on the mass of the superstructure.

The seismic behavior of liquid storage tanks is quite complex, especially when subjected to near-fault strong ground motions. These seismic events would have an effect on the sloshing motion of the liquid [3]. This thesis studies the seismic response of liquid storage tanks on isolated structure by FPS subjected to near field ground motions. A nonlinear time history analysis is performed on a base-isolated structure, and finally, the effect of the base isolation on the response of the liquid tank parameters is evaluated and presented.

1.2 The Objectives and Aim of The Thesis

The work in this thesis aims to analyze the seismic response of liquid storage tanks with different aspect ratios on isolated structures and compare their response with liquid storage tanks on fixed base structures. The evaluation of the seismic response of the tanks is based on base shear, overturning moment, and sloshing displacement.

The following tasks will be carried out in order to achieve the objectives:

- A literature review will be conducted on the seismic response of liquid storage tanks on base isolated structures to identify the recent developments and research needs in this domain.

- The theoretical foundations required for modelling and analysis of the isolated structure and the liquid storage tanks will be presented.
- The numerical models to be used in parametric analysis will be prepared and calibrated with the models available in the literature review. The isolated structure model developed by Sarlis and Constantinou will be used as the superstructure model and the model for the liquid storage tanks with 3 different aspect ratios will be created using a MATLAB Script.
- A parametric study will be conducted with a suite of 6 near field earthquake ground motions to evaluate the tank design parameters for fixed-base and base isolated cases. The storage tanks in the above-mentioned analyses will be considered to be totally anchored to the floor in order to experience the floor accelerations, and their masses will be considered to have a negligible effect on the overall seismic response of the structure.
- The results and key findings of the parametric study will be presented in the conclusions along with topics for further research.

1.3 Organization of the Thesis

This thesis is organized into five chapters, which are as follows:

In chapter one, an introduction to aseismic isolation liquid storage tanks is presented, and the aim and objective of the study are shown, as well as the thesis organization is described. Also, the literature review findings are presented.

In chapter two there are three main sections under this chapter. The first section presents an overview of seismic base isolation devices and their working principles. In the second section, the effects of base isolation systems on the structures are addressed. The third section examines the various types of base isolation devices, including their categories and subcategories.

In chapter three, the modeling and analysis of the two-dimensional base-isolated model structure with SAP2000 is described. Also, the isolation analysis properties are stated. In addition, it presents the seismic ground motion excitations selected for the purpose of the analysis of the study.

In chapter four, a brief description and literature review of seismic analysis of liquid storage tanks is addressed. Also, the formulaic and numerical evaluation of a simple procedure for analyzing liquid storage tanks is presented.

In chapter five, the parametric study and its results are presented. Three main parameters are the base shear, liquid displacement, and overturning moment of the liquid storage tanks.

Chapter six, which is the last chapter of the thesis, presents the conclusions and recommendations.

1.4 Literature Review

This section aims to present an assessment of the literature studies on further research on the seismic response of liquid storage tanks on isolated structures.

Harry W. Shenton III and Francis P. Hampton (1999) [4]: In this study, the seismic response of an isolated elevated water tank was analyzed using an isolated structure model that includes the isolation mechanism, frame structure, and sloshing liquid in a separate three-degree of freedom structure. The response spectrum is examined in order to determine the natural frequencies and mode shapes.

A full range of capacity and aspect ratios of the tank and the liquid elevations were studied. In comparison to a fixed base tank model, seismic isolation effectively reduces overturning moments, base shear, and frame structure drifts. When it came to the isolated structure, a single-mode solution was not sufficient since fluid motion had a significant impact on the overall structural response. As a result, isolation was more successful in the tank with the smallest capacity. Isolation, on the other hand, increased the relative convective displacement of fluid in the tank.

M. K. Shrimali and R. S. Jangid (2003) [5]: performed research on the seismic behavior of elevated steel liquid storage tanks. Those tanks are isolated by using linear elastomeric bearings under seismic events. The isolation devices are installed at the bottom and top of the supported structural steel frame tower in two different tank models. The tank models the liquid mass as a lumped mass, often known as sloshing mass, and the impulsive mass as a rigid mass.

Focusing on the tank wall and liquid mass values, the stiffness constant corresponding with these lumped masses is being evaluated. In this model, the steel tower structure's mass is lumped at the bottom and top. The response of two distinct tank forms, namely slender and broad tanks, was evaluated, and a parametric analysis was performed to determine the effect of significant system factors on seismic isolation efficacy. Among the parameters considered were the tank aspect ratio, tower structure time period, damping, and isolation system time period. The seismic response of the isolated tank was proven to be significantly reduced in this research. Furthermore, in terms of isolation, a tank with a rigid tower structure is more efficient than a tank with a flexible tower structure.

A. Tokhi and S. Arora (2019) [6]: In this study, intze water tanks, circular water tanks, and rectangular water tanks with RCC frame staging in zones of III and V were evaluated for seismic analysis and comparison in the empty, half, and fully filled conditions using STTAD Pro. According to the three conditions, the intze water tank has a higher base shear than the rectangular and circular water tanks in zone III, and vice versa in zone IV. When constructing an elevated water tank for full-filled situations, the maximum design base shear is critical.

In Zone III, the circular water tank has the maximum displacement when fully filled, while in Zone V, the intze tank had the most displacement. The time period is longer for an intze and circular tank in fully filled condition than for a rectangular tank and is independent of the other zones.

CHAPTER 2

SEISMIC BASE ISOLATION

2.1 Overview

Seismic isolation is a strategy for enhancing a structure's efficiency during earthquakes by altering how it reacts. In general, base isolation is an earthquake-prevention technique which is used to separate or decouple a structure's motion from ground shaking and minimize structural forces [7].

The forces transferred to the structure are minimized by isolating it from the ground's motion, resulting in a reduction in the demand imposed on the structure's members. Separate isolators must always protect the overall superstructure with predetermined dynamic properties. Some other isolators are often designed to provide significant damping. Displacement and yielding are concentrated at the base isolation material position, and the superstructure behaves almost identically to a rigid.

A conventional or fixed base structure experiences substantial story drifts during seismic events, as figure 2.1 shows, which can create long-term damage to the structure. On the other hand, isolated structures perform deformation mainly at the structure's base [8].

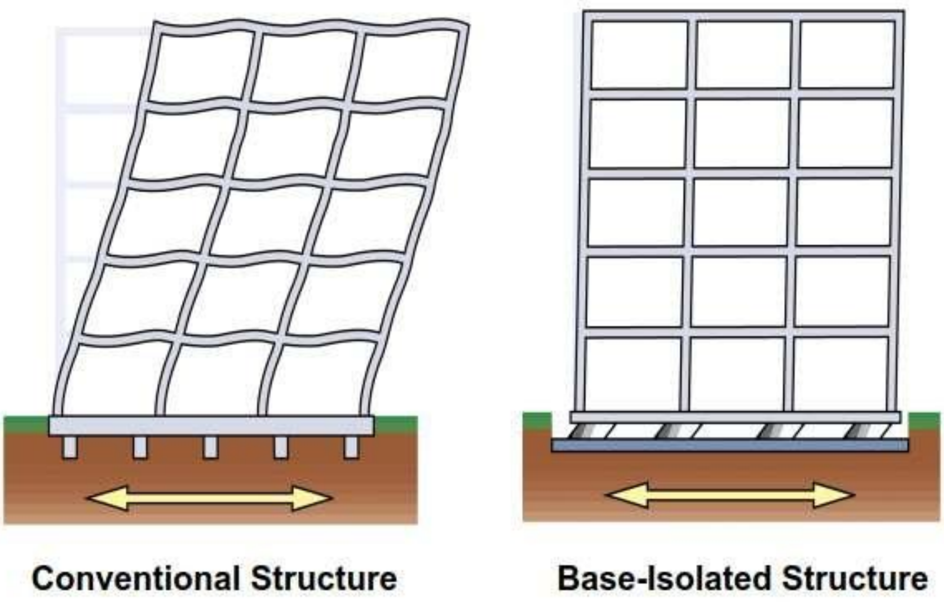

Figure 2.1: The behavior of fixed base and isolated structure [8].

2.2 Effects of seismic base isolation

Seismic base isolation is among the most successful structural control techniques that have been developed. It may be used for both new construction and retrofit existing buildings and bridges. The base displacements, base accelerations, floor accelerations, and relative floor displacements are often used to assess the efficiency of seismically isolated structures [9].

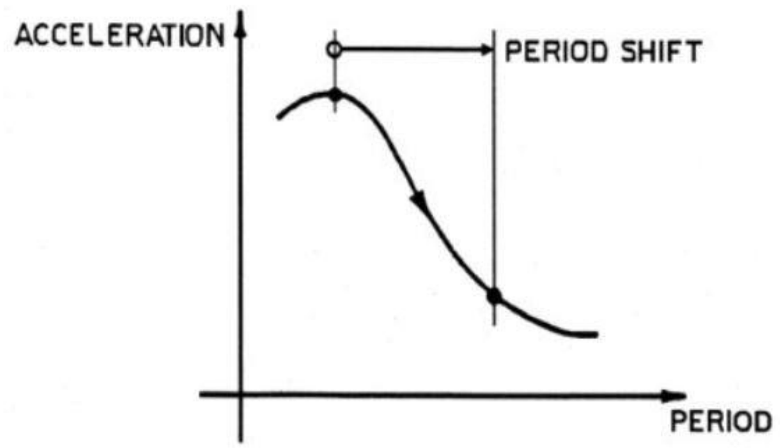

Figure 2.2: Effect of the period shift in isolated structures on accelerations [10].

Seismic isolation primarily increases the natural period, which decreases acceleration and forces required on the structure [10]; the period shift is shown in figure 2.2.

As the base isolation increases, the natural time, which improves displacement demand, shows in figure 2.3; moreover, the displacement demand is moved from the superstructure to the isolation system.

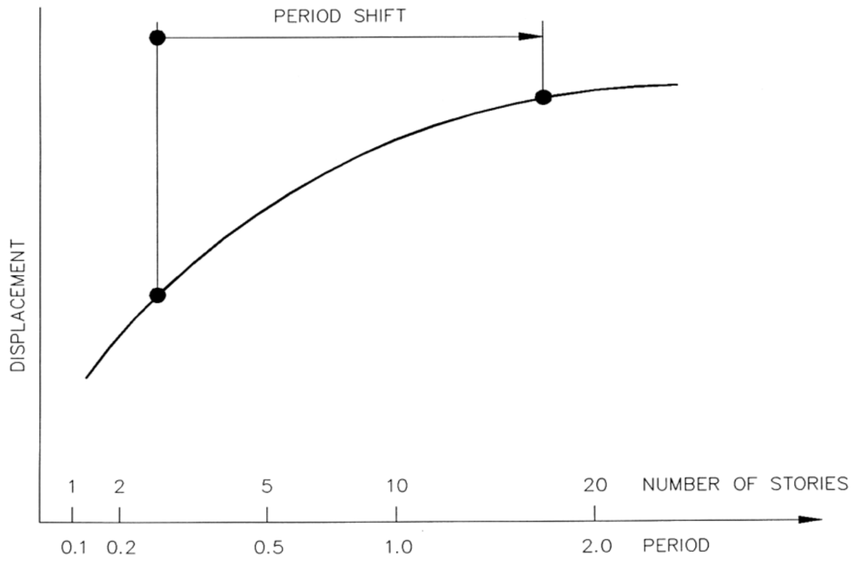

Figure 2.3: Effect of the period shift in isolated structures on displacement [11].

2.3 Seismic Base Isolation Systems

For the seismic-resistant of structures, several seismic isolation bearings have been studied and tested globally. This section provides an overview of each type of bearing's fundamental structure and mechanical properties. Isolation devices primarily comprise either elastomeric bearings or sliding bearings, though they have been mixed in some situations [12].

2.3.1 Elastomeric Bearings

Elastomeric bearings are a vast category of seismic isolation systems. These bearings are made up of flexible properties of natural and synthetic elastomeric rubber to obtain the suitable properties of an isolation system. The following are some popular elastomeric devices: (a) Natural rubber bearing (NRB), (b) Lead rubber bearing (LRB), and (c) High-damped rubber bearing (HRB).

Every elastomeric isolation bearing comprises multiple layers of rubber pads and stiffening plates of steel shims bound along with a strong, semi adhesive. The steel shims protect the rubber pads from lateral bulging while providing the device's vertical stiffness to support the building weight. The rubber layers are composed of an unfilled rubber that provides lateral flexibility [13].

2.3.1.1 Natural Rubber Bearings

Natural rubber bearings, also referred to as laminated rubber bearings, are made up of natural rubber, and a synthetic rubber material used for its hardness and endurance and exhibits natural rubber-like properties. Figure 2.4 illustrates a normal, natural rubber-bearing configuration. Natural rubber bearings are composed of alternate layers of rubber and steel shims. To create a laminate bearing, these layers are bonded together using a vulcanization process that involves pressure and heat. Steel shims provide vertical stiffness to the bearings and prevent the isolated structure from shaking. Steel shims also protect the rubber from bursting out when subjected to heavy axial compression loads [13].

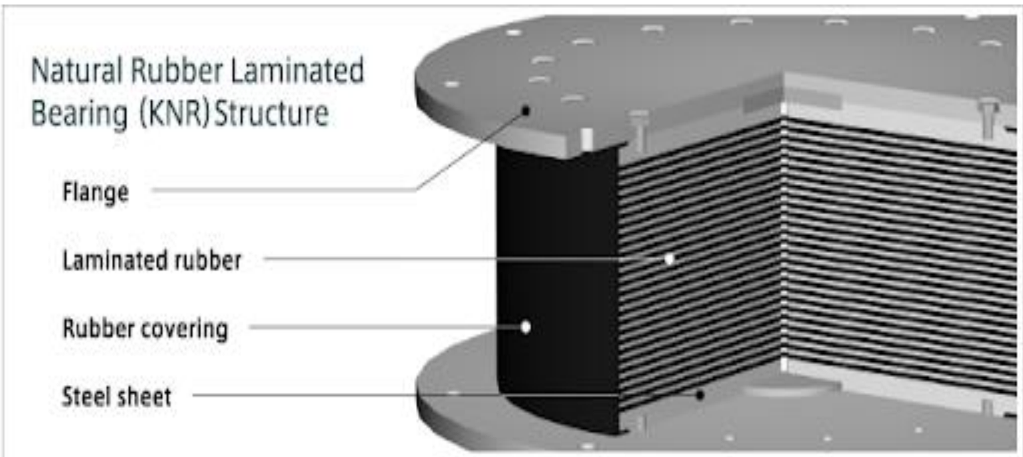

Figure 2.4: Natural rubber bearing [14]

2.3.1.2 Lead Rubber Bearings

Lead rubber bearings are more capable of providing enough stiffness for wind loads and improved damping characteristics than natural rubber bearings. The arrangement of a lead rubber bearing is similar to that of a natural rubber bearing, except for the presence of one or more circular lead plugs in the center, as illustrated in Figure 2.5. In connection with the rubber, the lead plug allows the device to behave bilinearly. Under low applied wind loads, the lead plug's high rigidity absorbs most of the load, and the configuration exhibits higher stiffness. However, when subjected to strong earthquake loads, lead deforms plastically, resulting in the stiffness of the device dropping to the stiffness of rubber [13].

Furthermore, energy is wasted in a hysteretic way during deformations of the lead plug. During strong seismic events, the lead plug deforms similarly to rubber but creates heat or releases kinetic energy by turning it into heat. As a result, the hysteretic activity of the plug pertains to a reduction in the amount of energy absorbed by the structure. Additionally, lead rubber bearings are simple to install, construct, evaluate, and design [13].

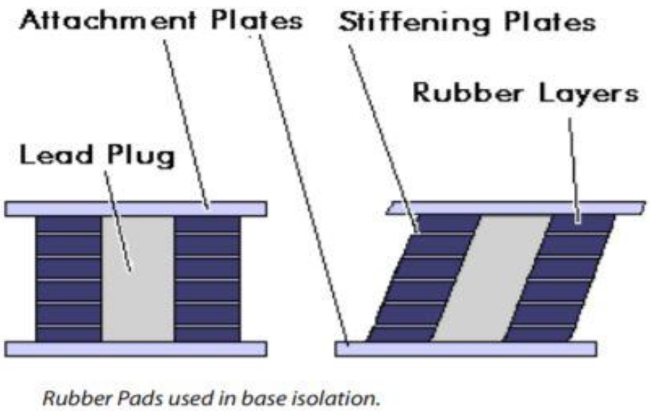

Figure 2.5: Lead rubber bearing [15].

2.3.1.3 High Damped Rubber Bearings

The use of natural rubber bearings with a high damping capacity avoids the need for supplemental damping systems. Besides the kind of elastomeric element utilized, their construction is identical to that of natural rubber bearings. Increased damping is accomplished by using materials such as carbon, oils, and resins. Fillers raised the damping to between 20% to 30% of critical damping. When shear strains are less than 20%, the high damping natural rubber bearings demonstrate a high degree of stiffness and damping. This behavior is helpful for reducing deflections caused by wind loads in service [13].

2.3.2 Sliding Bearings

Sliding bearing is another kind of seismic base isolation system wherein the sliding motion effectively reduces horizontal stiffness. Sliding bearings carry the structure's weight on a bearing that is supported by a sliding interface and provided with a low coefficient of friction. In most sliding bearings, the sliding interface is made of polytetrafluorethylene (PTFE), and the bearing substance is stainless steel. Sliding bearings usually use spherical surfaces or smooth flat sliding surfaces. The Friction

Pendulum System (FPS) bearing is now the most commonly utilized sliding seismic isolation bearing globally, and it has a spherical surface. According to pendulum mechanisms, FPS bearing, which has more than one mechanism, is multi-spherical FPS. The three common types of spherical FPS, as figure 3.6 shows, are (a) single FP bearing, (b) double FP bearing, (c) triple FP bearing [16].

2.3.2.1 Single Friction Pendulum Bearings

The traditional Friction Pendulum isolator is the Single Friction Pendulum bearing system. The single slider sustains the weight support at the structural member's center. The single FP bearing isolator also has a low height, which can be helpful in some applications. The Single FP isolator provides constant friction, stiffness, and dynamic period for all seismic events and displacement stages. An articulated slider on a spherical and a spherical surface is used in the bearing system. The slider is coated with PTFE (polytetrafluoroethylene), and stainless steel covers the spherical surface. Figure 2.6 depicts the geometrical construction of a single FP bearing and identifies the described components [17].

2.3.2.2 Double Friction Pendulum Bearings

The double concave FP device was shown to be an effective system for minimizing a structure's seismic response during an earthquake. The double concave FP bearing comprises two concave stainless-steel surfaces that face one another and are separated by an articulated slider. For a proper pressure distribution at the sliding interface, the sider's articulation is required to handle various movements over sliding surfaces at the top and the bottom [18]. The radii of curvature R_1 and R_2 on the upper and lower concave surfaces may be unequal.

Therefore, the coefficients of friction are μ_1 for one concave sliding surface and μ_2 for the other surface, which may not always be equal. The height of the sliders h_1 and h_2 are the vertical distances from the pivot point to the lower and upper concave surfaces consequently. The displacement of the sliders upon the upper concave and the lower concave surfaces are d_1 and d_2 and resulting in the whole bearing displacement capacity. Figure 2.6 shows the geometry of double concave friction system [18].

2.3.2.3 Triple Friction Pendulum Bearings

The triple FP bearing comprises four concave plates divided by an internal discrete slider assembly and has three different systems, as shown in figure 2.6. Concave surfaces on each side of a spherical inner slider with a low-friction device on both sides make up the outer slider [19].

This creates a first pendulum system that determines the isolation system's properties. The outer slider also comprises sliding interfaces between upper and bottom outer sliders and the bearing's main spherical surfaces. The second pendulum system is created as the bottom sliding surface comes into contact with a curved surface with a fixed radius of curvature. Finally, the third pendulum system is created as the upper sliding surface comes into contact with another spherical surface with a fixed radius of curvature. The features of these three pendulum systems can be designed to maximize the seismic isolated structure's efficiency when several degrees of seismic hazards are regarded [20].

2.4 Geometry of Triple Friction Pendulum Bearings

Triple FP bearings have the following geometrical and frictional properties, which are numbered from the bottom to the top of the concave plates. As the outer geometrical properties are equal, the inner properties are also identical: R_1=R_4, R_2=R_3, μ_2=μ_3, μ_1=μ_4, h_1=h_4, h_3=h_2, d_1=d_4, d_2=d_3. The outer concave plates have radii of curvature, and it can be inferred that this is the effective radius pendulum, which is the actual radius minus the slider height, and that is, $R_{eff1} = R_1 - h_1$, $R_{eff4} = R_4 - h_4$. The inner concave plates also have an effective radius pendulum which is the same as the outer plates; $R_{eff2} = R_2 - h_2$, $R_{eff3} = R_3 - h_3$.

The outer surfaces of the slide plates and rigid sliders are coated with a non-metallic sliding material characterized by coefficients of friction. The lower main spherical surface friction coefficient is smaller than the upper main spherical surface friction coefficient. The triple FP bearing is primarily based on the different sliders exceeding the maximum horizontal potential of their corresponding slider interfaces during motion [21].

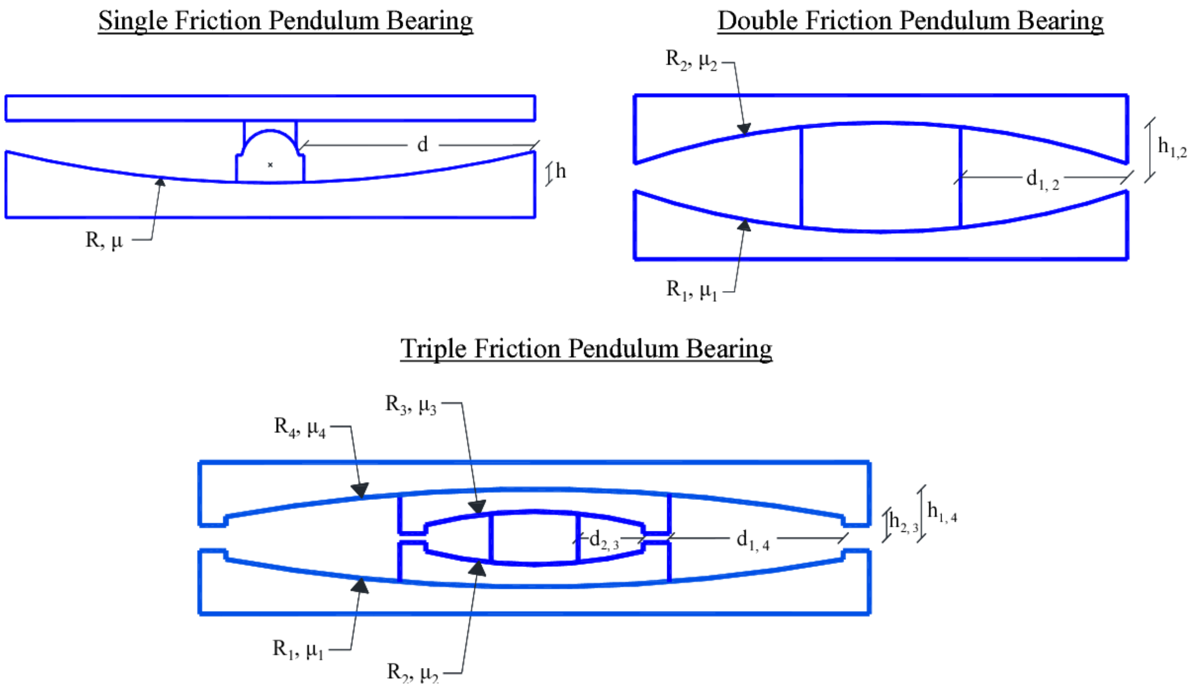

Figure 2.6: geometry of spherical friction pendulum bearings [22].

CHAPTER 3

MODELING AND ANALYSIS OF THE ISOLATED STRUCTURE

This part presents guidelines on modeling base isolated building. The isolated building model that was used in this study was taken from the study of Sarlis and Constantinou 2015 [23]. In this study, the parameters and modeling procedure will be explained. And finally, the model will be used for analyzing the seismic response of elevated tank. The type of isolation used is TFP bearing.

This part, in particular, presents the following:

- A summary description of the base isolated building.
- Presentation of the properties of TFP isolator.
- Defining time history input.
- Definition of load case.
- Comparison of the results to check the model.

3.1 Description of the Isolated Model

The isolated building model in Figure 3.1 that was used in this study is Sarlis and Constantinou's model as mentioned above. The structure is a two-dimensional segment of a three-dimensional building with five floors, including the ground level floor, which has a plan of 1920in x 768in (19.51m x 48.78m) and a length of 384inches (9.75m) between the columns on both the x and y axes and a height of 192inches (4.88m). Each floor has a weight of 1080kips (4804 kN) and the total weight of the structure including the base floor is 5400kips (24020 kN). Six isolators support the two-dimensional building, and each isolator carries 900kips (4003 kN). All floor connections are modeled as a rigid diaphragm, with the floor mass given at the joints and each joint assigned equal mass.

Structural damping of 2% of critical for all modes is used when modelling the isolated structure. The TCU-065-E component of the 1999 Chi-Chi, Taiwan earthquake is used in the analysis [23]. The vibration periods of the first four modes when the model is fixed base is presented in Table 3.1.

Table 3.1: Periods of Vibration of Superstructure when Fixed at the Base

Mode	Period (sec)
1	0.776
2	0.253
3	0.138
4	0.093

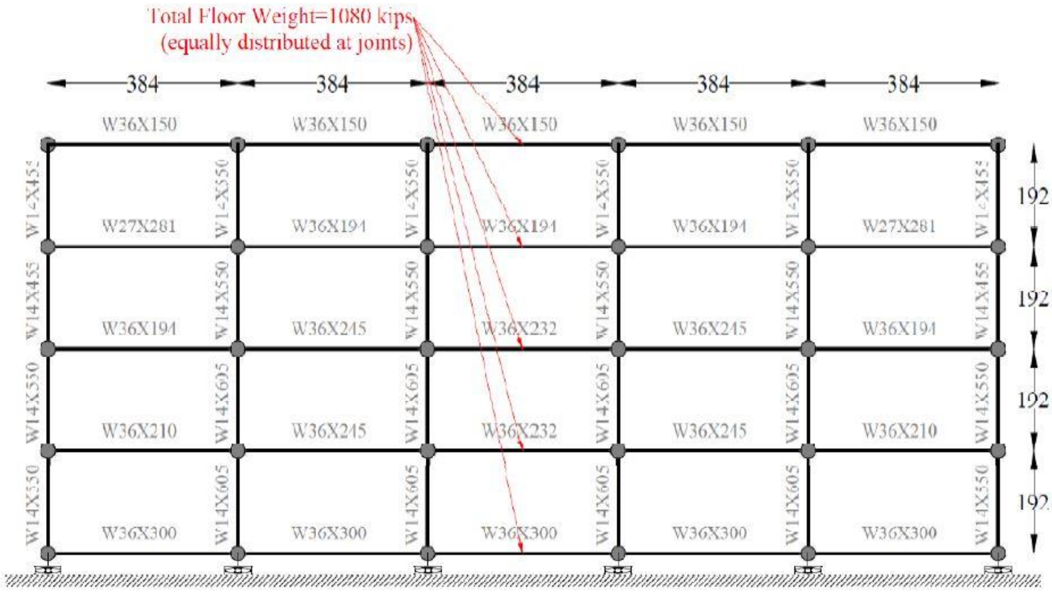

Figure 3.1: Schematic of four-story planar structure (dimensions in inches) [23]

3.2 Properties of the Isolators

The isolator properties that were used in the analysis are listed in Table 3.2.

Table 3.2: Isolator properties of TFP isolator [23]

Properties	**Values**
$R_{eff1} = R_{eff4}$ (inch), cm	(82.5) 210
$R_{eff2} = R_{eff3}$ (inch), cm	(7.5) 19.1
$d_1 = d_4$ (inch), cm	(17.8) 45.2
$d_2 = d_3$ (inch), cm	(0.94) 2.39
$\mu_1 = \mu_4$	0.108
$\mu_2 = \mu_3$	0.030
$a_1 = a_2 = a_3 = a_4$ (inch/ sec) cm/sec	(2.54) 62.23

3.3 Triple Pendulum Isolator Link Element Properties

Triple Pendulum Isolator Link Element under the define section properties to the link support properties command in SAP2000 was used to model the triple friction pendulum bearings. This element has three displacement degrees of freedom, U1, which is vertical, U2 and U3, which are horizontal. R!, R2 and R3, represent the rotational degrees of freedom. The constraints applied in the model are presented in Figure 3.2.

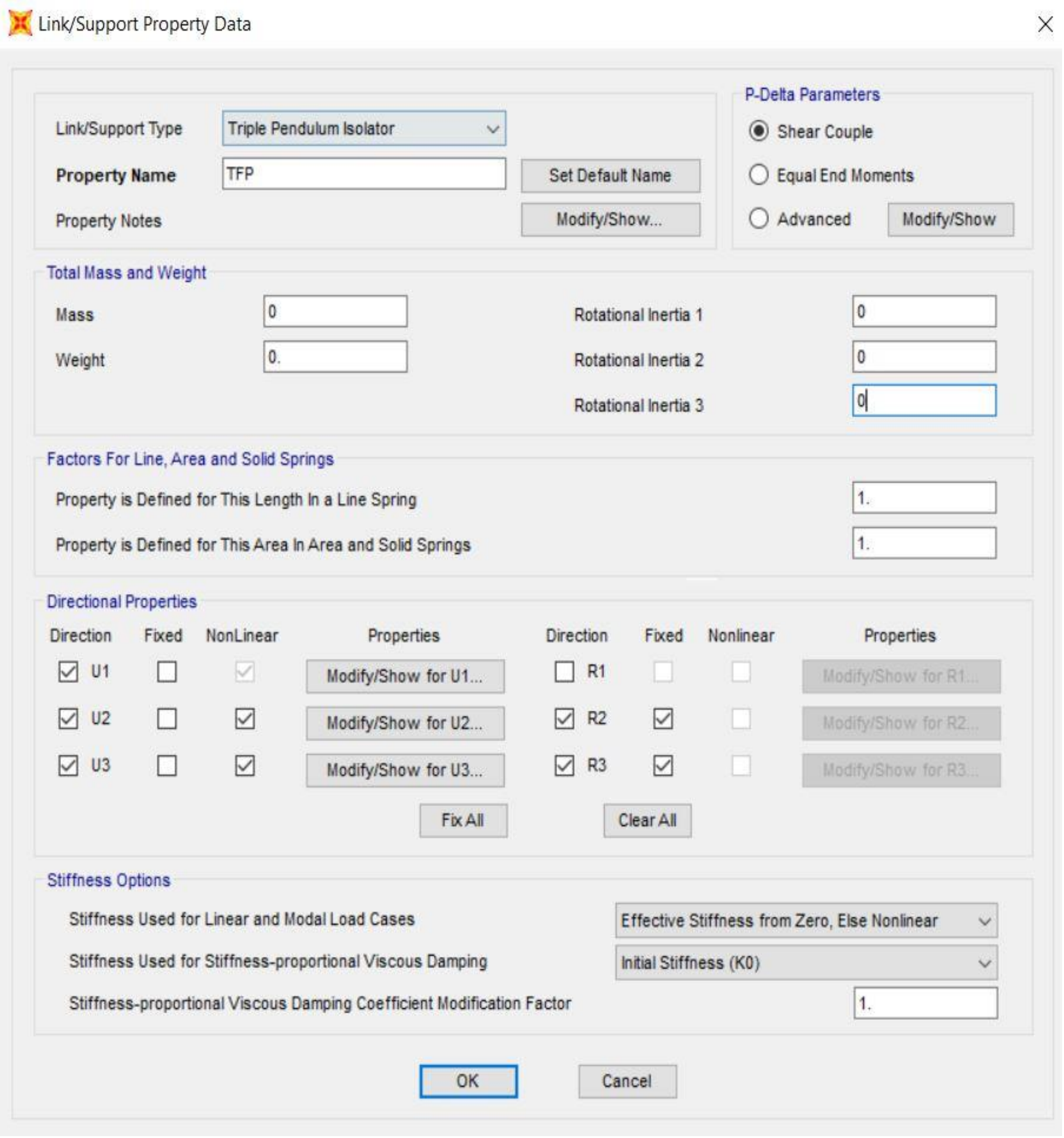

Figure 3.2: Link/support property data of TFP on SAP2000

Table 3.3 shows the numerical values of the parameters used for each of the six isolators in the SAP2000 link element, that will be filled in the SAP2000 interface window shows in Figure 3.3 and 3.4, Further details of the TFP used in this study may be found in Sarlis and Constantinou (2010).

There are properties of sliding surfaces which are listed below:

1. Stiffness: is the shear stiffness at the stop just before sliding starts.
2. Coefficient of friction-slow: Friction Coefficient when the velocity is at zero.
3. Coefficient of friction-fast: Friction Coefficient when the velocity at a fast rate.
4. Rate parameter: inverse of the characteristic velocity for friction
5. Radius: Actual radius of the concave surface.
6. Stop distance: transversal displacement allowed before reaching a stiff stop

Table 3.3: Values of Properties of the TFP Isolator Link Element in SAP2000 [23]

Element Mass (Kip-s2/in) kN-s2/cm		(0.003) 0.00525		
Effective Stiffness (Kip/in) kN/cm		(9.675) 16.94		
Vertical Stiffness (Kip/in) kN/cm		(71176.7) 124649.5		
Rotational/Tortional Stiffness		R1=0, R2=Fixed, R3=Fixed		
Rotational Moment of Inertia		1.0		
Properties of Sliding Surfaces	Outer Top	Outer Bottom	Inner Top	Inner Bottom
Stiffness (Kip/in) kN/cm	(3000) 5254	(3000) 5254	(3000) 5254	(3000) 5254
Friction of Coefficient-Slow	0.065	0.035	0.015	0.015
Friction of Coefficient-Fast	0.13	0.07	0.03	0.03
Rate Parameter	(2.54) 1	(2.54) 1	(2.54) 1	(2.54) 1
Radius (in) cm	(82.5) 210	(82.5) 210	(7.5) 19	(7.5) 19
Stop Distance (in) cm	(18) 45.7	(18) 45.7	(2) 5.08	(2) 5.08

Figure 3.3 depicts U1 which is the axial DOF. this DOF is linear, and it is necessary to specify the elastic vertical stiffness.

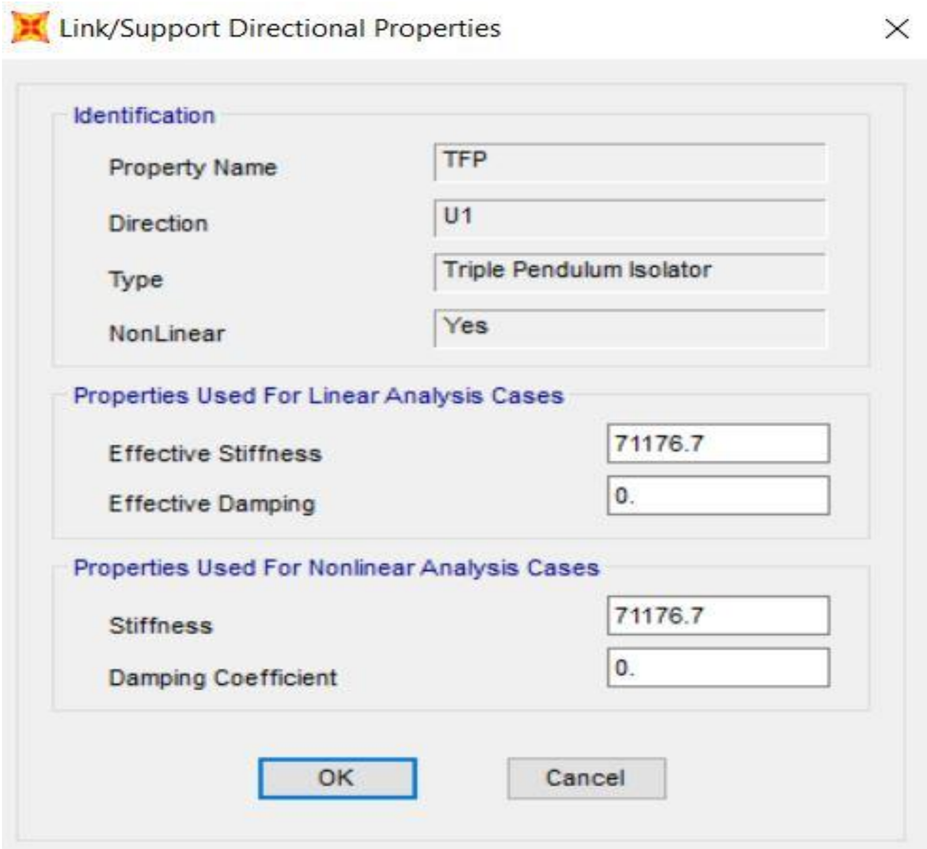

Figure 3.3: U1 directional properties on SAP2000

Figure 3.4 shows U2 and U3 and they are shear DOF in the two orthogonal directions. For elastic analysis, the stiffness associated with these two degrees of freedom should be stated as the effective isolator stiffness. And in the nonlinear analysis, the sliding surface properties will be determined.

Also, there will be a torsion degree of freedom that will be designed as R1, and the rotational stiffnesses R2 and R3 were fixed in this study. The torsional stiffness (elastic DOF) of FP isolators is relatively small, hence a value of zero is appropriate.

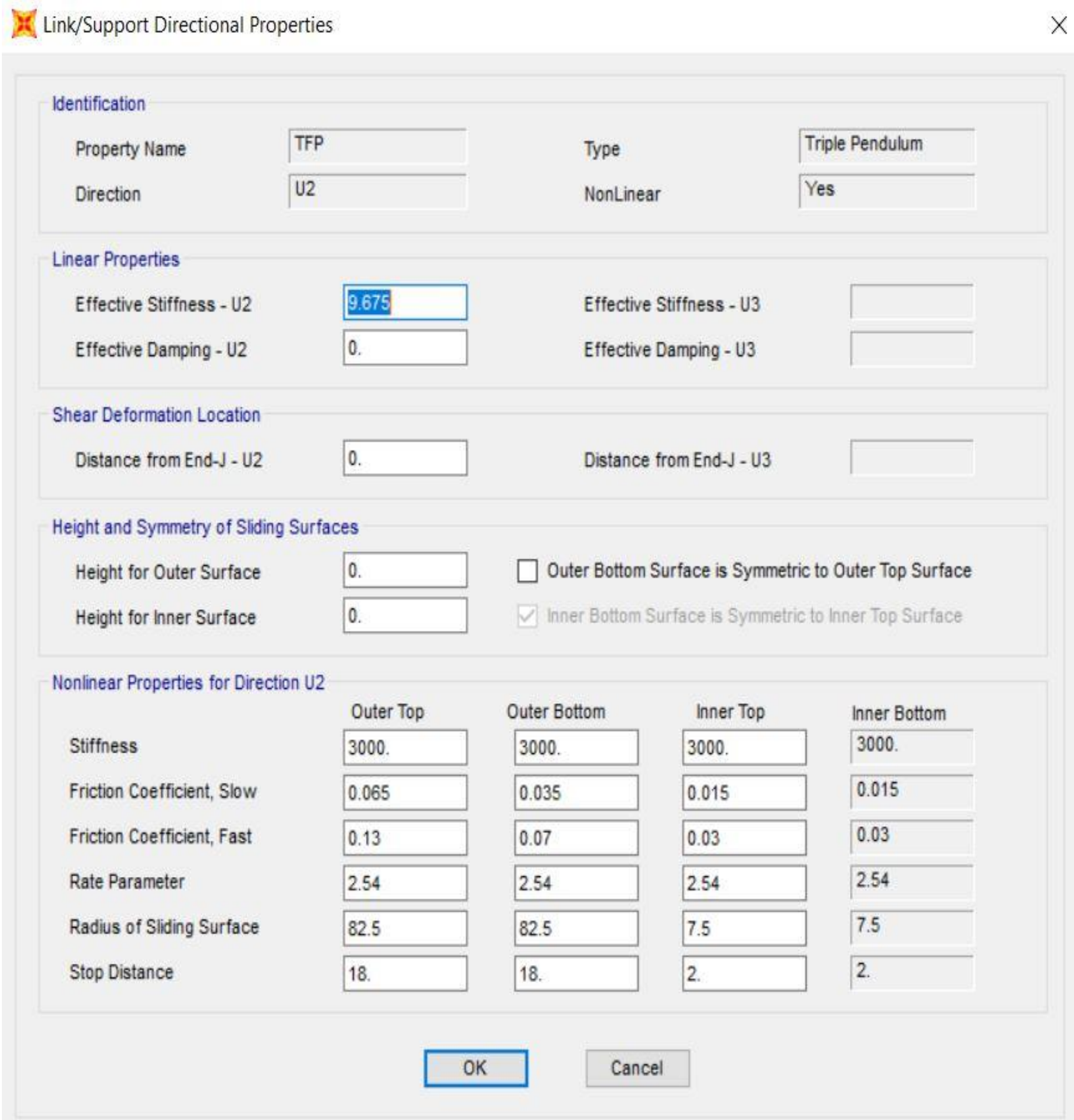

Figure 3.4: U2 and U3 directional properties on SAP2000.

3.4 Defining Time History Input

In this study, defining for the time history input, two function types will be used. First, under the time history function, a seismic event excitation will be uploaded by choosing a function "from file," as Figure 3.5 shows. The second one will be the ramp function, which is under the time history function types for applying the dead load, and it will be mentioned a RAMP. As Figure 4.6 shows, the slope of the ramp function will be 10 seconds in length.

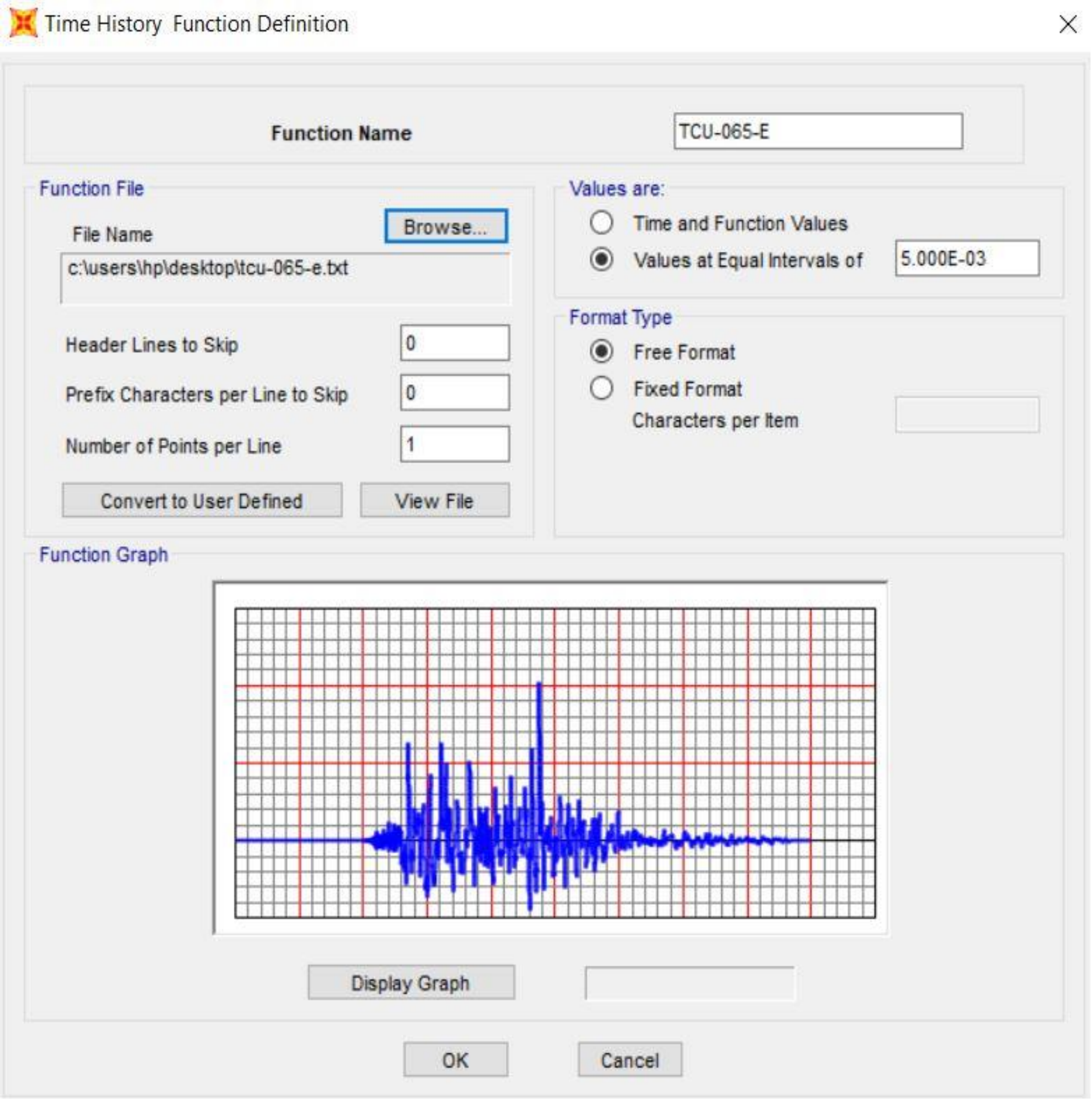

Figure 3.5: Definition of acceleration time history on SAP2000

The base isolators used in this study are friction pendulum isolators, which implies that their behavior is determined by friction forces, which states that the isolator must be loaded with the vertical load before the seismic analyses began. Thus, a time history will be used to define the dead load.

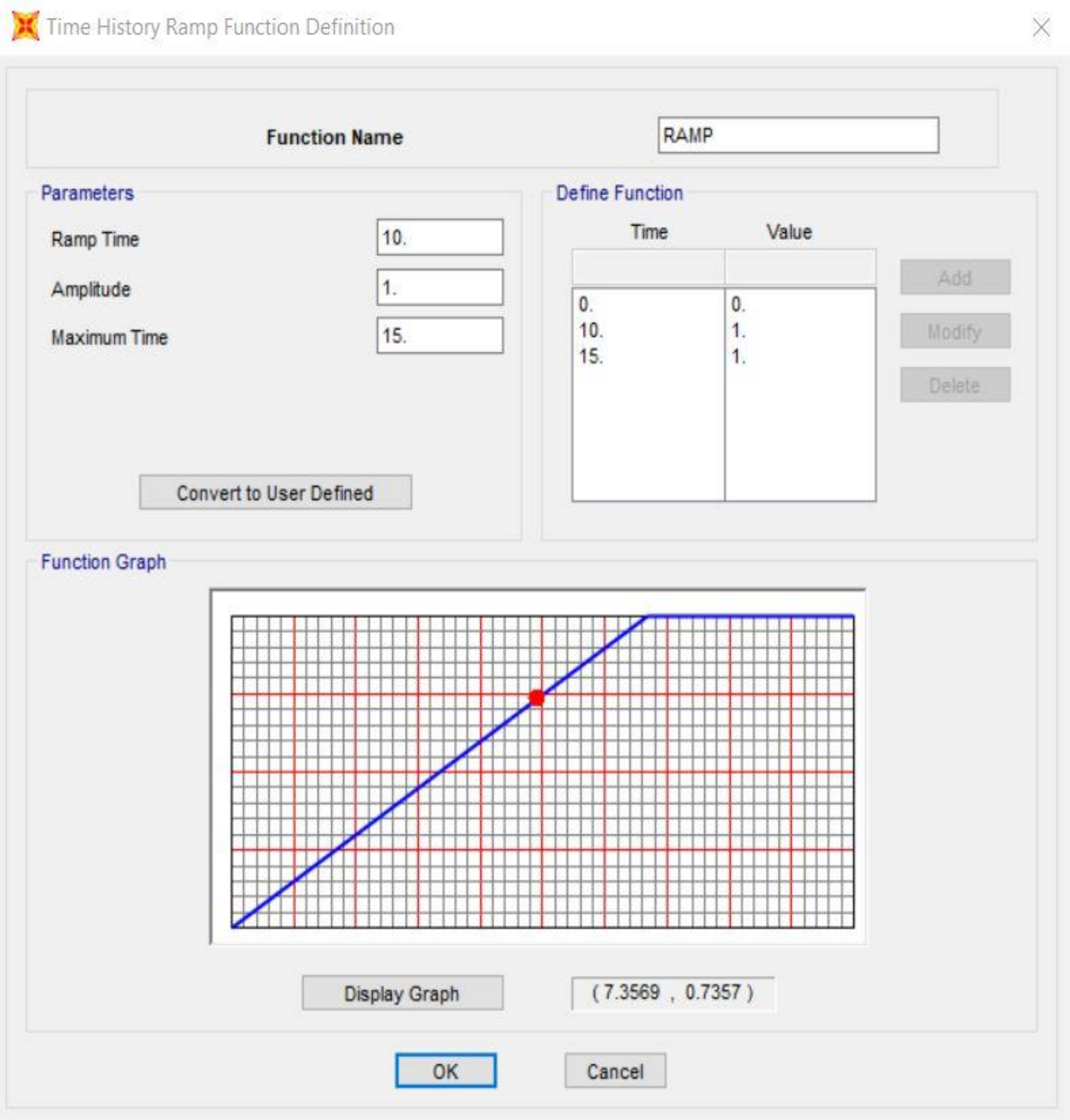

Figure 3.6: Definition of time history ramp function on SAP2000.

3.5 Defining Load Case

A load case specifies how load patterns are applied (static or dynamic), how the structure responds (linear or nonlinear), and how analysis is carried out (through modal analysis, direct integration, etc.) Two default load cases will be defined, the dead and the model cases; both of which will be modified.

The model case: ritz vectors were used as the type of modes. In order to perform fast nonlinear analysis, load dependent ritz vectors must be used. The number of Ritz vector modes to be used in fast nonlinear analysis must be specified. A total number of 200 modes were asked, in this study.

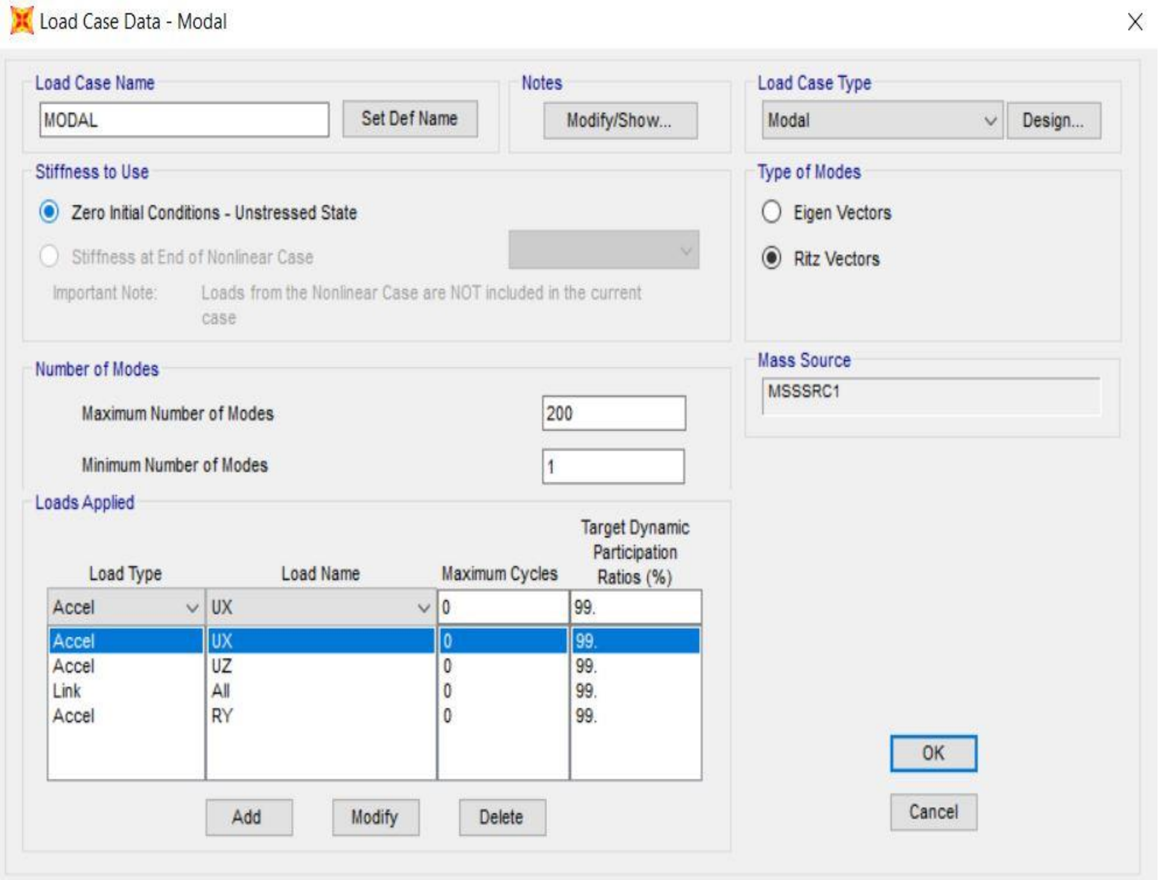

Figure 3.7: Load case model on SAP2000

The dead load case: The load will be applied using the ramp function. For the ramp loading, 150-time steps at 0.1 sec intervals were used.

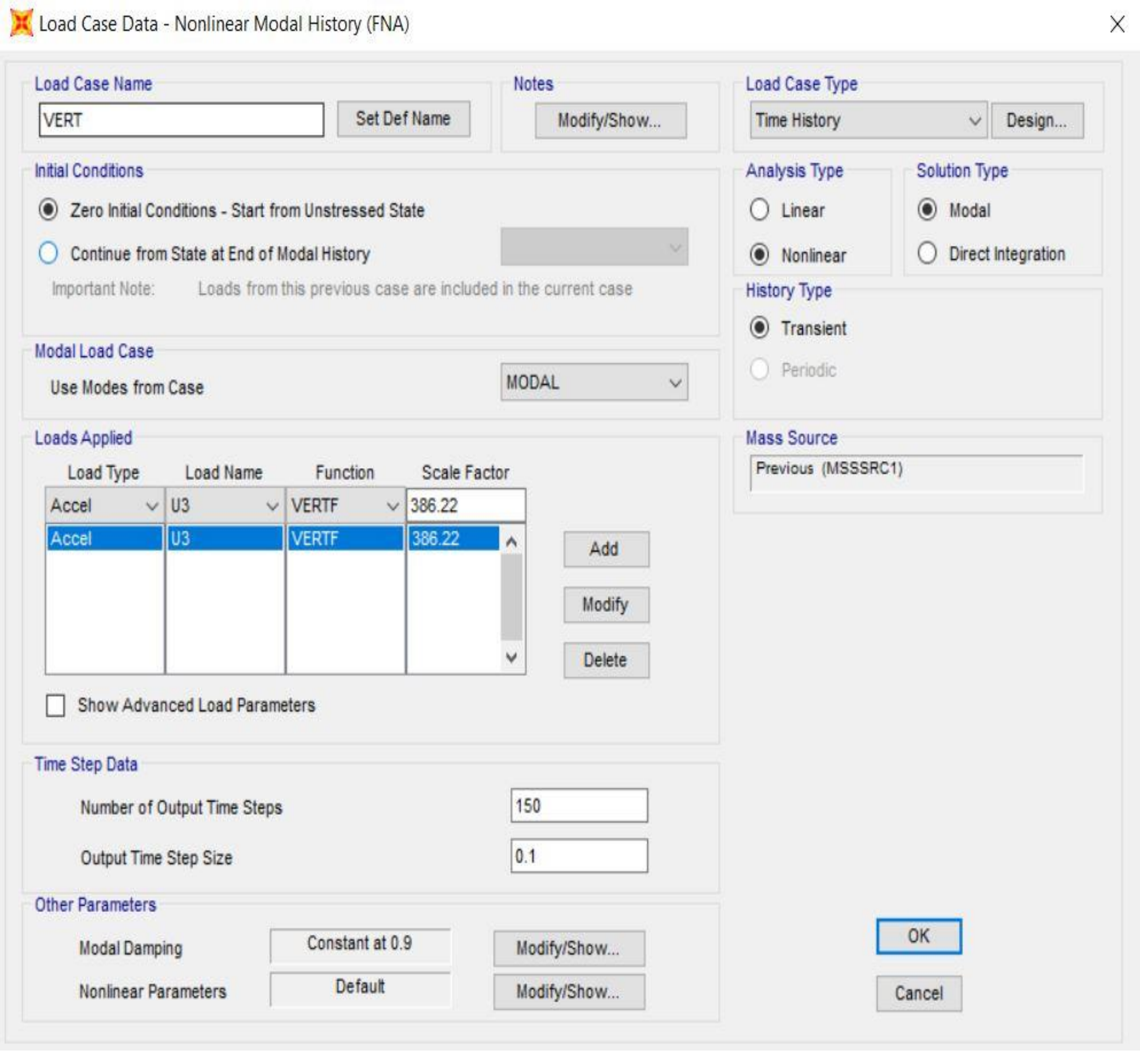

Figure 3.8: FNA vertical load case on SAP2000

Afterward, a new load case for the nonlinear time history will also be added. It will be called FNA. For this load case, it will be started from the conclusion of the dead load case. The load applied will be an acceleration by using the excitation record event function, and it will be scaled from g units. A modal damping constant of 2% was used, along with 900, 000-time steps at 0.001sec intervals.

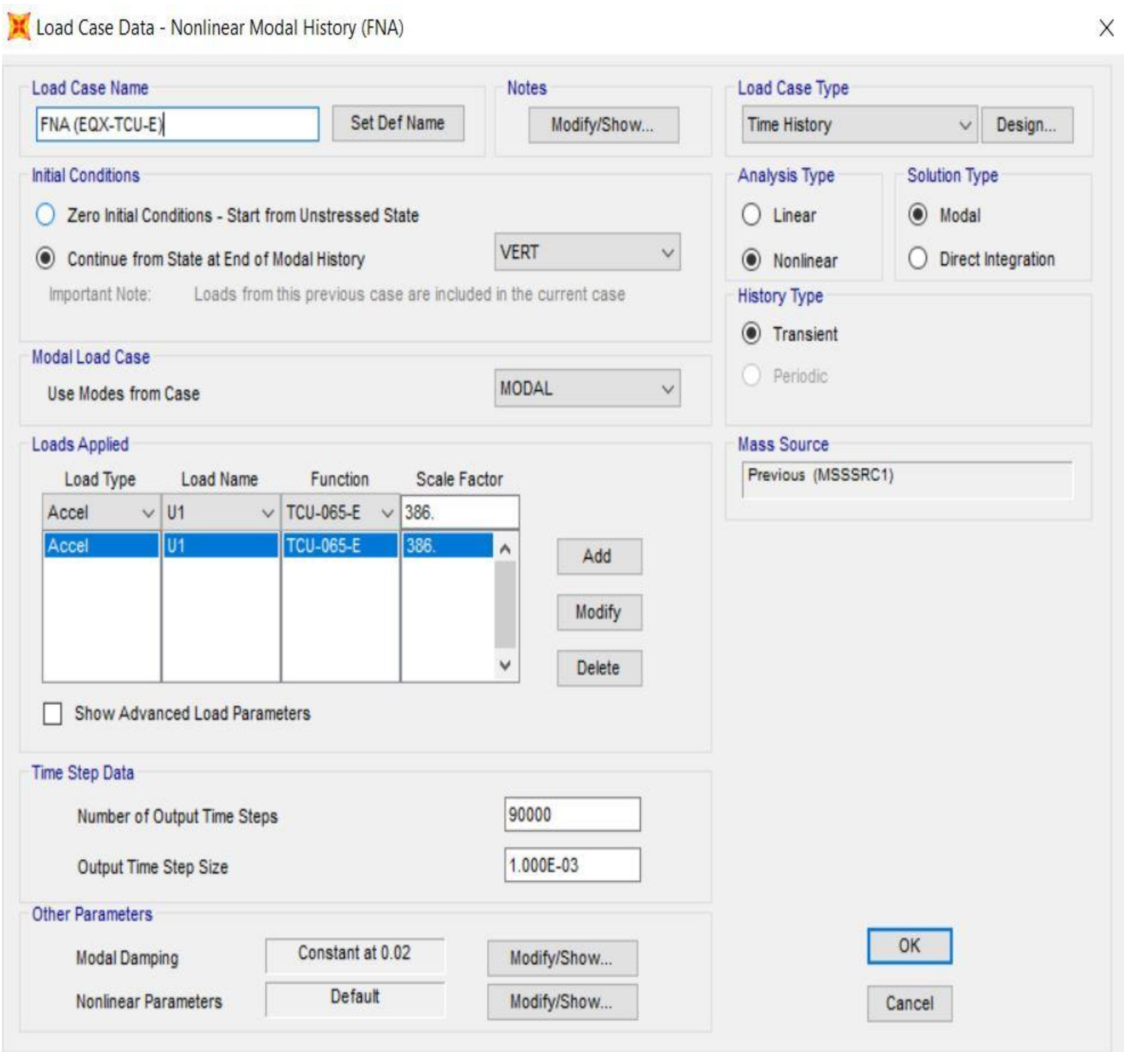

Figure 3.9: FNA excitation load case on SAP2000

3.6 Comparison of The Results to Check the Model

Figures 3.10 to 3.15 show the results of the analysis re-obtained in the SAP2000 of this study by the model, which are then compared to the paper report of Sarlis and Constantino [23].

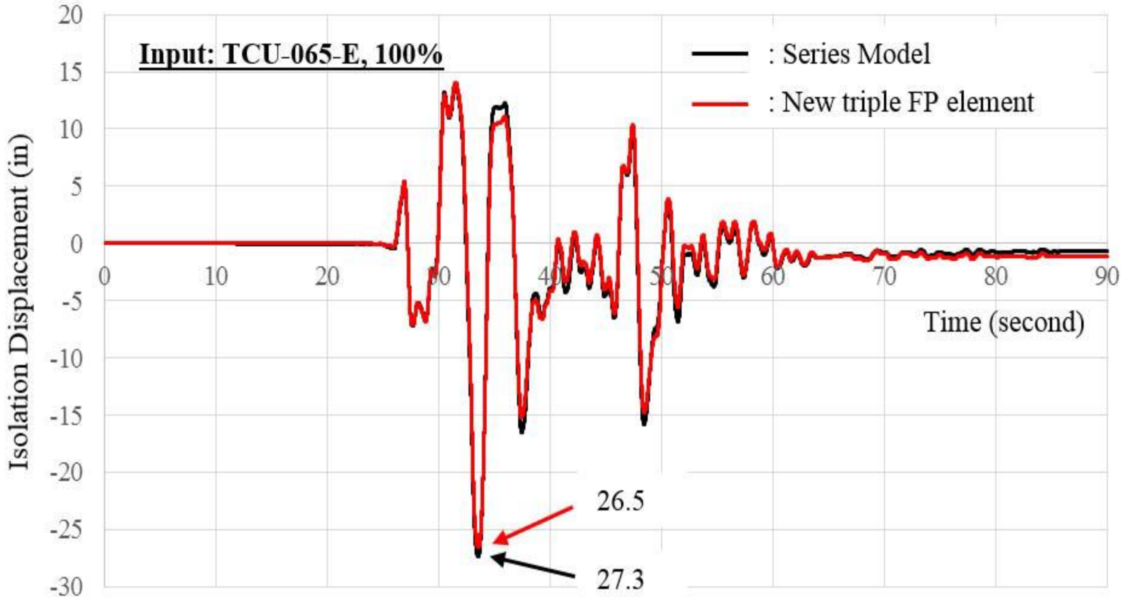

Figure 3.10: Comparison of Isolator Displacement Histories (Constantino report) [23]

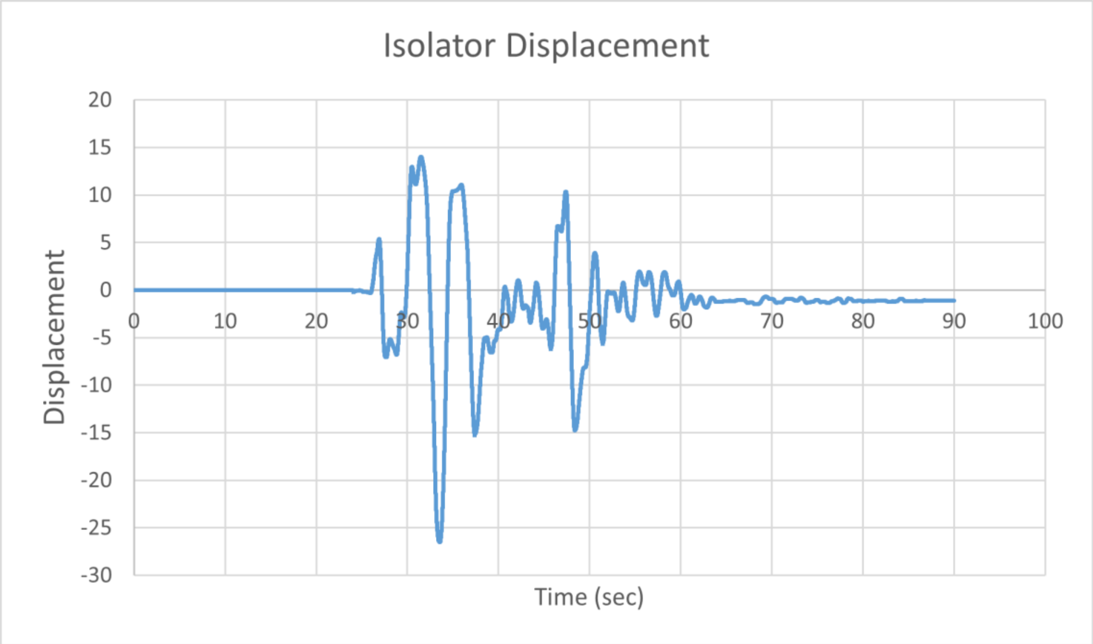

Figure 3.11: Comparison of Isolator Displacement Histories (This report)

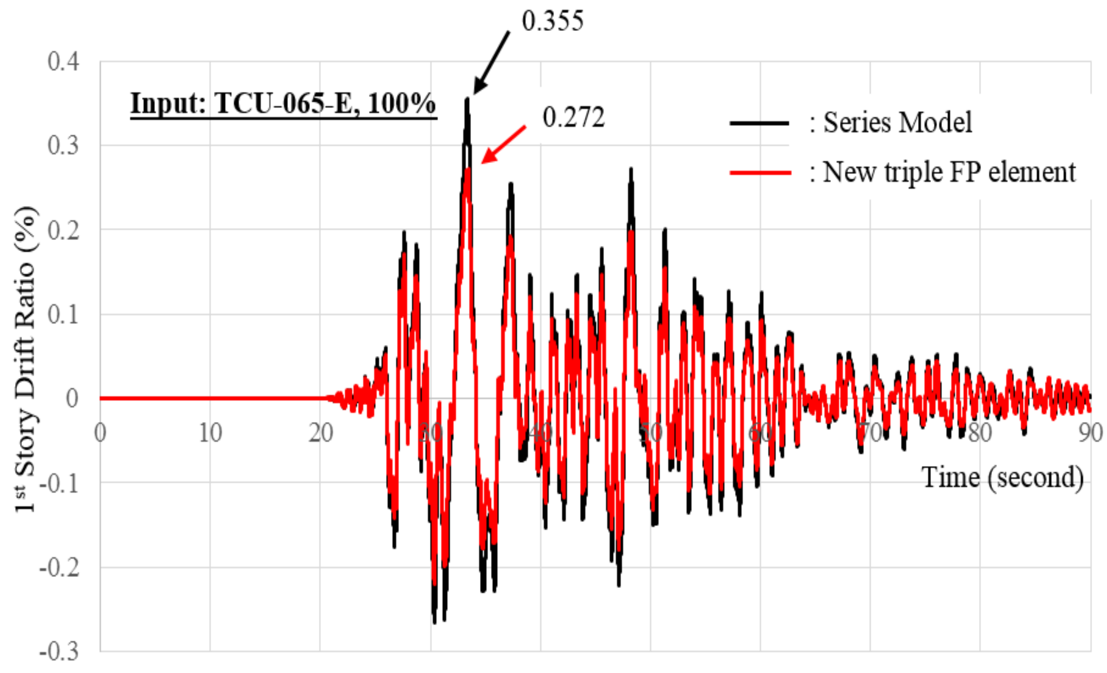

Figure 3.12: Comparison of First Story Drift Ratio Histories (Constantino) [23]

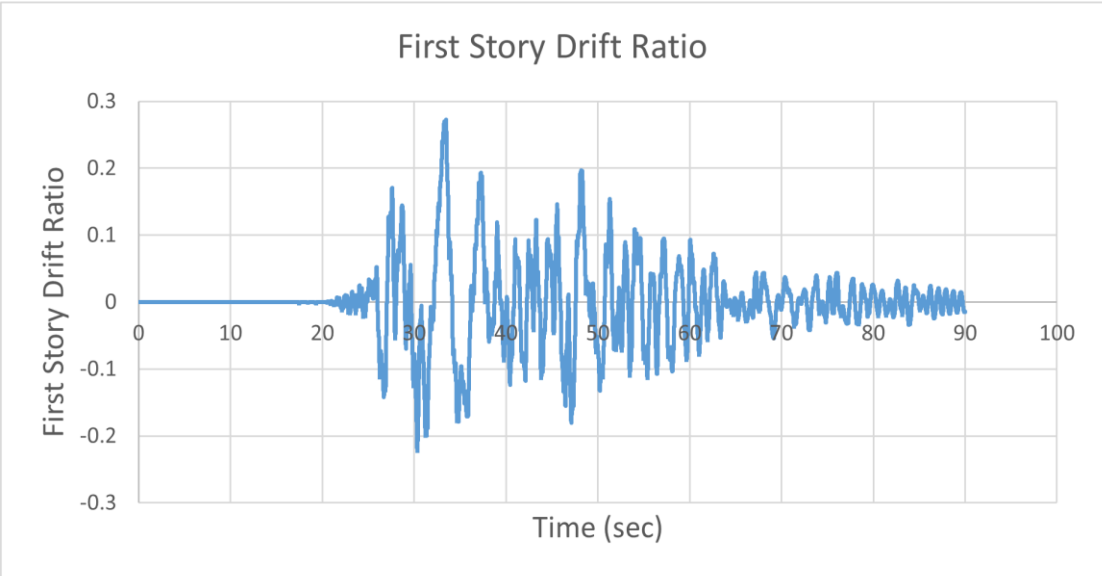

Figure 3.13: Comparison of First Story Drift Ratio Histories (this report)

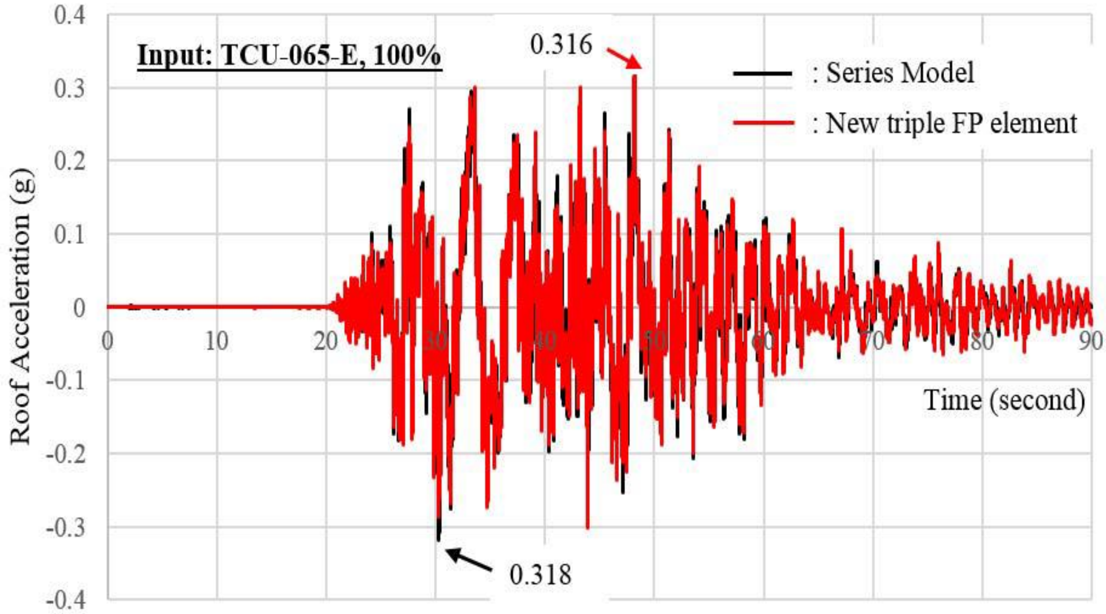

Figure 3.14: Comparison of Roof Acceleration Histories (Conistantio) [23]

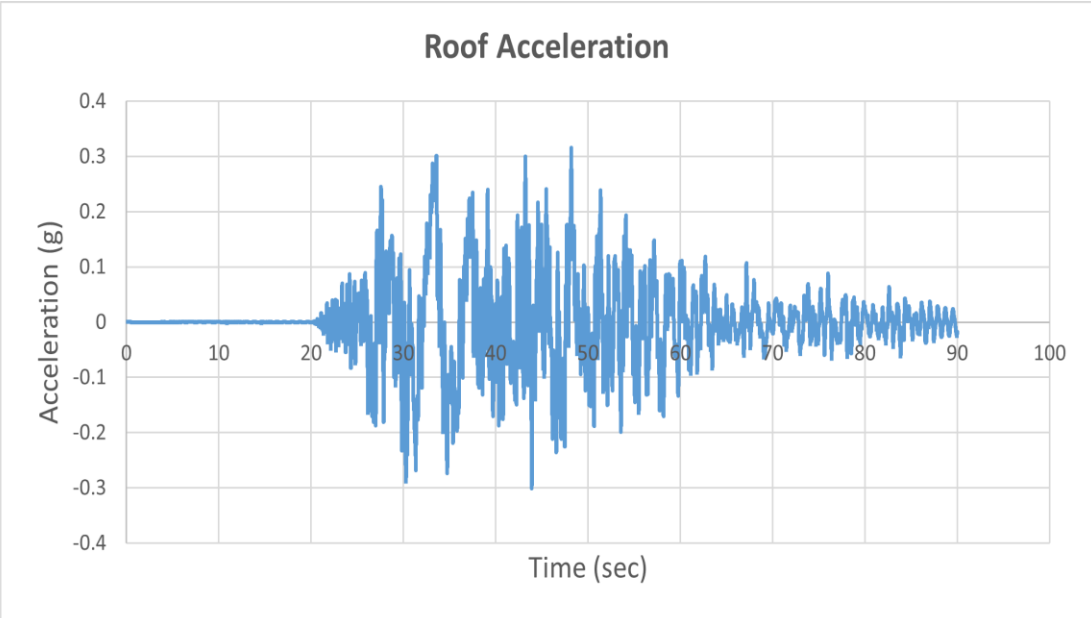

Figure 3.15: Comparison of Roof Acceleration Histories (This report)

3.7 Ground Motion Excitation

Selection of earthquake loading for the purpose of designing and/or analyzing the response of a structure is not a straightforward process due to the nature of seismic excitation. One possible method for the response of earthquake loading is to assume that the structure is subjected to a collection of seismic events that are more likely to occur in the area where the structure is located, and then apply that assumption to the structure [24]. In this study, a set of six near-field seismic events was applied unidirectionally to the seismically isolated structure. The Strong Ground Motion database of the Pacific Earthquake Engineering Research (PEER) Center was used. As it was mentioned, all the events that have been chosen are near field, meaning that their distances are less than 10 km from the fault rupture. These near-field ground motions are characterized by large amplitude, high PGV and PGD. And, in particular, the PGA is high in this kind of motion since the PGAs of near-fault earthquakes are often high and reach the 0.4g PGA recommended by various Building Earthquake Codes.

Each of the seismic events obtained from the PEER Data Base, for this study, had a time history in only one direction, and that direction was H1. All of the events have been processed and analyzed with scaling by the SEISMOMATCH program. Some of the peak values of the scaled ground motion parameters are mentioned in table 3.4 and their acceleration, displacement, and velocity spectrum charts (with 5% damping) are shown in Figure 3.16 to 3.33.

Table 3.4: Ground Motion Records

No	Event	RSN	Year	MW	H1		
					PGA (g)	PGV (cm/s)	PGD (cm)
1	Imperial Valley-06	165	1979	6.53	0.56	48.03	23.37
2	Coalinga-01	368	1983	6.36	0.58	70.15	82.23
3	Kocaeli, Turkey	1176	1999	7.51	0.51	55.85	38.53
4	Chi-Chi, Taiwan	1244	1999	7.62	0.58	50.63	22.60
5	Iwate, Japan	5619	2008	6.9	0.65	38.87	73.68
6	Darfield, New Zealand	6897	2010	7	0.65	42.84	20.40

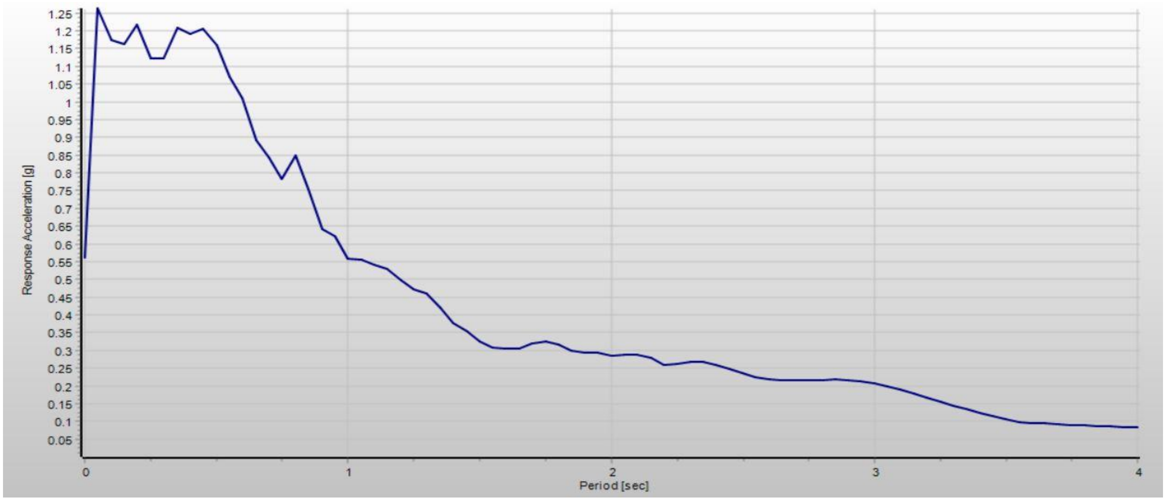

Figure 3.16: Imperial Valley-06 spectral acceleration

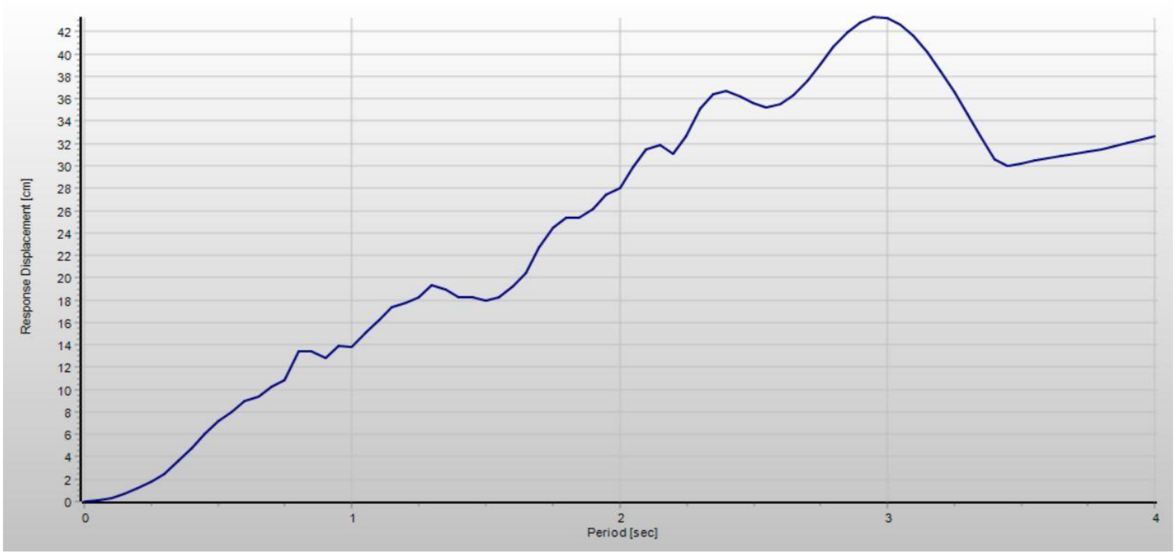

Figure 3.17: Imperial Valley-06 spectral displacement

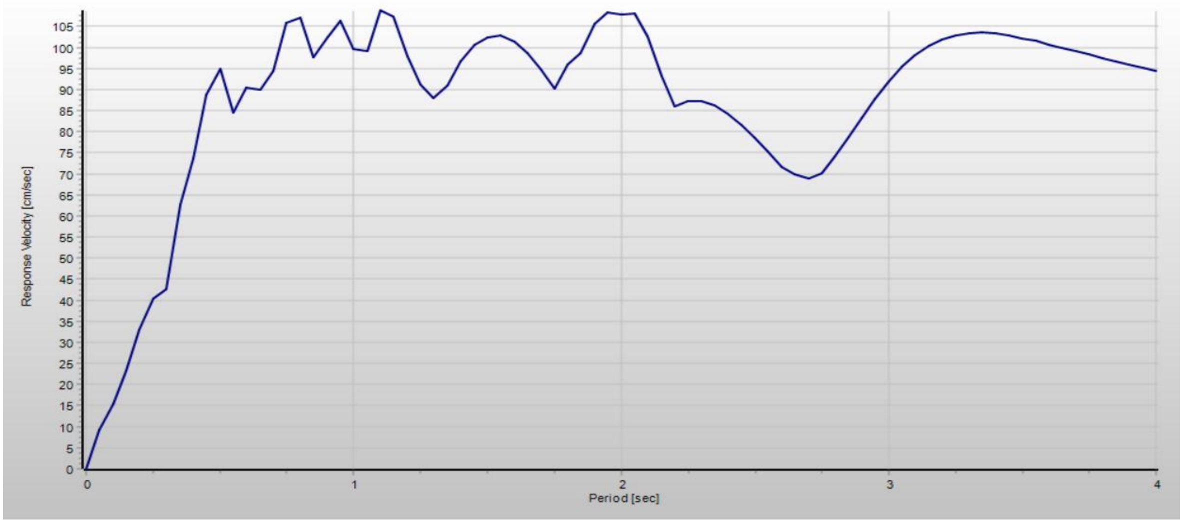

Figure 3.18: Imperial Valley-06 spectral velocity

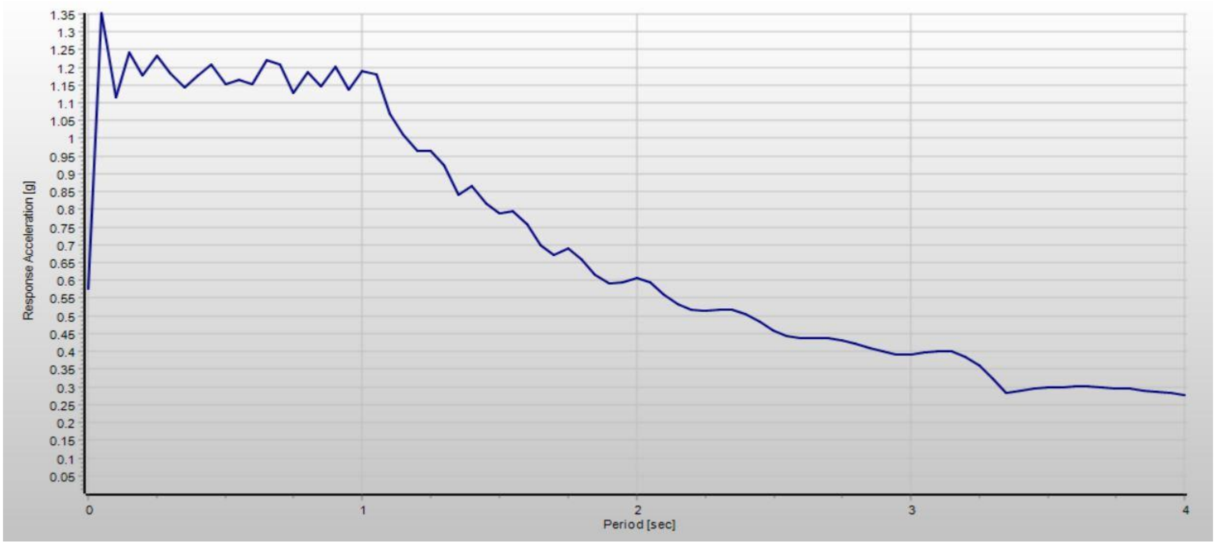

Figure 3.19: Coalinga-01 spectral acceleration

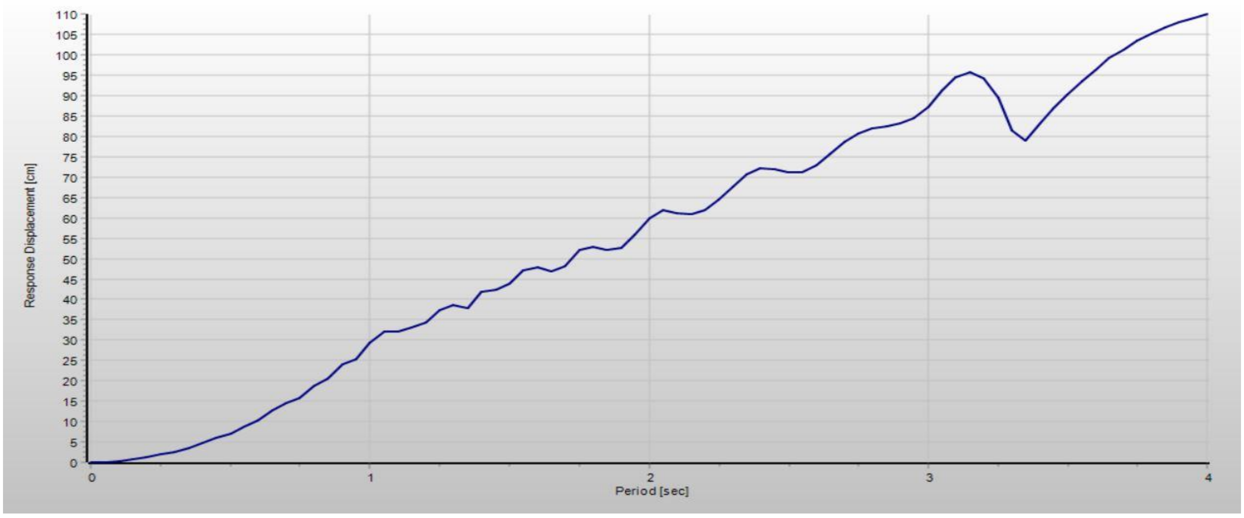

Figure 3.20: Coalinga-01 spectral displacement

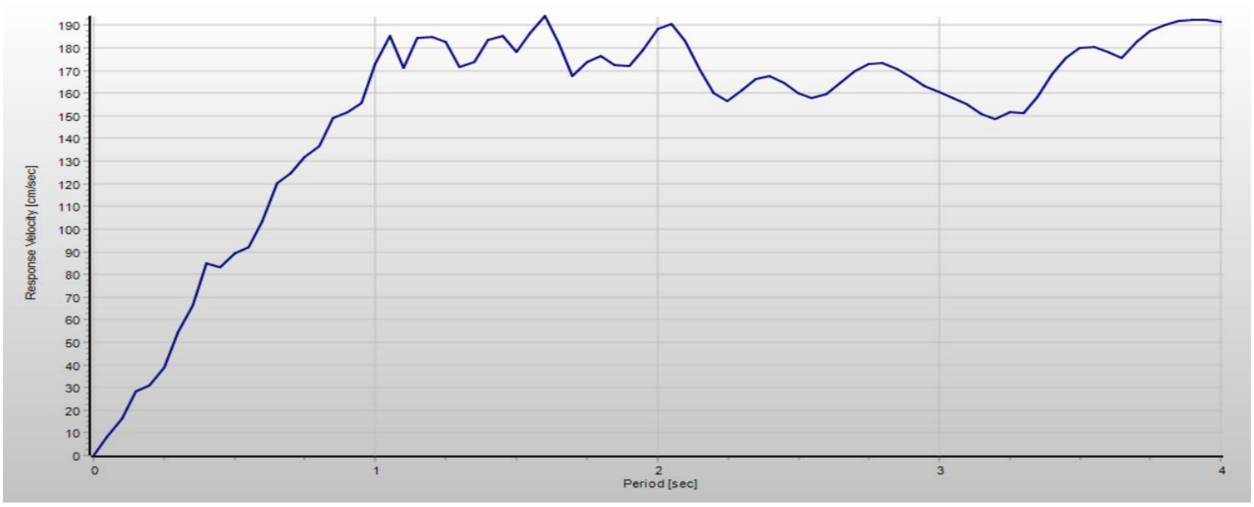

Figure 3.21: Coalinga-01 spectral velocity

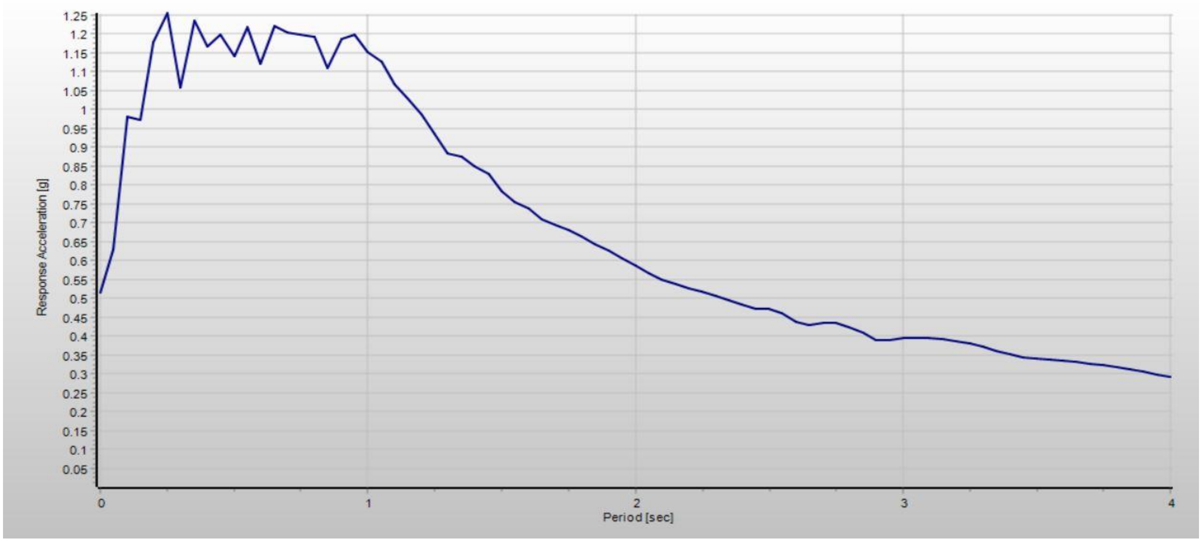

Figure 3.22: Kocaeli spectral acceleration

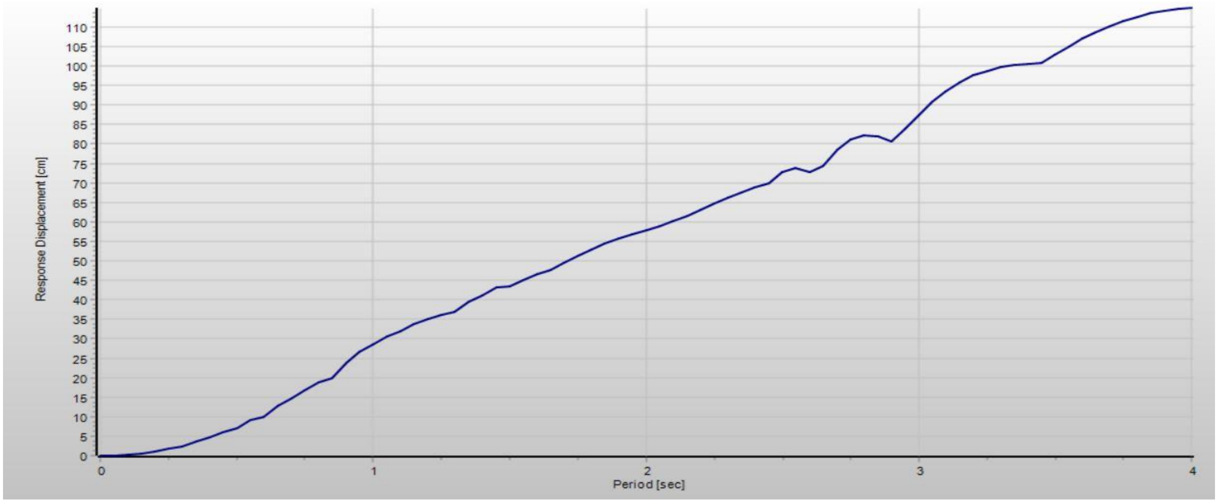

Figure 3.23: Kocaeli spectral displacement

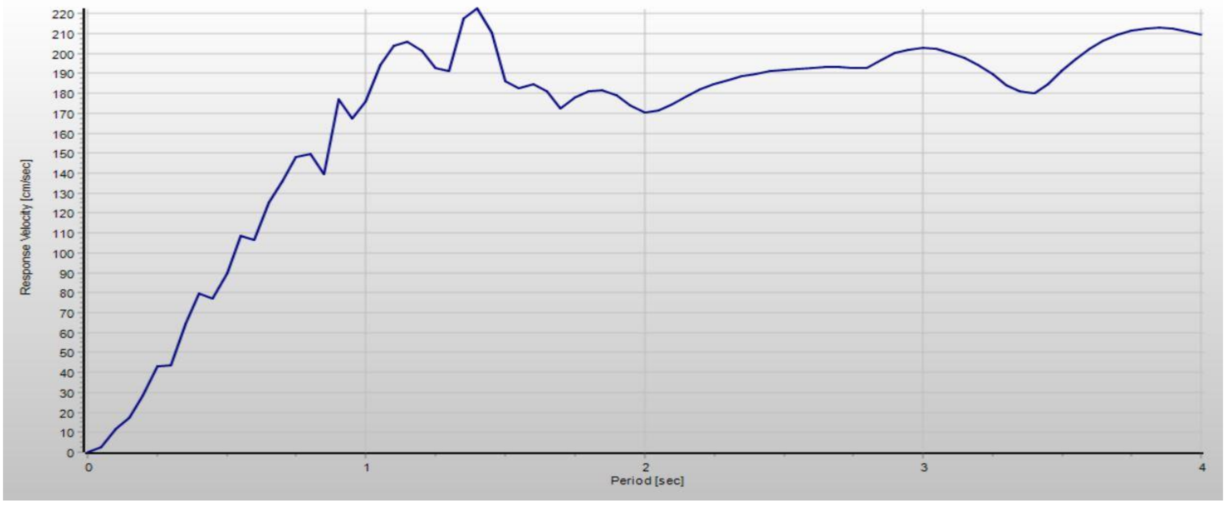

Figure 3.24: Kocaeli spectral velocity

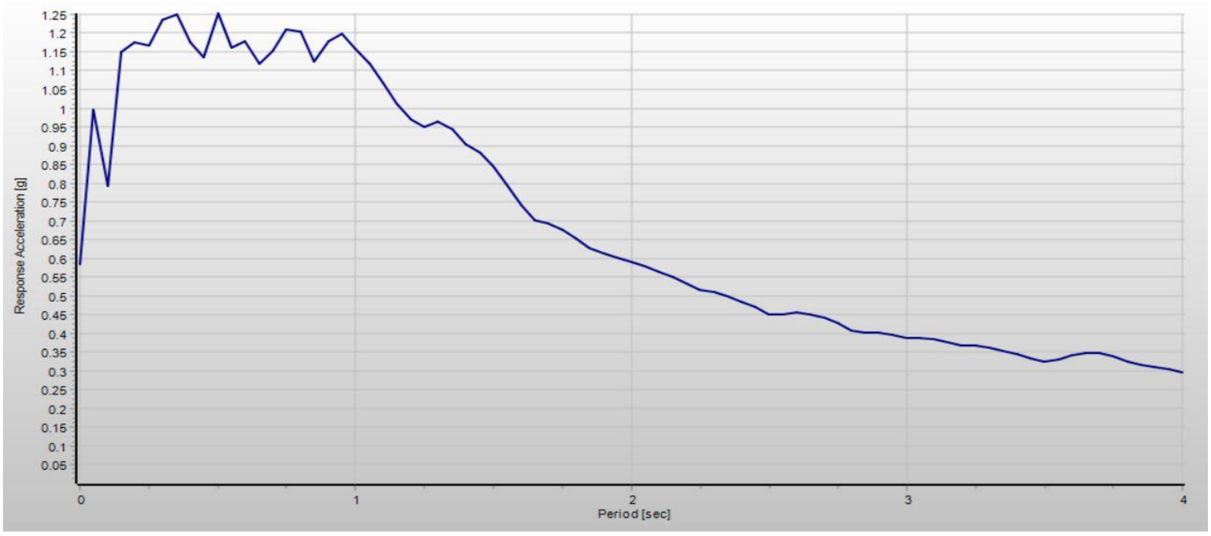

Figure 3.25: Chi-Chi spectral acceleration

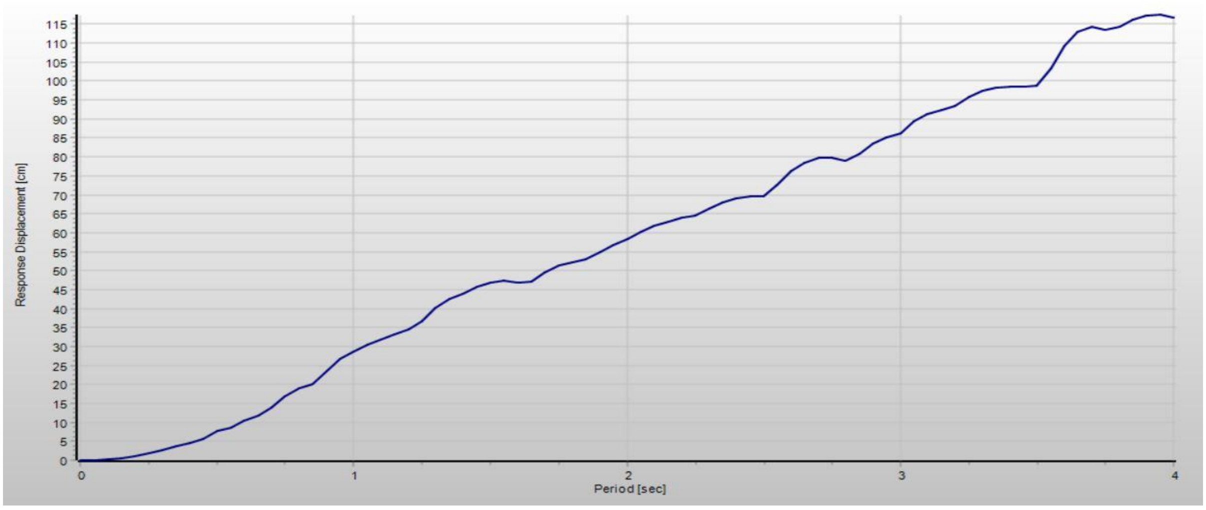

Figure 3.26: Chi-Chi spectral displacement

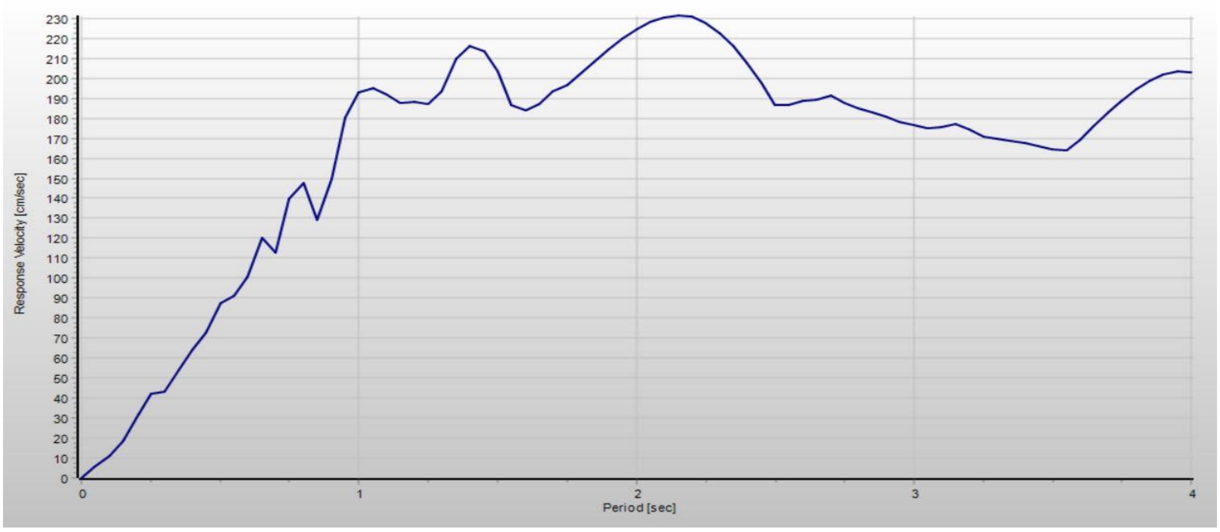

Figure 3.27: Chi-Chi spectral velocity

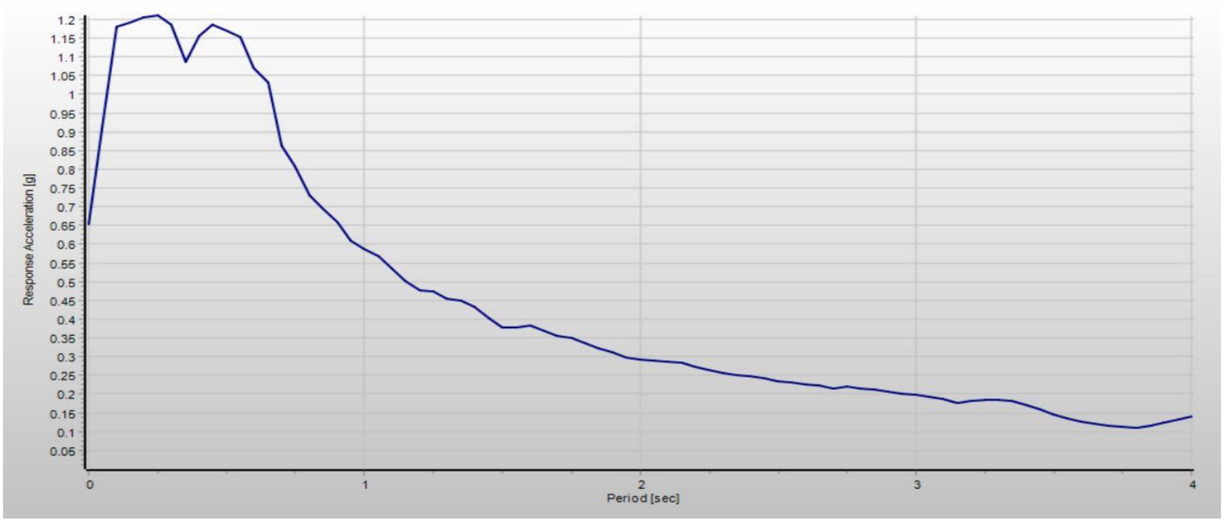

Figure 3.28: Iwate spectral acceleration

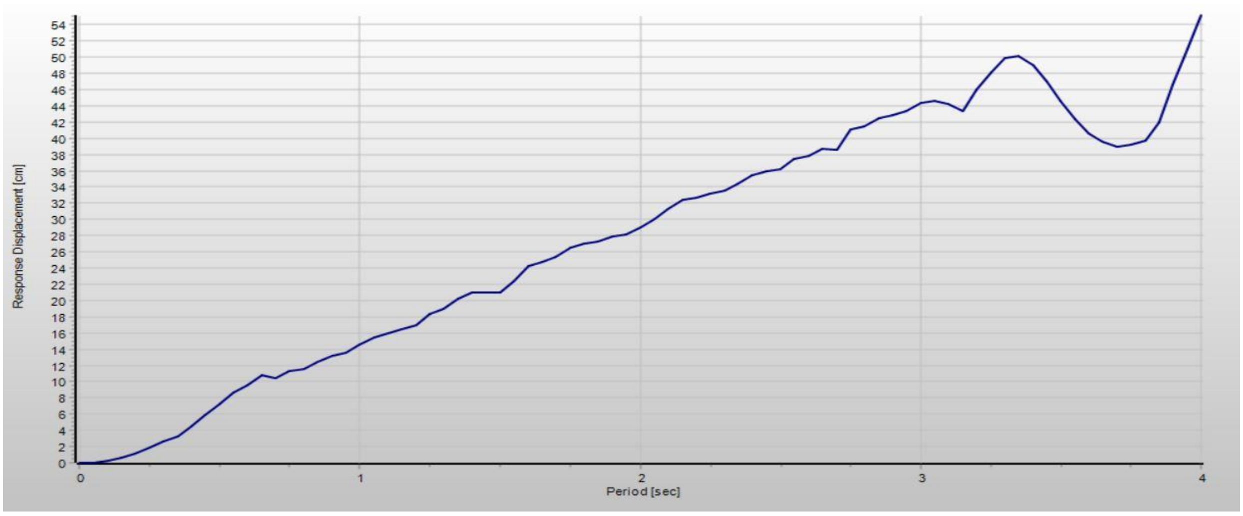

Figure 3.29: Iwate spectral displacement

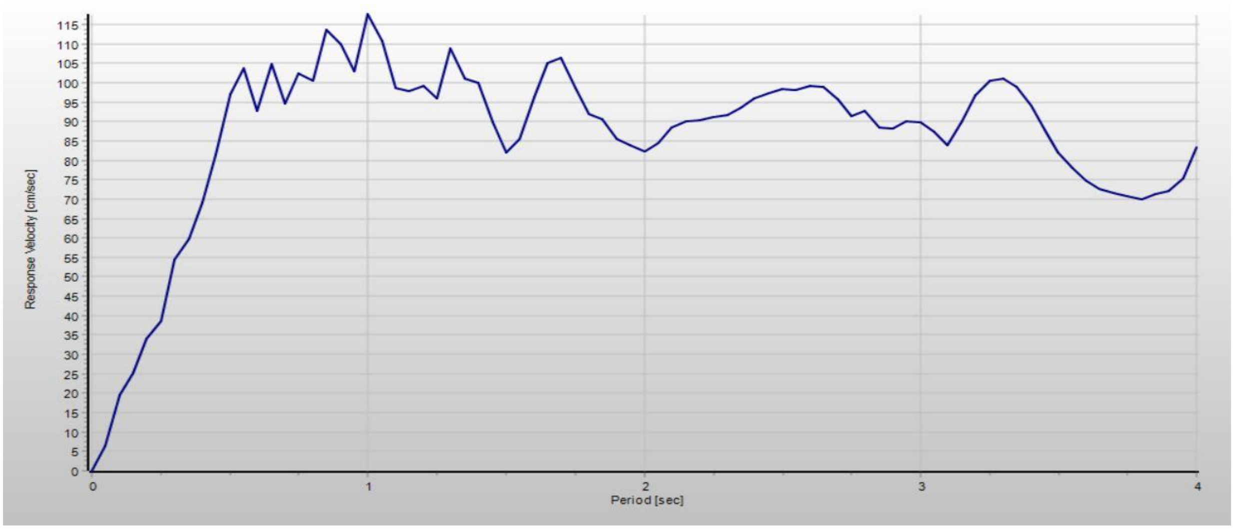

Figure 3.30: Iwate spectral velocity

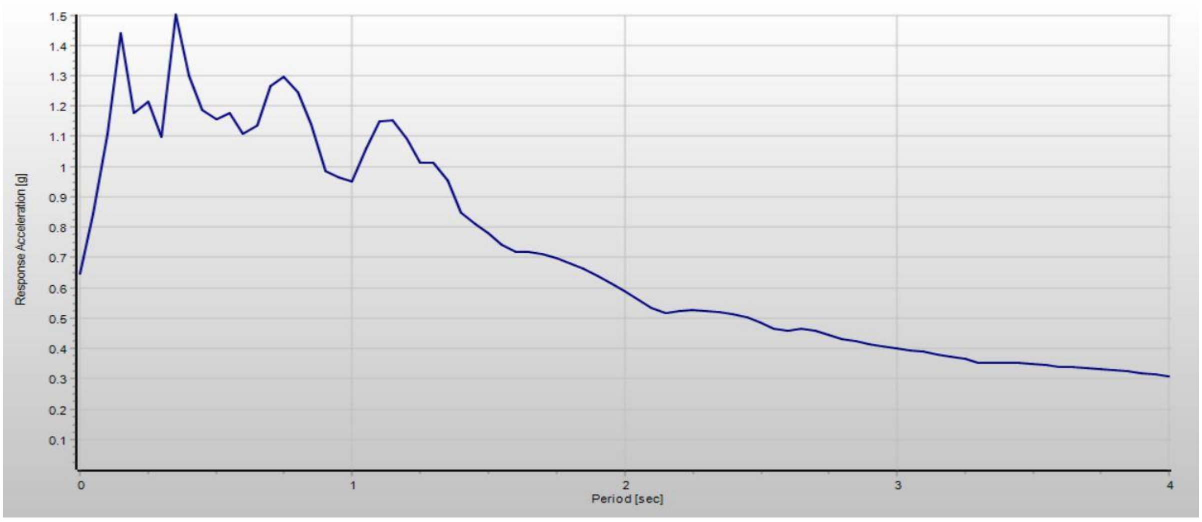

Figure 3.31: Darfield spectral acceleration

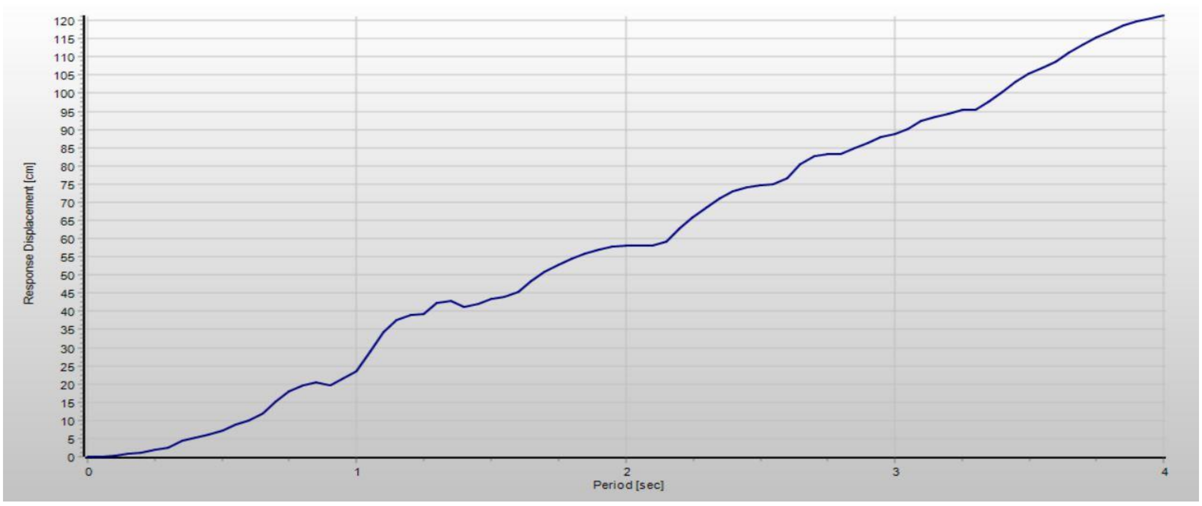

Figure 3.32: Darfield spectral displacement

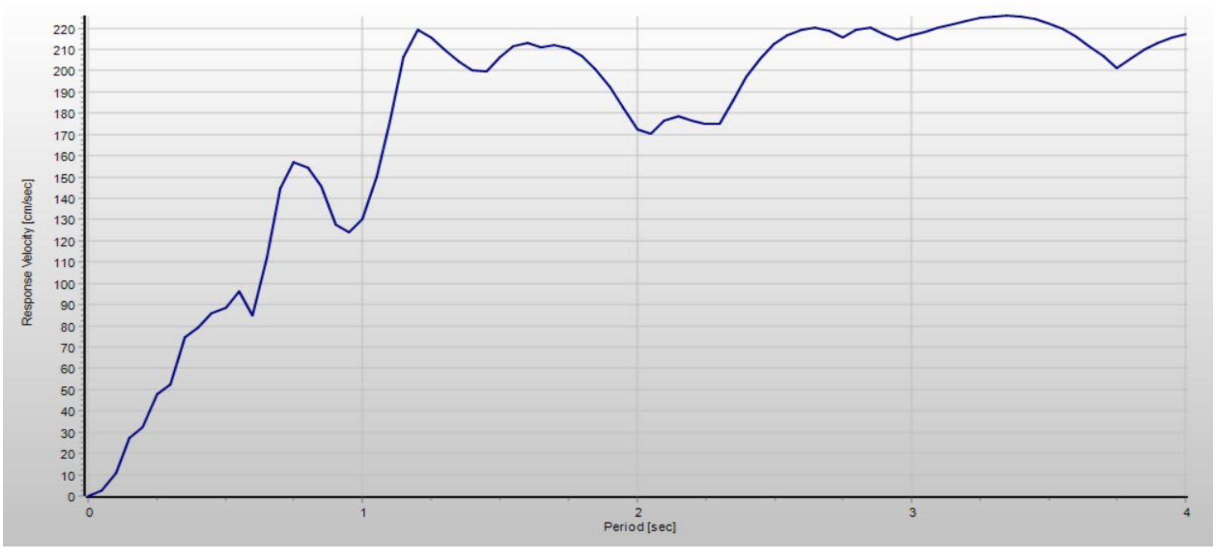

Figure 3.33: Darfield spectral velocity

3.8 Scaling of the Ground Motion Events

To use seismic records in the design or evaluation of a structural system for earthquake hazards, it is suggested that they should be taken from records whose magnitude, source-to-site distance, and type of faulting are close to the maximum earthquake considered at the site. They are various ground motion scaling procedures. In this study, a non-stationary spectral matching procedure was being analyzed. Time domain spectral matching is used to create acceleration time histories in non-stationary spectral matching techniques. The spectral accelerations of each created acceleration time history are fitted almost precisely to the target spectrum using this method. Figure 3.34 shows the collection of all matched accelerograms, and they are named according to their record sequence number (RSN). Although the resulting motions may not be realistic in some cases, this is not considered an issue for structural analysis [25]. Figure 3.35 shows the target earthquake spectrum that was created by using the spectra of all of the selected events to generate the target earthquake spectrum and Figure 3.36 represents a collection of accelerograms showing events that have been unscaled.

In this study, spectral matching was performed through the use of the SeismoMatch software. SeismoMatch is a software that allows earthquake accelerograms to be adjusted in order to match a specified target response spectrum.

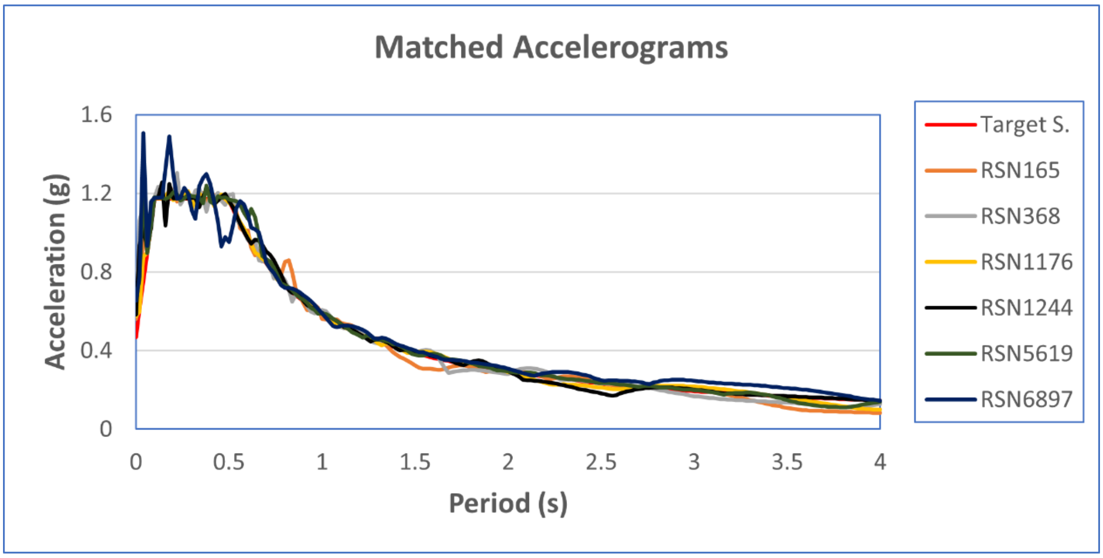

Figure 3.34: Collection of all matched accelerograms.

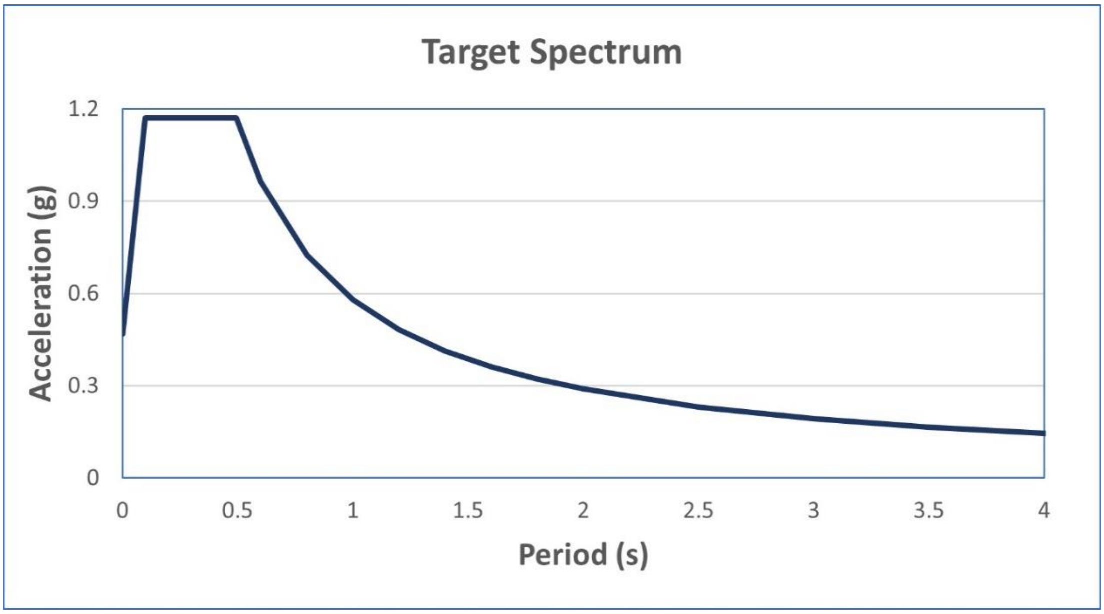

Figure 3.35: Target Spectrum to Which the Ground Motions Have Been Scaled

CHAPTER 4

LIQUID STORAGE TANK

4.1 Liquid Storage Tank Models

Three steel liquid storage tanks with an isolated and fixed base structure system were considered in this study. These liquid storage tanks are placed on the floors of the structure, and their elevation heights will vary depending on the floor heights. The shapes of the tanks are cylinders, and they are named liquid storage tanks one, two, and three (LST1, LST2, and LST3). Their capacities are 7.854, 4.712, and 1.964 cubic meters, respectively. Section 4.2 provides a brief explanation of the elevated tanks, and Section 3.6 illustrates the frame structure in considerable detail. Table 4.2 provides a description of the tank's technical specification function of the height-to-radius ratio (H/r). Additionally, Table 4.1 includes mechanical parameters for the tanks and liquid that are obtained by the methods described in [26].

4.2 Mechanical Analogue Model

Housner, presented a two-mass model for liquid storage tanks that is more suitable and is widely used in the majority of international codes [27]. The pressure exerted on the liquid as a response to the dynamic motion of the tank can be divided into two components – impulsive and convective. When a liquid tank is subjected to a horizontal seismic event, both the tank wall and the liquid experience horizontal acceleration. The liquid in the tank's lower part acts like a mass rigidly coupled to the tank wall. This mass is referred to as "impulsive liquid mass" since it accelerates together with the wall, generating hydrodynamic force to be exerted on the tank wall and, likewise, on the bottom. Sloshing motion occurs in the upper liquid mass of the tank. This mass is referred to as "convective liquid mass," and it generates a convective hydrodynamic force on the tank's wall and bottom.

4.3 Seismic Analysis of Tank and Modeling of Liquid

The tank was analyzed and detailed as per the simple procedure for tank analysis and modelling of liquids proposed by Malhotra that was based on the work of Veletsos and co-workers [26]. Malhotra made some adjustments to the procedure that made it easier to apply for design. This study will follow the same procedure that was presented with the following modifications:

- Only the first impulsive and first convective modes are used to represent the tank-liquid system.
- Combining the first impulsive mode with the higher impulsive modal mass and the first convective mode with the higher convective modal mass.
- Modifying the impulsive and convective heights to accounting for the overturning effect of the higher modes.
- The impulsive period formula is being generalized so that it may be applied to steel and concrete tanks with uniform wall thicknesses.

As an example, the calculation of the liquid storage tank (LST1) parameters is described here, step by step, in order to provide a comprehensive explanation and all the other analyzed results are listed in the Appendix A by the help of MATLAB and also the MATLAB code scripts for the analysis are in the Appendix B. Before analyzing a numerical evaluation, the formulaic parameters are presented and discussed in detail in the following section through equations 4.1 to 4.6 by using Malhotra's approach.

4.4 Model Parameter Properties

The impulsive (T_{imp}) and convective (T_{con}) natural periods are [26]

$$T_{imp} = C_i \frac{H\sqrt{\rho}}{\sqrt{H/r}\, x \sqrt{E}} \qquad (4.1)$$

$$T_{con} = C_c \sqrt{r} \qquad (4.2)$$

Where:

h is the uniform thickness of the tank wall, ρ is the liquid density (mass), and E is the tank's modulus of elasticity. The Ci and Cc coefficients can be found in Table 1. Ci is a dimensionless coefficient, whereas Cc is represented in $s/\sqrt{m}$. For tanks with non-uniform wall thickness, h can be computed by taking a weighted average of the tank wall's wetted height and assigning the highest weight towards the tank's base, where the strain is greatest [26].

4.5 Seismic Response Parameters

The formulations of main parameters of the seismic response of liquid storage tank are presented here [26].

1. Base shear:

$$Q = (m_i + m_r + m_W) \text{ x } S_e(T_{im}) + m_c S_e(T_{con}) \quad (4.3)$$

Where:

The m_i and m_c are impulsive and convective masses that are obtained using the data in the Table 4.2 and m_W is the mass of tank wall, while m_r the mass of tank roof. $S_e(T_{imp})$ is the impulsive spectral acceleration and $Se(T_{con})$ the convective spectral acceleration (obtained from a 0.5% damped response spectrum) [26].

2. Overturning moment above the base plate

$$M = (m_i h_i + m_r h_r + m_w h_w) \text{ x } S_e(T_{im}) + m_c h_c S_e(T_{con}) \quad (4.4)$$

Where:

The h_i and h_c are the heights of the centroids of the impulsive and convective hydrodynamic pressure walls, respectively, and are obtained from table 4.2. and h_w and h_r are the heights of the tank wall and roof's centers of gravity, respectively [26].

3. The overturning moment below the base plate [26].

$$M' = (m_i h'_i + m_r h_r + m_w h_w) \text{ x } S_e(T_{im}) + m_c h'_c S_e(T_{con}) \quad (4.5)$$

Where: the heights hi' and hc' are obtained from Table 4.2.

4. Liquid displacement due to the sloshing [26].

$$d = R \frac{S_e(T_{con})}{g} \quad (4.6)$$

Where: the g is the acceleration due to gravity.

Table 4.1: Mechanical parameters for the tanks and liquid

Properties	Unit	Value of The Three Tanks		
A. General properties		**LET1**	**LET2**	**LET3**
Height	m	2.5	1.5	2.5
Radius	m	1	1	0.5
Volume	m^3	7.854	4.712	1.964
Gravitational Acc.	m/s^2	9.81	9.81	9.81
B. Liquid Properties				
Liquid Height	m	2	1	1.5
Liquid Density	kg/m^3	1000	1000	1000
Mass of Liquid	kg	$6.28x10^3$	$3.14x10^3$	$1.18x10^3$
C. Wall Properties				
Wall Thickness (Uniform)	m	0.005	0.005	0.005
Modulus of Elasticity	N/m^2	$2*10^{11}$	$2*10^{11}$	$2*10^{11}$

Table 4.2: Technical specification function of the height-to-radius ratio (H/r) [26].

H/r	C_i	C_c [s/m]	m_i/m_l	m_c/m_l	h_i/H	h_c/H	h_c'/H	h_i'/H
0.3	9.28	2.09	0.176	0.824	0.4	0.521	2.64	3.414
0.5	7.74	1.74	0.3	0.7	0.4	0.543	1.46	1.517
0.7	6.97	1.6	0.414	0.586	0.401	0.571	1.009	1.011
1	6.36	1.52	0.548	0.452	0.419	0.616	0.721	0.785
1.5	6.06	1.48	0.686	0.314	0.439	0.69	0.555	0.734
2	6.21	1.48	0.763	0.237	0.448	0.751	0.5	0.764
2.5	6.56	1.48	0.81	0.19	0.452	0.791	0.48	0.796
3	7.03	1.48	0.842	0.158	0.453	0.825	0.472	0.825

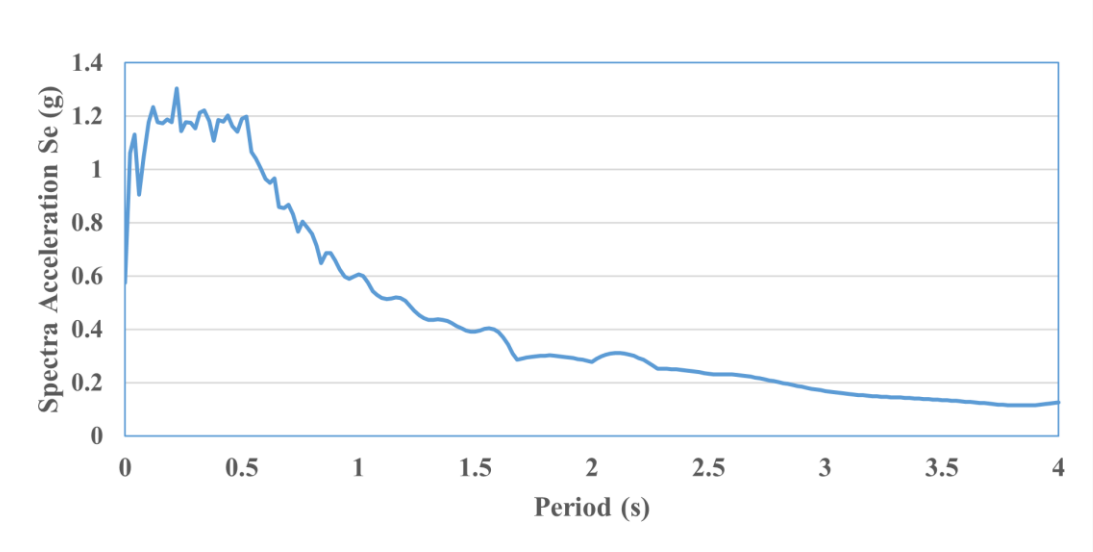

Figure 4.1: 5% damped spectral acceleration for ground motion (Imperial Valley-06).

Example: Here is the solution analysis for the liquid storage tank 1 (LST1) when the tank is on the ground. It is assumed that it is rigid to a concrete mat foundation. The radius of the tank is 1 m, and the total height of the tanks is 2.5 m. The ratio of liquid height to radius is (H/r = 2). The total mass of water in the tank (m_l) is 6283.19 kg. The total mass of the tank wall (m_w) is 612.61 kg, and the height of its center of gravity is 1.25 m. The mass of the tank roof (m_r) is 122.52 kg and the height of its center of gravity (h_r) is 2.5 m. The 5% damped spectral acceleration for ground motion (Imperial Valley-06) is shown in figure 4.1. All the other tank material and properties are in given in table 4.1.

Step 1: Model properties

From Table 4.2: H/r = 2, Ci = 6.21, C_C = 1.48

$$T_{im} = 6.21\frac{2\sqrt{1000}}{\sqrt{0.005/1}\,x\sqrt{2x10^{11}}} = \; 0.01242s$$

$$T_{con}{=}1.48\sqrt{1} \; = 1.48s$$

Step 2: Seismic responses

From Table 4.2: $H/r = 2$, $m_i/m_l = 0.763$, $m_c/m_l = 0.237$

$m_i = 0.763 \times 6.28 \times 10^3 = 4.62 \times 10^3$ kg

$m_c = 0.237 \times 6.28 \times 10^3 = 1.49 \times 10^3$ kg

From Table 4.2: $H/r = 2$, $h_i/H = 0.448$, $h_c/H = 0.751$, $hi'/H = 0.5$ $hc'/H = 0.764$

From figure 4.1: $T_{im} = 0.01242s$, $Se\,(T_{im}) = 0.604\ g$, $T_{com} = 1.48s$, $Se\,(T_{con}) = 0.33701$

$$Q = (4.62 + 0.6126 + 0.1225)x10^3 \text{ x } 0.604 + 1.489x10^3x0.337 = 3.74\ kN$$

$$M = (4.62x0.896 + 0.6126x1.25 + 0.1225x2.5)\ x10^3x\ 0.604 + 1.489x10^3x1.502x0.337 = 3.9\ kN$$

$$d = 1\frac{1.48}{9.807} = 0.15\ m$$

CHAPTER 5

RESULTS AND DISCUSSION

5.1 Overview

The seismic response of the three liquid storage tanks (LST1, LST2, and LST3) models will be investigated in this section. The results of the analyses for both the isolated and fixed base liquid storage tank analyses are described here. We will explore how the liquid in the tanks on the floors of the structure, described in Section 3.6, responds to two conditions: isolated and non-isolated.

The entire process of analysing the results can be summarized as follows:

- ❖ Develop a model of a two-dimensional base isolated structure by using nonlinear dynamic history analysis as explained in Chapter 3.
- ❖ Again, develop the same previous structure by using the same method of analysis (NLDH), but with a fixed base.
- ❖ Analyze three geometrically different liquid storage tanks that have a cylindrical shape (see chapter 4).
- ❖ Assume placing the tanks at the center of each floor and apply the floor accelerations to them to analyze their response.
- ❖ Finally, evaluate and compare the response results of the tank parameters from both frame structures (isolated and non-isolated).

In this study, six near-fault earthquakes were used. The responses of the liquid storage tanks were observed by a parametric analysis, and the following results are presented for both isolated and non-isolated conditions:

1. The total base shear
2. The liquid displacement due to the sloshing
3. The overturning moment

5.2 Base Shear

Base shear values were computed and presented in Figures 5.1 to 5.6. In general, all three liquid storage tanks were analyzed under six near-field seismic events in two cases (fixed and isolated) and showed the effectiveness of isolation in reducing the base shear demand. In order to make a comparative evaluation, the base shear of the tank was divided by its weight. It is clear that the values are reduced in the isolated condition. According to the tanks on floor variations, base shear increases as the elevation of the tank rise, mostly, however, the top floor has the maximum base shear in all tanks.

The floor variation of base shear forces under Imperial Valley seismic events for liquid storage tanks (LST1, LST2, and LST3) in two conditions (isolated and non-isolated) are compared and presented in the pictures in Figure 5.1. As expected, the base shear is decrease in all of the floors, except the base floor of LST2 and LST3.

Considering floor elevations (Figure 5.1), the base shear forces in base, first and second, third and fourth floor due to LST1 reduce, respectively, by 0.25%, 15%, 22%, 24%, and 35% assuming isolation model; and the base shear forces in, first and second, third and fourth floor due to LST2 reduce respectively, by 31%, 30%, 30% and 45%, assuming isolation model, while there is an increase in the base floor. On the other hand, due to LST3, the base shear forces in the first and second, third and fourth floor reduce respectively by 5%, 19%, 35%, and 44% for the isolation model.

In general, the foregoing result indicates that base isolation reduces the seismic response of the entire system, particularly on the top four floors. Furthermore, the base shear force is comparatively larger as the elevation of the tanks increases.

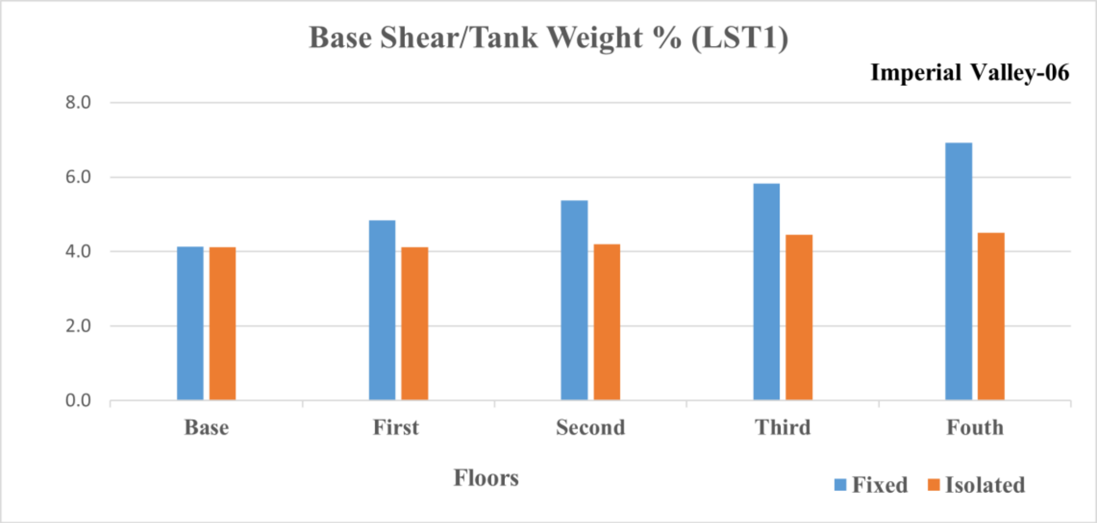

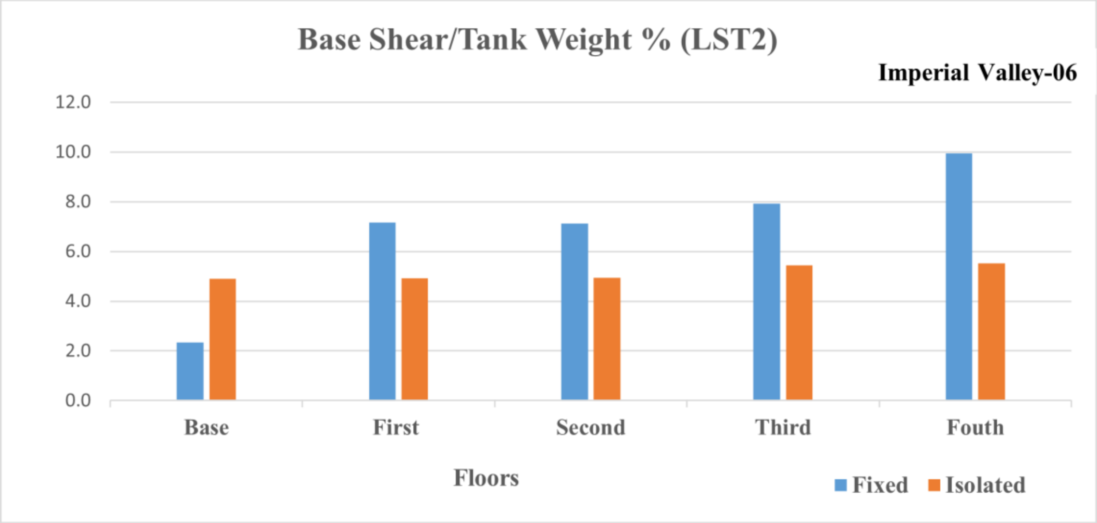

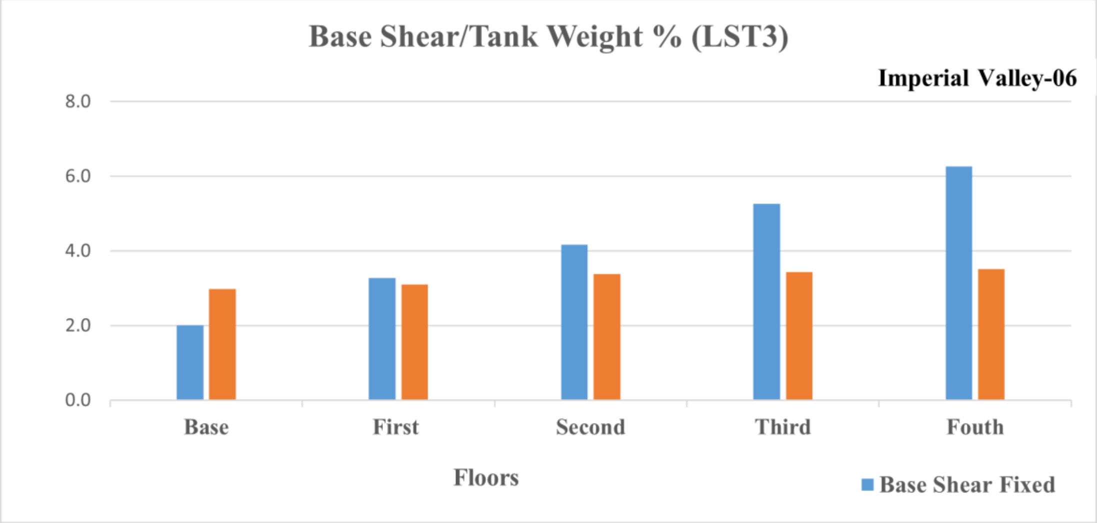

Figure 5.1: Base shear variation of three liquid storage tanks on fixed and isolated condition under Imperial Valley-06

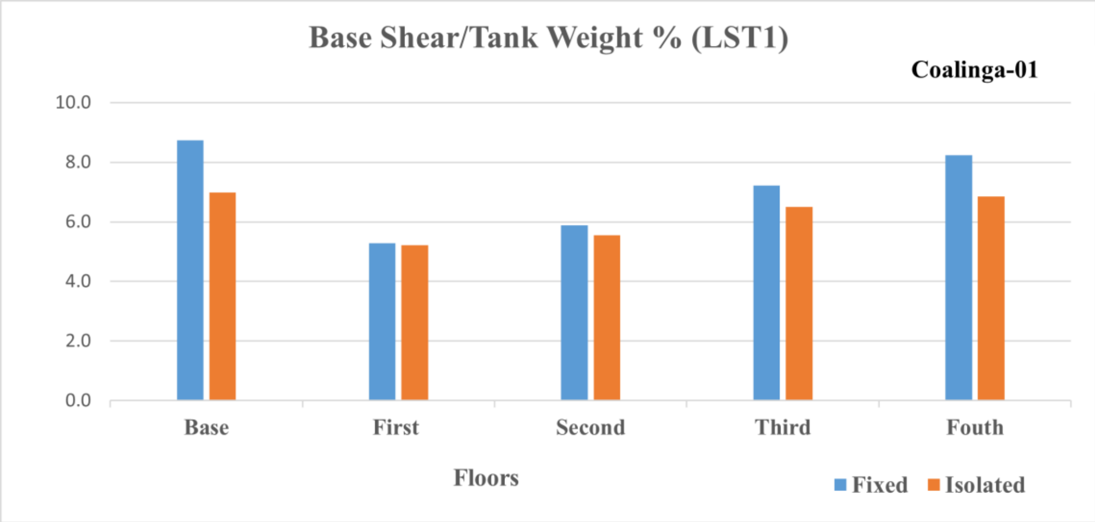

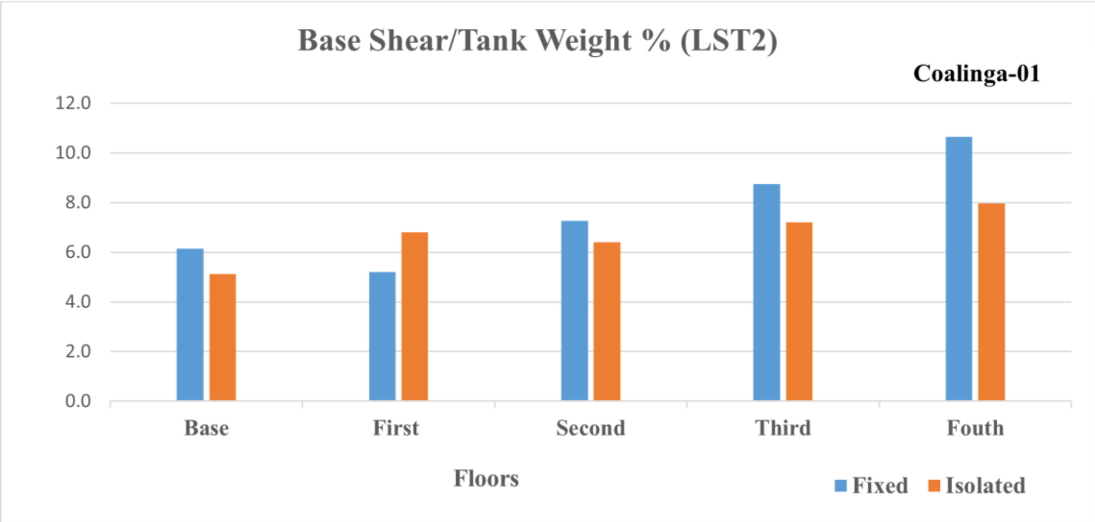

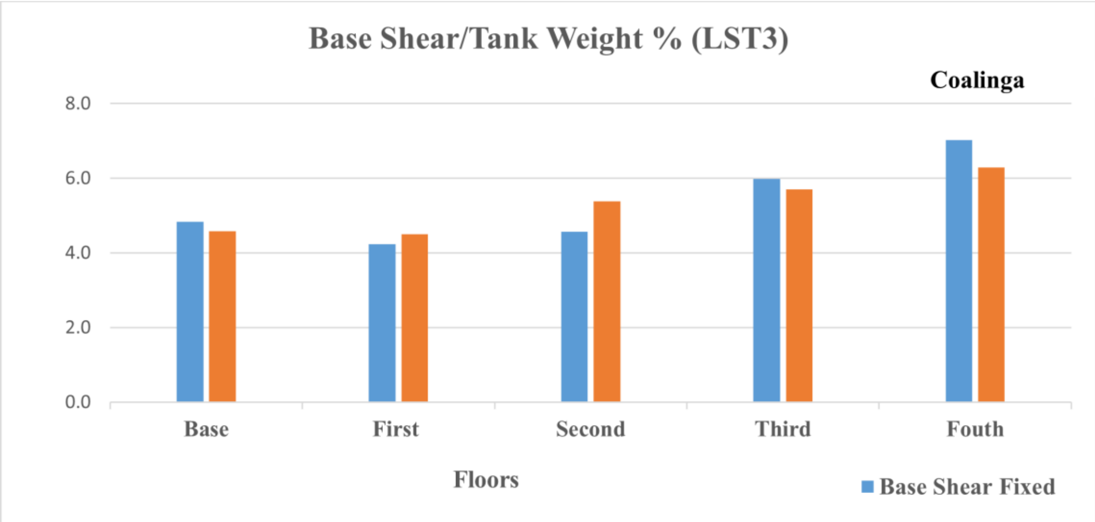

Figure 5.2: Base shear variation of three liquid storage tanks on fixed and isolated condition under Coalinga

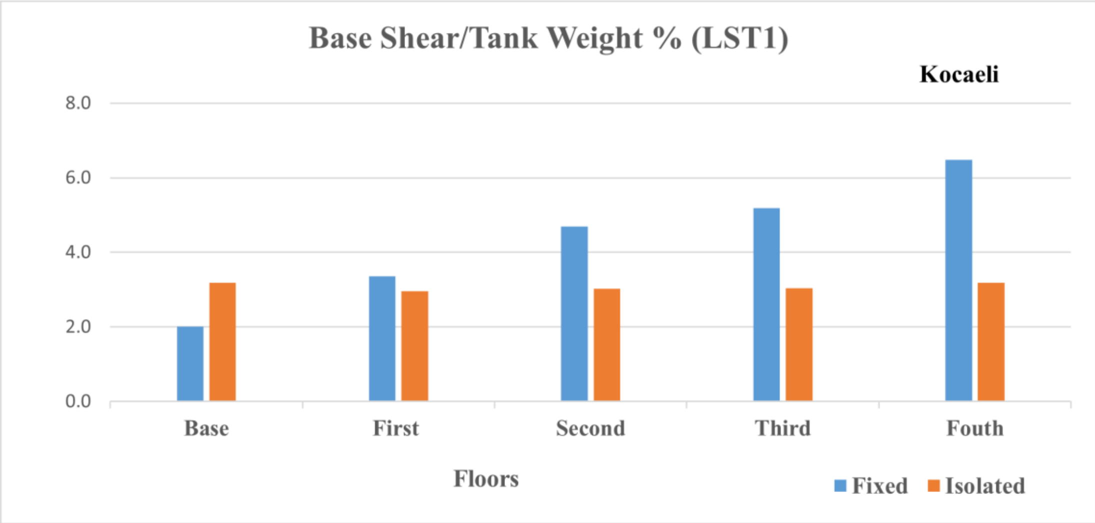

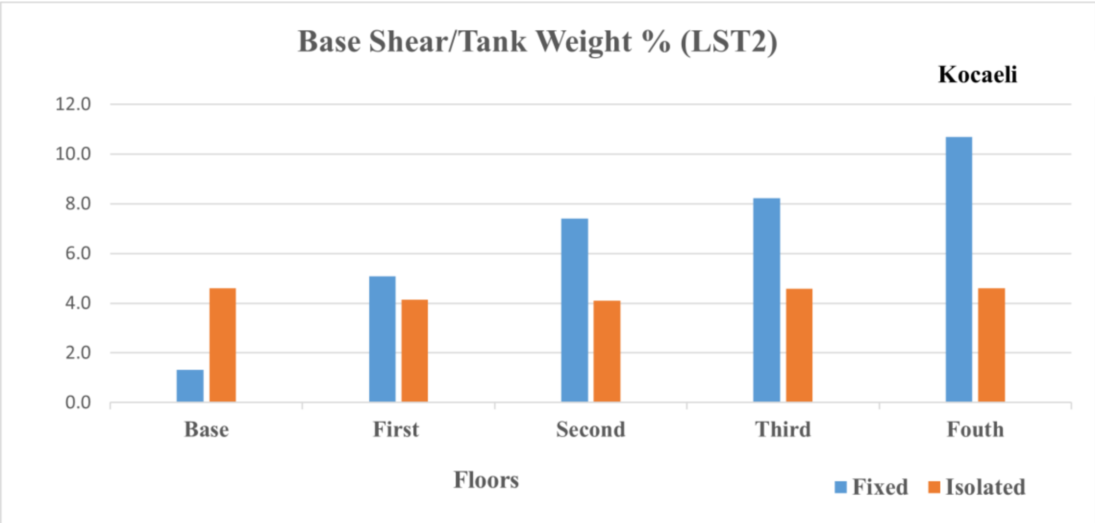

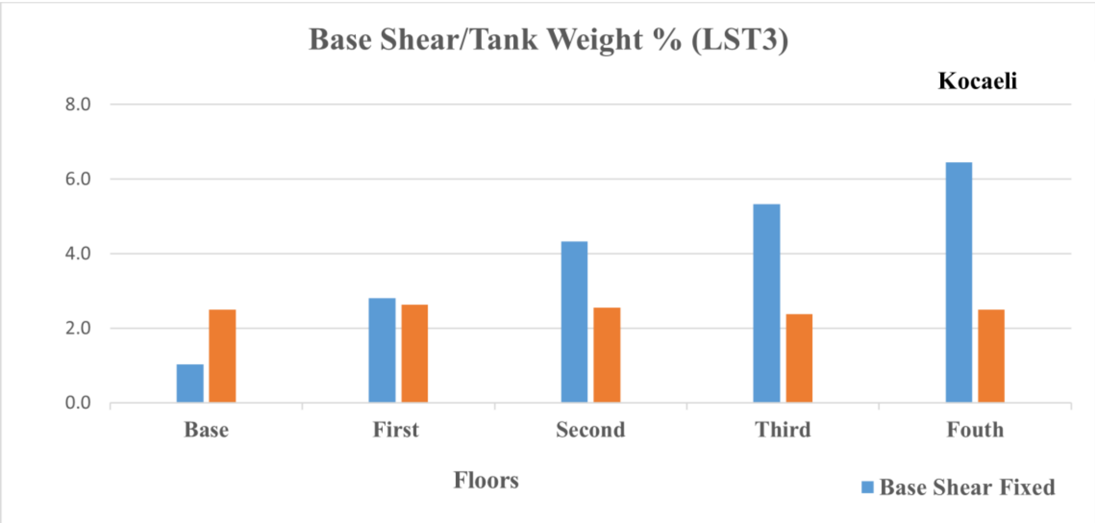

Figure 5.3: Base shear variation of three liquid storage tanks on fixed and isolated condition under Kocaeli

Figure 5.4: Base shear variation of three liquid storage tanks on fixed and isolated condition under Chi-Chi

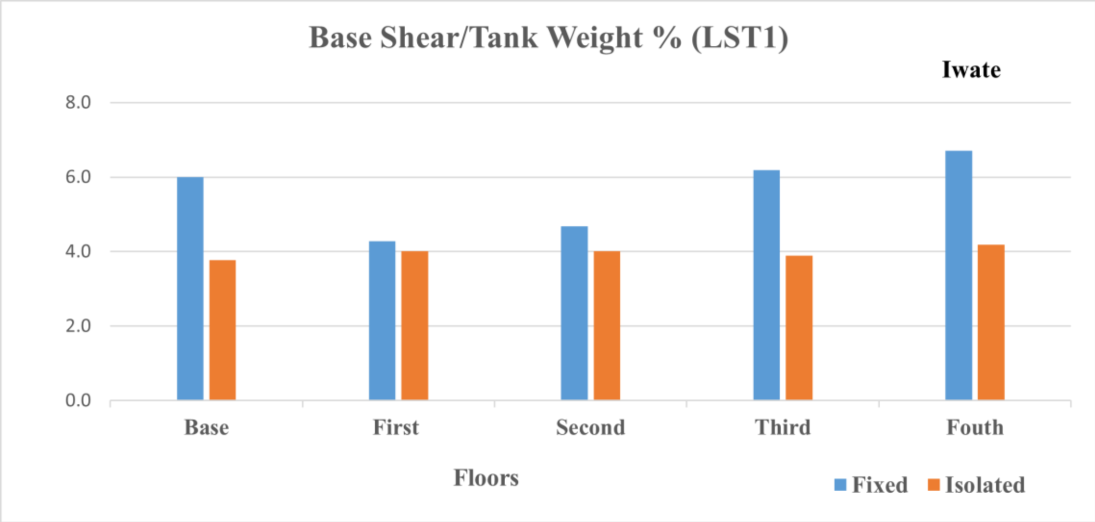

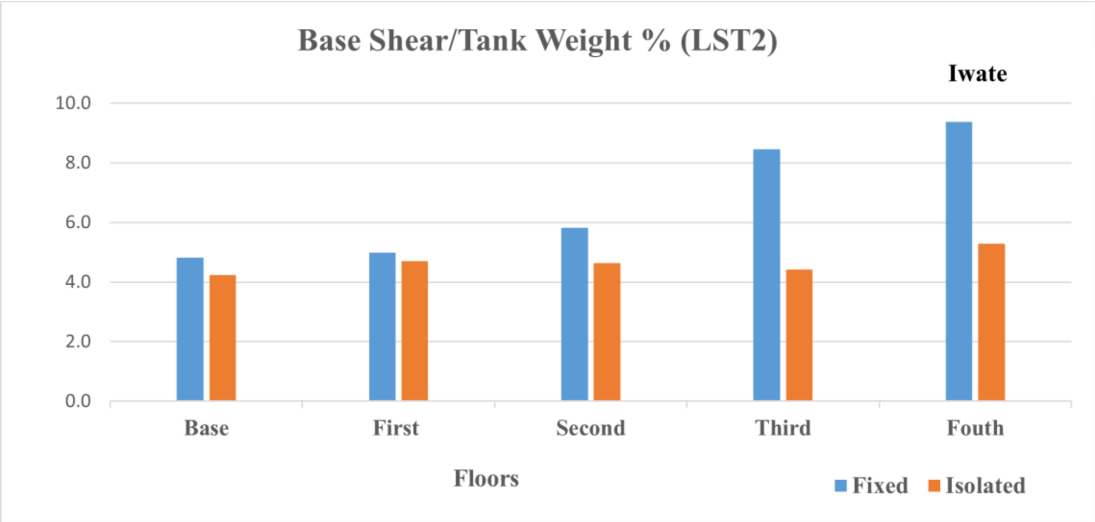

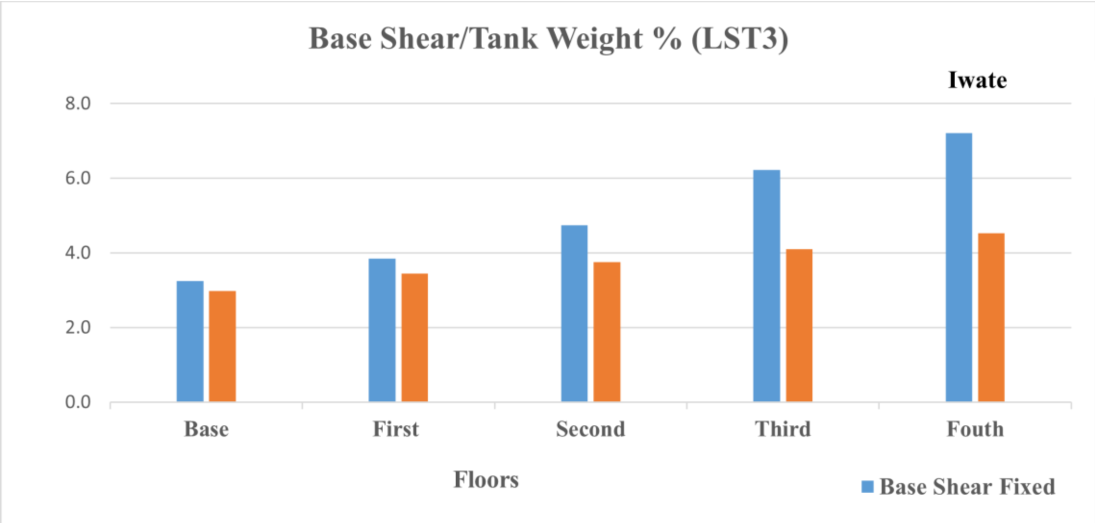

Figure 5.5: Base shear variation of three liquid storage tanks on fixed and isolated condition under Iwate

Figure 5.6: Base shear variation of three liquid storage tanks on fixed and isolated condition under Darfield

5.2 The Liquid Displacement Due to The Sloshing

Liquid displacement heights values were analyzed and presented in Figures 5.7 to 5.11. In general, all three liquid storage tanks were analyzed under six near-field seismic events in two cases (fixed and isolated) and showed the effectiveness of isolation in decreasing liquid displacement due to the sloshing in the majority of the case, but the base floor is not decreasing. In order to make a comparative evaluation, the displacement sloshing heights of the tanks, each figure presents when all the tanks are on same floor.

When the tanks are placed on the base floor, the liquid displacement heights due to the sloshing under six near-field seismic events for liquid storage tanks (LST1, LST2, and LST3) in two conditions (isolated and non-isolated) are compared and presented in the pictures in Figure 5.7. The first two liquid storage tanks (LST1 and LST2) are obtained close values while the LST3 is lower in all the events.

Considering to base floor (Figure 5.7), the liquid displacement heights in Imperial Valley-06, Coalinga-01, Kocaeli, Chi-Chi, Iwate, and Darfield due to LST1 increase, respectively, by 170%, 54%, 397%, 13%, 24% and 99% assuming isolation model; also, the liquid displacement heights in Imperial Valley-06, Coalinga-01, Kocaeli, Chi-Chi, Iwate and Darfield due to LST2 increase, respectively, by 171%, 47%, 386%, 11%, 23% and 96% assuming isolation model.

On the other hand, due to LST3, the liquid displacement heights in Imperial Valley-06, Coalinga-01, Kocaeli, Chi-Chi, Iwate, and Darfield due to LST2 increase, respectively, by 222%, 64%, 528%, 13%, 87% and 127% assuming isolation model.

The abovementioned result on the base floor indicates that base isolation increases the displacement liquid heights, considerably. But in general, according to the compared results between non-isolated and isolated tanks, the maximum displacements are significantly decreased due to base isolation in the majority of cases.

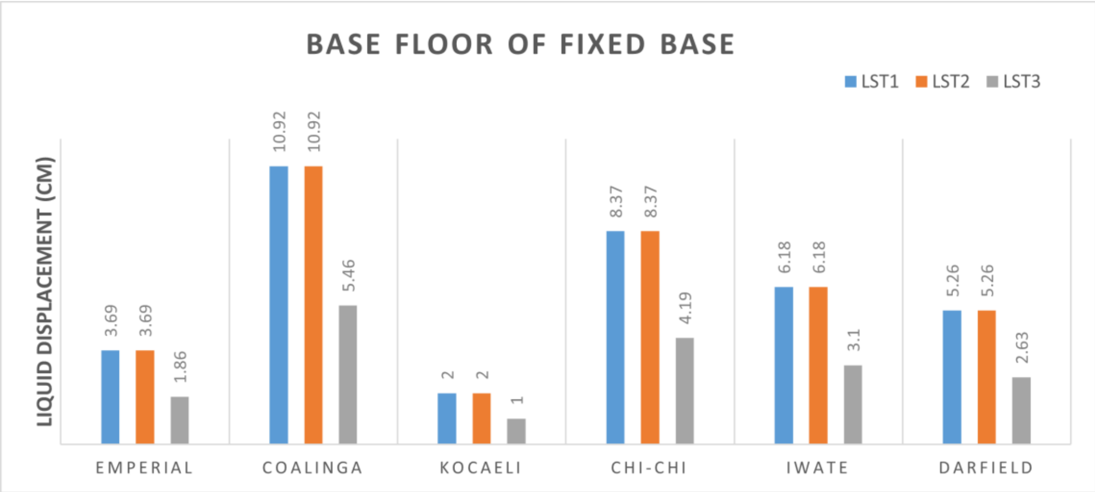

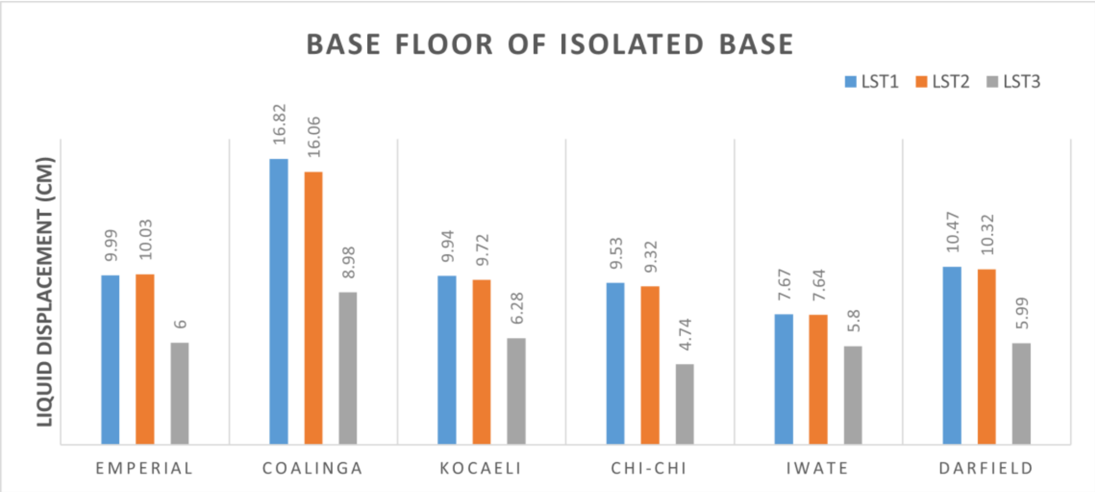

Figure 5.7: Base floor of liquid displacement of fixed and base isolation

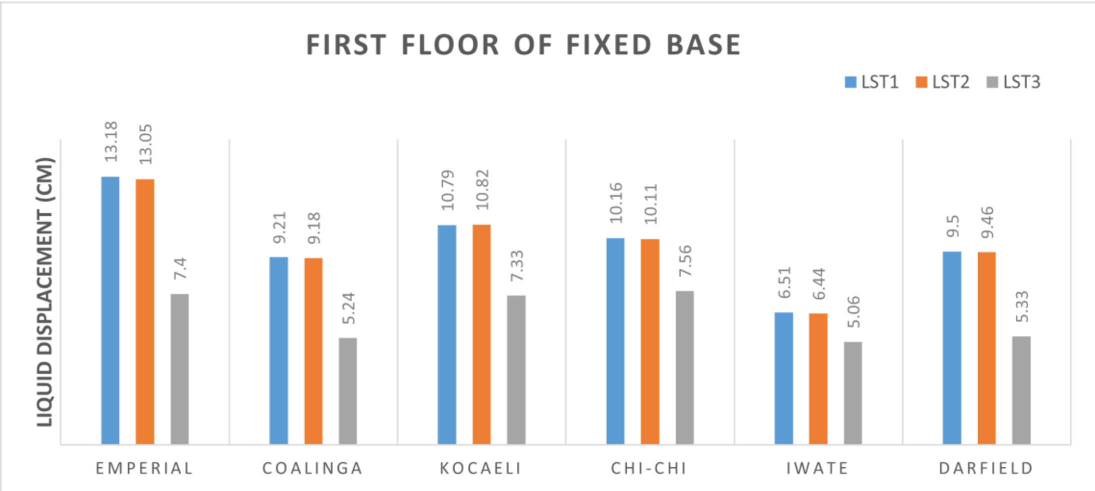

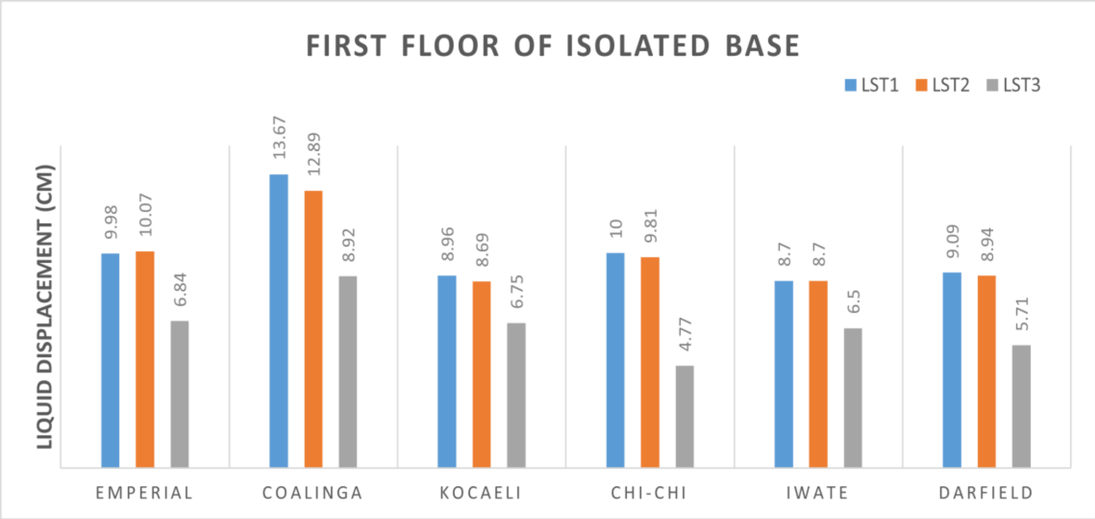

Figure 5.8: First floor of liquid displacement of fixed and base isolation

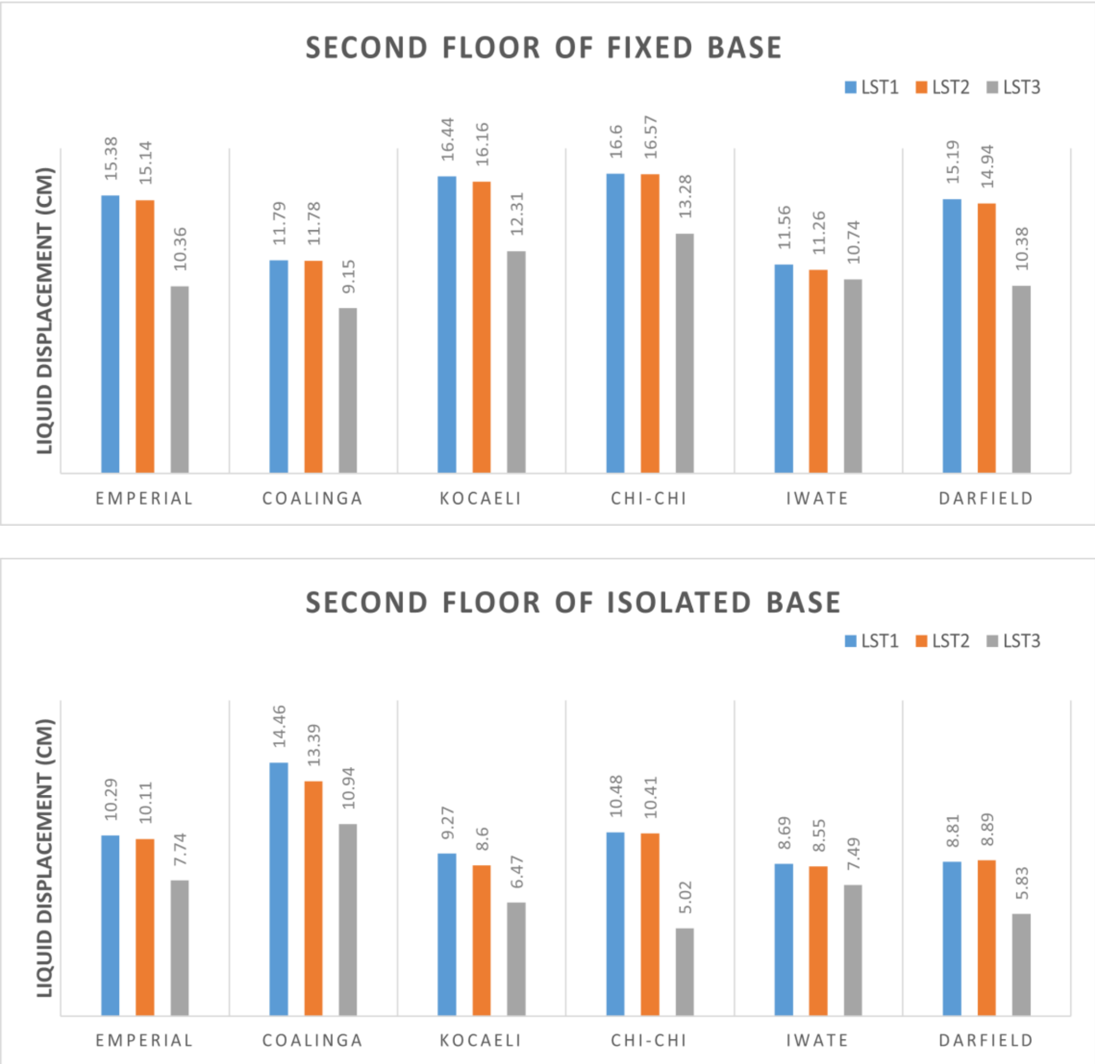

Figure 5.9: Second floor of liquid displacement of fixed and base isolation

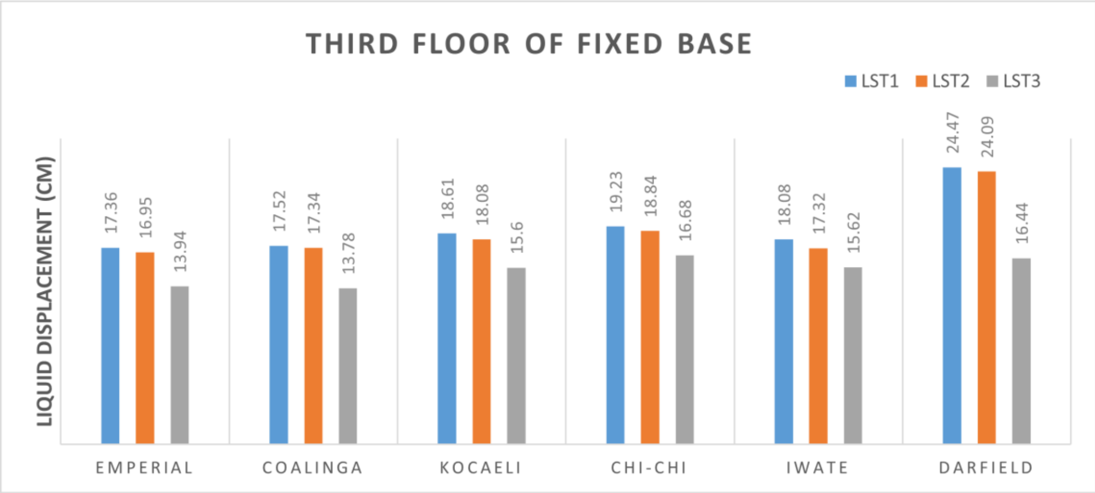

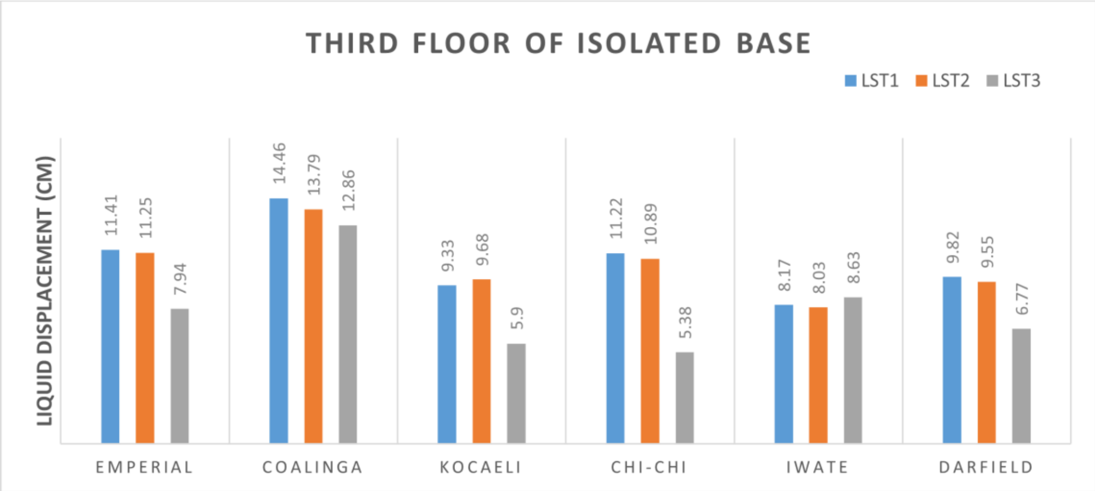

Figure 5.10: Third floor of liquid displacement of fixed and base isolation

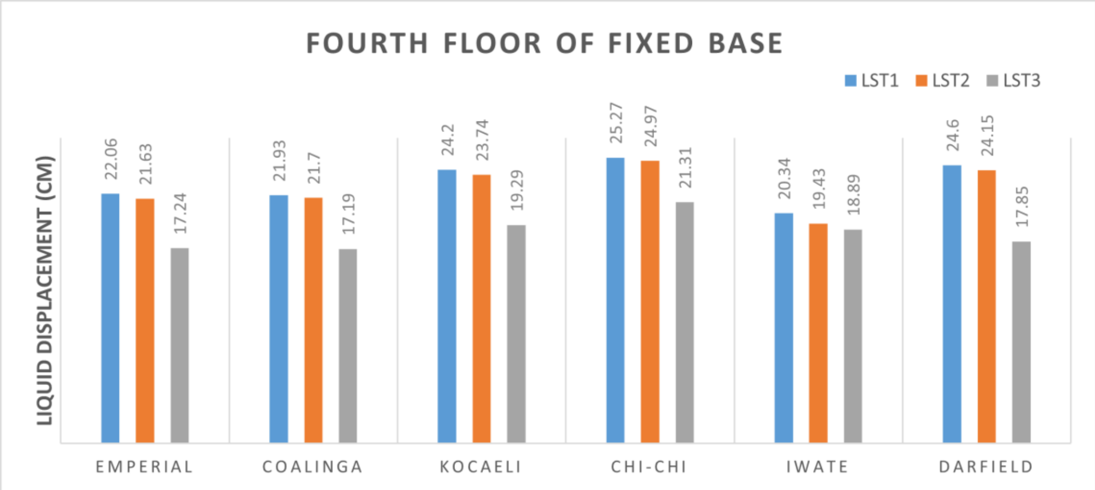

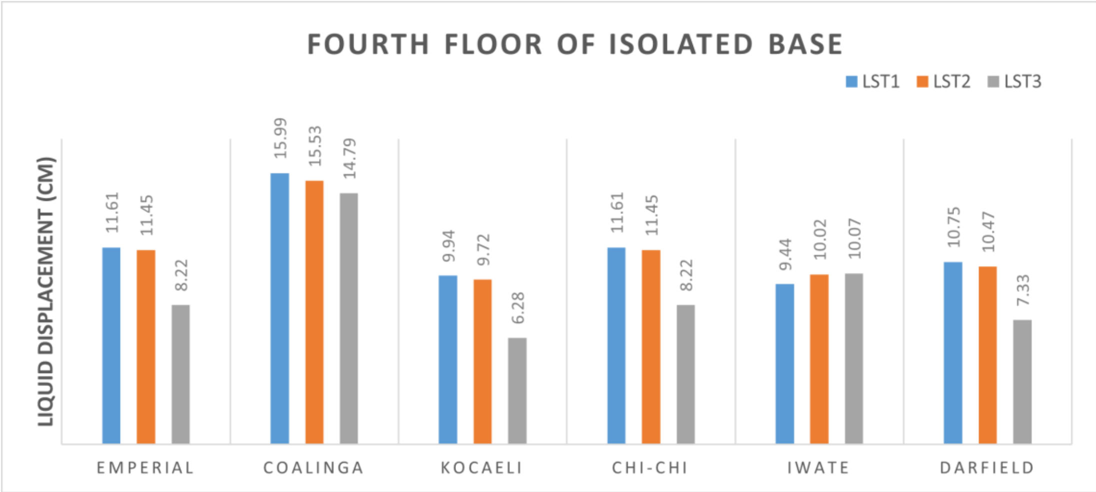

Figure 5.11: Fourth floor of liquid displacement of fixed and base isolation

5.3 Overturning Moment

The overturning moment values were analyzed and presented in Figures 5.12 to 5.16; all of those values are normalized by dividing the isolated values over its corresponding fixed base values. In general, all three liquid storage tanks were analyzed under six near-field seismic events in two cases (fixed and isolated) and showed the effectiveness of isolation in decreasing the overturning moments, but there are few findings at the base, first and second floor which are not decreasing. According the second and the first floor, under the Coalinga-01 excitation values is not decreasing in all the three storage tanks, but the base floor, due to the LST1, LST2 and LST3, the overturning moments in Imperial Valley, Kocaeli, and Darfield are not decreasing.

The findings of the overturning moments that are compared here appear in APPENDIX A.

Considering to top floor (the fourth floor), the overturning moment in Imperial Valley-06, Coalinga-01, Kocaeli, Chi-Chi, Iwate, and Darfield due to LST1 decrease, respectively, by 39%, 20%, 54%, 49%, 42% and 50% assuming isolation model; also, the overturning moments in Imperial Valley-06, Coalinga-01, Kocaeli, Chi-Chi, Iwate, and Darfield due to LST2 decrease, respectively, by 45%, 26%, 57%, 54%, 44% and 55% assuming isolation model. On the other hand, due to LST3, the overturning moments in Imperial Valley-06, Coalinga-01, Kocaeli, Chi-Chi, Iwate, and Darfield due to LST2 decrease, respectively, by 46%, 12%, 64%, 59%, 40% and 54% assuming isolation model.

Considering to the third floor, the overturning moment in Imperial Valley-06, Coalinga-01, Kocaeli, Chi-Chi, Iwate, and Darfield due to LST1 decrease, respectively, by 27%, 8%, 44%, 31%, 42% and 52% assuming isolation model; also, the overturning moments in Imperial Valley-06, Coalinga-01, Kocaeli, Chi-Chi, Iwate, and Darfield due to LST2 decrease, respectively, by 32%, 18%, 45%, 38%, 48% and 58% assuming isolation model. On the other hand, due to LST3, the overturning moments in Imperial Valley-06, Coalinga-01, Kocaeli, Chi-Chi, Iwate, and Darfield due to LST2 decrease, respectively, by 38%, 5%, 58%, 55%, 38% and 54% assuming isolation model.

Corresponding to the second floor, there will be an increase the overturning moment in Coalinga-01, in all the storage tanks, LST1, LST2, and LST3, respectively, by 13%, 12% and 14% assuming isolation model. But all the other excitations at this floor will be decreasing as follows: the Imperial Valley-06, Kocaeli, Chi-Chi, Iwate, and Darfield due to LST1 decrease, respectively, by 25%, 38%, 32%, 17%, and 35% assuming isolation model; also, the overturning moments in Imperial Valley-06, Kocaeli, Chi-Chi, Iwate, and Darfield due to LST2 decrease, respectively, by 31%, 45%, 33%, 21%, and 38% assuming isolation model. On the other hand, due to LST3, the overturning moments in Imperial Valley-06, Coalinga-01, Kocaeli, Chi-Chi, Iwate, and Darfield due to LST2 decrease, respectively, by 21%, 43%, 49%, 24% and 38% assuming isolation model.

According to the compared results between non-isolated and isolated tanks, the overturning moments are significantly decreased due to base isolation in the majority of cases. As the height of the tank elevation decreases, the percentage reduction also decreases, and the top floor has the maximum value on all of the tanks.

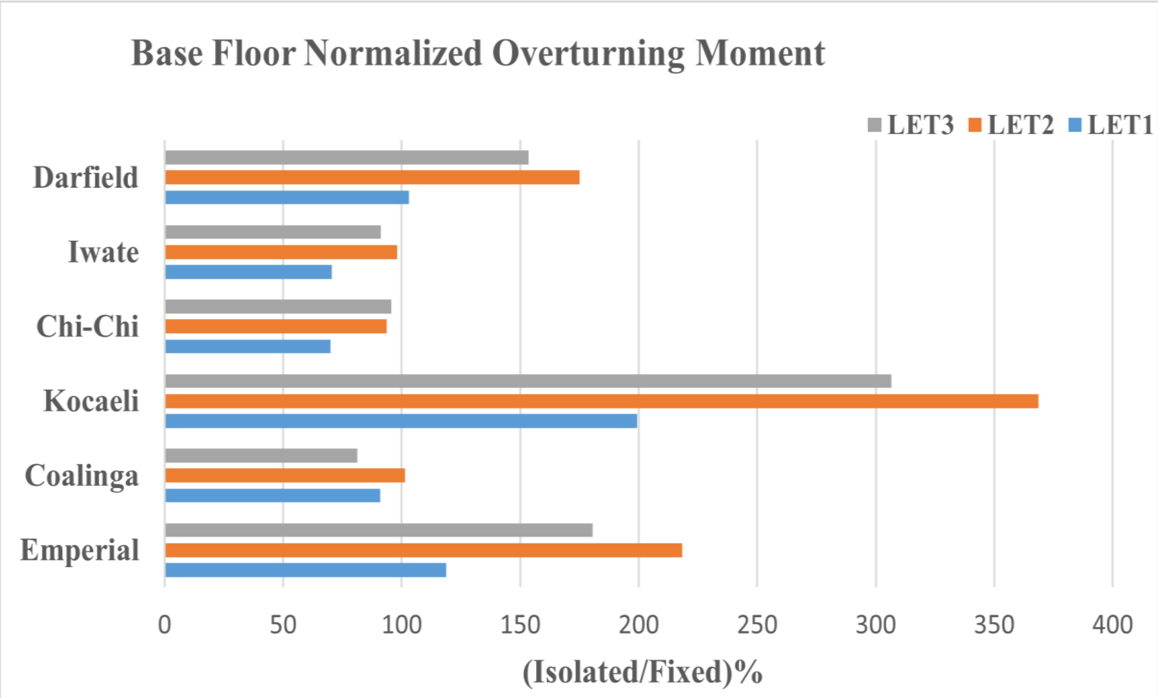

Figure 5.12: Base floor of overturning moment of fixed and base isolation

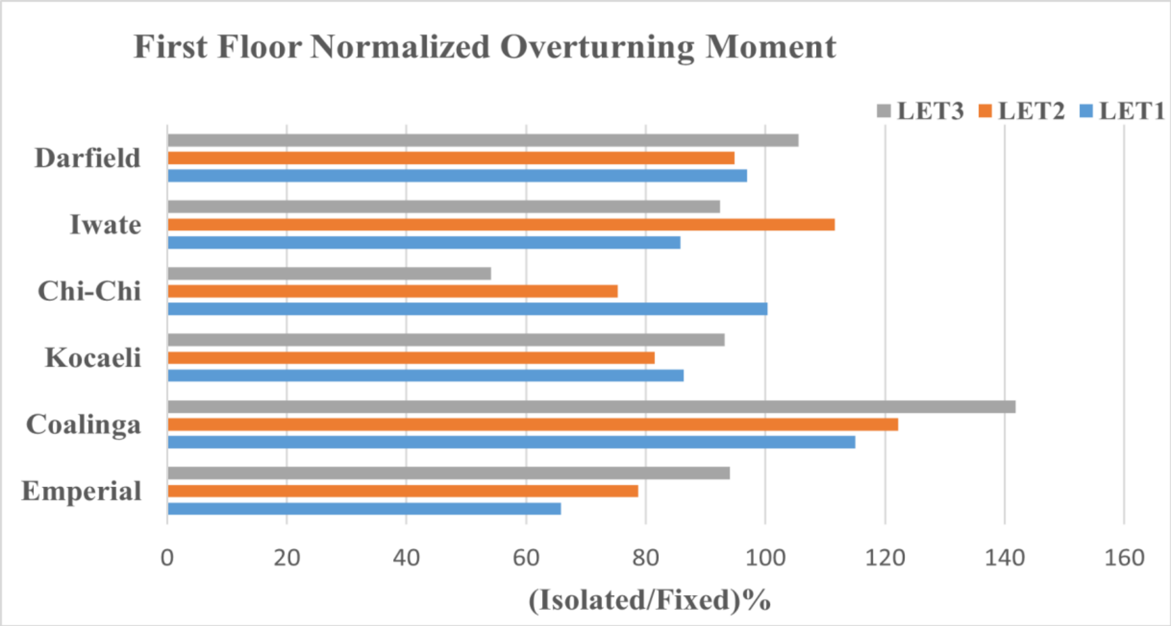

Figure 5.13: First floor of overturning moment of fixed and base isolation

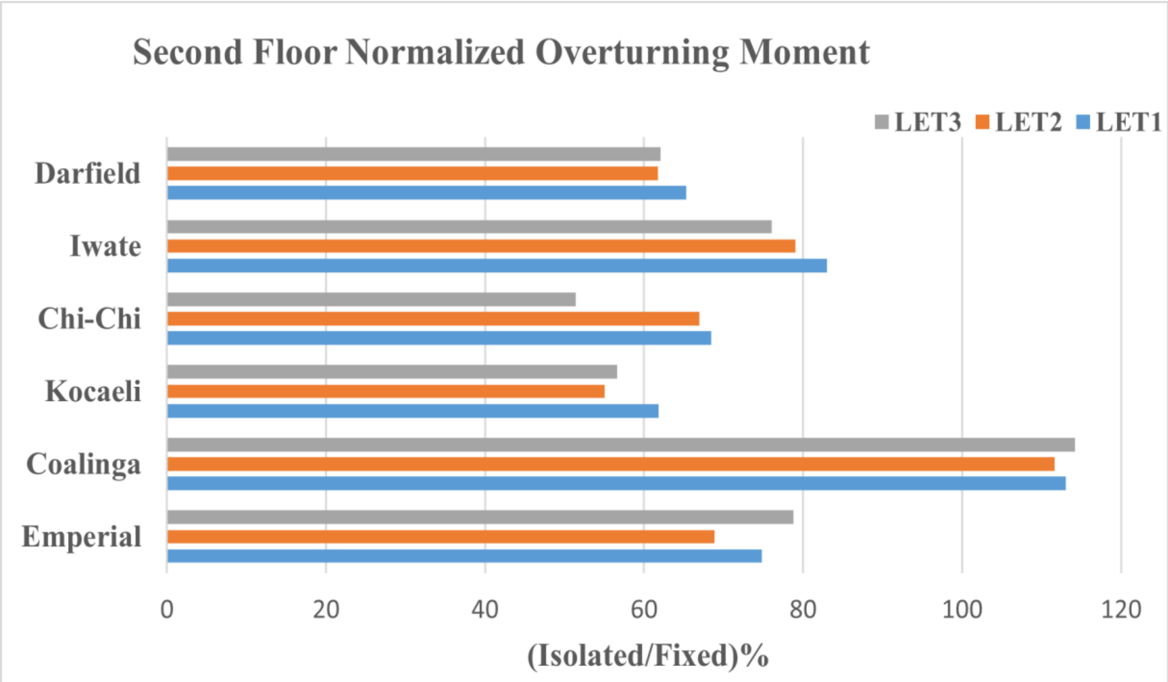

Figure 5.14: Second floor of overturning moment of fixed and base isolation

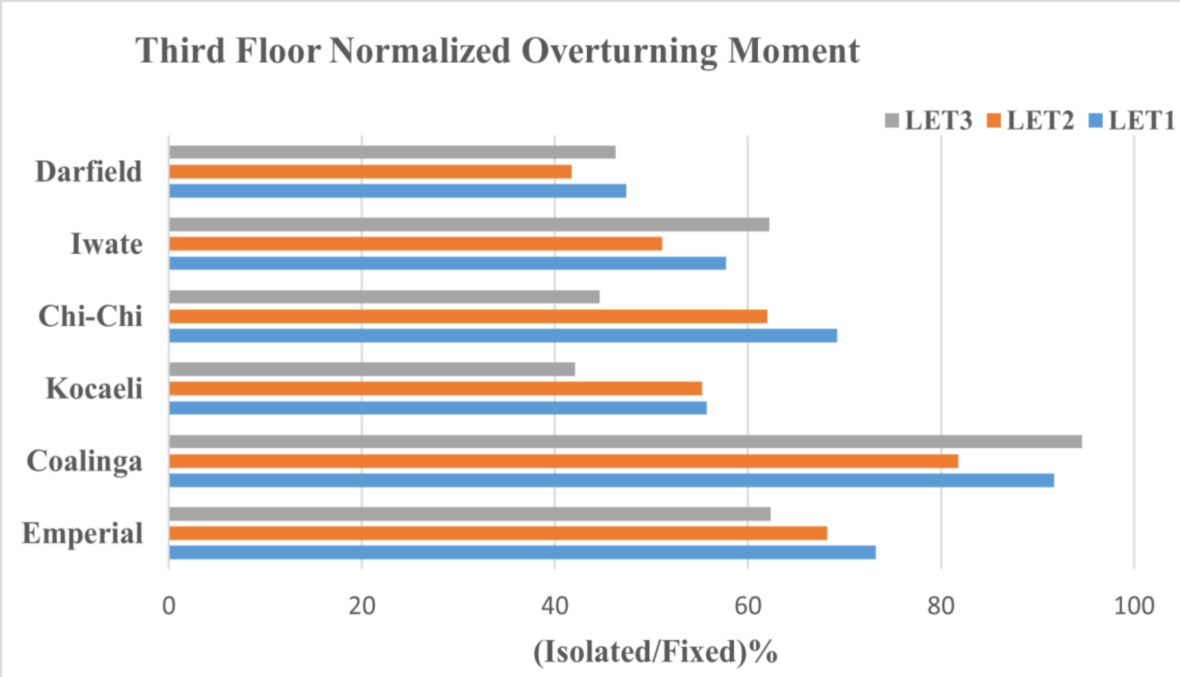

Figure 5.15: Third floor of overturning moment of fixed and base isolation

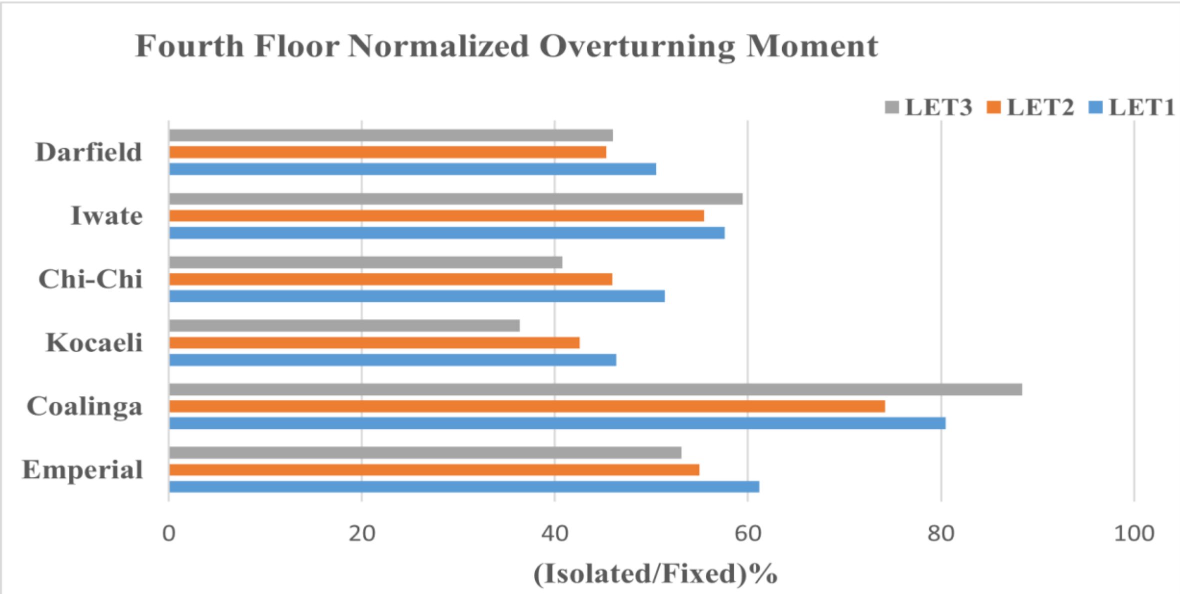

Figure 5.16: Fourth floor of overturning moment of fixed and base isolation

CHAPTER 6

CONCLUSION AND RECOMENDATION

6.1 Conclusion and Recommendation

The seismic response of liquid storage tanks supported by a base-isolated structure was analyzed using six near-field horizontal earthquake ground motions. Then, the seismic response of the isolated tanks was compared to the response of tanks on fixed base structure in order to determine the effectiveness of seismic isolation. The liquid storage tanks that were investigated in this thesis had three aspect ratios, namely LST1, LST2, and LST3. In this study, nonlinear time history analysis was used to determine the seismic demands of the liquid storage tanks. Afterwards, parametric analyses were carried out in order to determine the impacts of various essential structural parameters on seismic base shear forces, liquid displacement, and overturning moments of base isolated liquid storage tank structures. Overall, the use seismic isolation devices considerably decrease the amount of base shear, overturning moment, and liquid displacement. The following conclusions may be made from the results acquired from the evaluations of the six near-field selected earthquake records when the typical assumed parameters for the isolation system and the tank are taken into consideration:

1. For the practical range of tank aspect ratios, seismic isolation is efficient in decreasing overturning moments, base shear, and liquid displacement. The relative decreases are highest for smaller aspect ratio tanks as compared to the similar fixed-base design. In low-capacity tanks with a high aspect ratio, isolation showed the lowest improvements for the range of parameters evaluated.

2. During seismic excitations, liquid displacement, base shear, and overturning moments can be controlled more efficiently by isolated structures than fixed base structures. In general, the percentage reduction of the overturning moment and base shear increases on the tanks located on the upper floors of the isolated structure in comparison with the tanks on the fixed base structure. The maximum percentage reduction is found on the top floor. There is one exception among the floors: the base floor with the base-isolator, which was not decreased.

This study investigated the influence of seismic isolation on the base shear, overturning moment and liquid sloshing displacement for small scale tanks on structures. Due to limited size of the tanks considered in the study, the influence of the sloshing action on the overall response of the structure was neglected and this influence can be considered as a topic for further research.

REFERENCES

[1] J. J. Connor, "Introduction to Structural Motion Control." Massachusetts Institute of Technology.

[2] Skinner, R., and G. McVerry "Base Isolation for Increased Earthquake Resistance Buildings," *vol. 8, no. June 1975.*

[3] Vern, Sourabh, et al, "Evaluation of the seismic response of liquid storage tanks," *Earthquakes and Structures, vol. 21, no. 2, pp. 205–217, 2021.*

[4] H. W. Shenton and F. P. Hampton, "Seismic Response of Isolated Elevated Water Tanks," *J. Struct. Eng., vol. 125, no. 9, pp. 965–976, 1999.*

[5] M. K. Shrimali and R. S. Jangid, "The seismic response of elevated liquid storage tanks isolated by lead-rubber bearings*," Bull. New Zeal. Soc. Earthq. Eng., vol. 36, no. 3, pp. 141–164, 2003.*

[6] A. Tokhi and S. Arora, "Seismic Analysis and Comparison of Overhead INTZE Water Tank, Circular Water Tank and Rectangular Water Tank and Response Spectrum Analysis," *Int. J. Civ. Eng. Technol., vol. 10, no. 3, pp. 2519–2527, 2019.*

[7] C. Kircher, "Chapter 12: Seismically Isolated Structures," *Fema P-751, pp. 1–64, 2012.*

[8] M. D. Symans, "Seismic Protective Systems: Seismic Isolation," *Instr. Mater. Complement. FEMA 451, pp. 1–87, 2004.*

[9] C. L. Mullen, "An introduction to seismic isolation," *Soil Dyn. Earthq. Eng., vol. 12, no. 7, pp. 1–354, 1993.*

[10] E. Blandford et al., "Advanced seismic base isolaton methods for modular reactors," *no. November 2014, pp. 1–132, 2010.*

[11] F. Naeim, "Seismic design handbook," *p. 450, 1997.*

[12] T. A. Morgan and S. A. Mahin, "The Use of Base Isolation Systems to Achieve Complex Seismic Performance Objectives Tokyo Institute of Technology," *Pacific Earthq. Eng. Res. Cent., no. July, 2011.*

[13] J. M. K. and Farzad Naeim, “Design of Seismic Isolated Structures: From Theory to Practice,” *Earthq. Spectra, 2000*.

[14] http://www.kawakinct.co.jp/english/buildings/a_s01.html

[15] S. Standards, “Two Activities — Base Isolation for Earthquake Resistance Base on Background Base Isolation for Earthquake Resistance,” *City, pp. 1–9, 1906*.

[16] M. C. Constantinou, “Friction Pendulum Double Concave Bearing,” *pp. 1–48, 2004.*

[17] N. V. Nguyen, et al. “Performance of Single Friction Pendulum bearing for isolated buildings subjected to seismic actions in Vietnam,” *IOP Conf. Ser. Earth Environ. Sci., vol. 143, no. 1, pp. 1–12, 2018.*

[18] J. W. Baker, “Behaviour of the double concave Friction Pendulum bearing,” *Pacific Conf. Earthq. Eng., no. 056, pp. 1403–1424, 2007.*

[19] H. Moeindarbari and T. Taghikhany, “Seismic optimum design of triple friction pendulum bearing subjected to near-fault pulse-like ground motions,” *Struct. Multidiscip. Optim., vol. 50, no. 4, pp. 701–716, 2014.*

[20] T. Morgan and S. Mahin, “The optimization of multi-stage friction pendulum isolators for loss mitigation considering a range of seismic hazard,” *Proceedings of the 14th World Conference on Earthquake Engineering. Beijing, China.*

[21] Daniel M. Fenz and Michael C. Constantinou, “Spherical sliding isolation bearings with adaptive behavior: Experimental verification Daniel,” *Pacific Conf. Earthq. Eng., no. 056, pp. 185–205, 2007.*

[22] I. E. Kavvadias, et al, “Finite element modeling of single and multi-spherical friction pendulum bearings,” *Compdyn 2017 - Proc. 6th Int. Conf. Comput. Methods Struct. Dyn. Earthq. Eng., vol. 2, no. June, pp. 4408–4416, 2017.*

[23] S. Kitayama and M. C. Constantinou, “Evaluation of Triple Friction Pendulum Isolator Element in Program Sap2000,” *pp. 1–33, 2015.*

[24] N. D. Lagaros, et al, “Encyclopedia of Earthquake Engineering,” *Encycl. Earthq. Eng., no. June 2015, 2014.*

[25] Abrahamson, N. A. “Non-stationary spectral matching. Seismological research letters,” *Vol. 63, 1992. pp. 30.*

[26] P. K. Malhotra, et al. “Simple procedure for seismic analysis of liquid-storage tanks,” *Struct. Eng. Int. J. Int. Assoc. Bridg. Struct. Eng., vol. 10, no. 3, pp. 197–201, 2000.*

[27] Housner, G. W., and M. A. Haroun. "Dynamic analysis of liquid storage tanks I II.” *(1980).*

[28] Rostampour, M.A. (2022). Elastic Response Spectra, ElasticSpec.m (https://www.mathworks.com/matlabcentral/fileexchange/78029-elastic-response-spectra), MATLAB Central File Exchange. Retrieved February 10, 2022.

APPENDIX A

Results for different important parameters of the tank analysis of different geometric elevated tanks (LST1, LST2, and LST3) that are supported on a fixed and isolated base structure by the help of MATLAB coding are recorded in tabular form in Tables I and VI, which are composed of base shear, overturning moment, and displacement.

Table I: Base Shear, Overturning Moment and Sloshing Displacement of LST1 (Isolated)

Case	Elevation	Time History	Base Shear (kN)	Overturning Moment (kNm)	Sloshing Displacement (m)
Base Isolatted Model	Base Floor	Imperial Valley 06	2.5994	3.2590	0.0999
		Coalinga-01	4.3967	5.5061	0.1682
		Kocaeli, Turkey	2.0053	2.6987	0.0994
		Chi-Chi, Taiwan	2.9862	3.5833	0.0953
		Iwate, Japan	2.3748	2.8568	0.0767
		Darfield	2.3725	3.0864	0.1047
	First Floor	Imperial Valley 06	2.5974	3.2565	0.0998
		Coalinga-01	3.2851	4.4596	0.1367
		Kocaeli, Turkey	1.8605	2.4817	0.0896
		Chi-Chi, Taiwan	3.0496	3.6806	0.1000
		Iwate, Japan	2.5262	3.0839	0.0870
		Darfield	2.1148	2.7305	0.0909
	Second Floor	Imperial Valley 06	2.6426	3.3242	0.1029
		Coalinga-01	3.4964	5.0295	0.1446
		Kocaeli, Turkey	1.907	2.5513	0.0927
		Chi-Chi, Taiwan	3.1234	3.7901	0.1048
		Iwate, Japan	2.5272	3.0836	0.0869
		Darfield	2.0748	2.6703	0.0881
	Third Floor	Imperial Valley 06	2.8063	3.5701	0.1141
		Coalinga-01	4.0953	5.2284	0.1446
		Kocaeli, Turkey	1.9159	2.5644	0.0933
		Chi-Chi, Taiwan	3.2283	3.9490	0.1122
		Iwate, Japan	2.4508	2.9692	0.0817
		Darfield	2.2247	2.8942	0.0982
	Fourth Floor	Imperial Valley 06	2.8351	3.6133	0.1161
		Coalinga-01	4.3214	5.3667	0.1599
		Kocaeli, Turkey	2.0053	2.6988	0.0994
		Chi-Chi, Taiwan	2.8351	3.6133	0.1161
		Iwate, Japan	2.6352	3.2470	0.0944
		Darfield	2.3582	3.0961	0.1075

Table II: Base Shear, Overturning Moment and Sloshing Displacement of LST1 (Fixed)

Case	Elevation	Time History	Base Shear (kN)	Overturning Moment (kNm)	Displacement (m)
Fixed Base Model	Base Floor	Imperial 06	2.6060	2.7444	0.0369
		Coalinga-01	5.5042	6.0547	0.1092
		Kocaeli, Turkey	1.2698	1.3542	0.0200
		Chi-Chi, Taiwan	4.7315	5.1206	0.0837
		Iwate, Japan	3.7804	4.0496	0.0618
		Darfield	2.7383	2.9975	0.0526
	First Floor	Imperial Valley 06	3.0511	4.9449	0.1318
		Coalinga-01	3.3290	3.8775	0.0921
		Kocaeli, Turkey	2.1155	2.8723	0.1079
		Chi-Chi, Taiwan	3.0225	3.6685	0.1016
		Iwate, Japan	2.6976	3.5953	0.0651
		Darfield	2.1711	2.8173	0.0950
	Second Floor	Imperial Valley 06	3.3864	4.4412	0.1538
		Coalinga-01	3.7106	4.4476	0.1179
		Kocaeli, Turkey	2.9562	4.1258	0.1644
		Chi-Chi, Taiwan	4.2217	5.5370	0.1660
		Iwate, Japan	2.9473	3.7140	0.1156
		Darfield	3.0247	4.0869	0.1519
	Third Floor	Imperial Valley 06	3.6750	4.8743	0.1736
		Coalinga-01	4.5423	5.6999	0.1752
		Kocaeli, Turkey	3.2715	4.6005	0.1861
		Chi-Chi, Taiwan	4.3950	5.7033	0.1923
		Iwate, Japan	3.8980	5.1430	0.1808
		Darfield	4.3682	6.1114	0.2447
	Fourth Floor	Imperial Valley 06	4.3607	5.9051	0.2206
		Coalinga-01	5.1890	6.6701	0.2193
		Kocaeli, Turkey	4.0870	5.8258	0.2420
		Chi-Chi, Taiwan	5.2862	7.0367	0.2527
		Iwate, Japan	4.2271	5.6380	0.2034
		Darfield	4.3837	6.1362	0.2460

Table III: Base Shear, Overturning Moment and Sloshing Displacement of LST2 (Isolated)

Case	Elevation	Time History	Base Shear (kN)	Overturning Moment (kNm)	Displacement (m)
ISOLATED BASE	Base Floor	Imperial 06	1.5704	0.9456	0.1003
		Coalinga-01	1.6387	1.3750	0.1606
		Kocaeli, Turkey	1.4703	0.8911	0.0972
		Chi-Chi, Taiwan	1.6658	0.8801	0.0932
		Iwate, Japan	1.3579	0.7998	0.0764
		Darfield	1.5817	0.9563	0.1032
	First Floor	Imperial Valley 06	1.5755	0.9488	0.1007
		Coalinga-01	2.1795	1.1944	0.1289
		Kocaeli, Turkey	1.3274	0.8031	0.0869
		Chi-Chi, Taiwan	1.7333	1.0218	0.0981
		Iwate, Japan	1.5064	0.8911	0.0870
		Darfield	1.3958	0.8408	0.0894
	Second Floor	Imperial Valley 06	1.5820	0.9528	0.1011
		Coalinga-01	2.0502	1.3379	0.1339
		Kocaeli, Turkey	1.3137	0.7946	0.0860
		Chi-Chi, Taiwan	1.8166	1.0731	0.1041
		Iwate, Japan	1.4845	0.8776	0.0855
		Darfield	1.3888	0.8366	0.0889
	Third Floor	Imperial Valley 06	1.7399	1.0501	0.1125
		Coalinga-01	2.3056	1.3720	0.1379
		Kocaeli, Turkey	1.4654	0.8881	0.0968
		Chi-Chi, Taiwan	1.8832	1.1141	0.1089
		Iwate, Japan	1.4119	0.8329	0.0803
		Darfield	1.4808	0.8932	0.0955
	Fourth Floor	Imperial Valley 06	1.7682	1.0675	0.1145
		Coalinga-01	2.5482	1.5214	0.1553
		Kocaeli, Turkey	1.4703	0.8911	0.0972
		Chi-Chi, Taiwan	1.7682	1.0675	0.1145
		Iwate, Japan	1.6897	1.0040	0.1002
		Darfield	1.6088	0.9721	0.1047

Table IV: Base Shear, Overturning Moment and Sloshing Displacement of LST2 (Fixed)

Case	Elevation	Time History	Base Shear (kN)	Overturning Moment (kNm)	Displacement (m)
FIXED BASE	Base Floor	Imperial 06	0.7511	0.4330	0.0369
		Coalinga-01	1.9656	1.3552	0.1092
		Kocaeli, Turkey	0.4213	0.2417	0.0200
		Chi-Chi, Taiwan	1.8156	0.9389	0.0837
		Iwate, Japan	1.5395	0.8162	0.0618
		Darfield	0.9263	0.5463	0.0526
	First Floor	Imperial Valley 06	2.2913	1.2049	0.1305
		Coalinga-01	1.6653	0.9773	0.0918
		Kocaeli, Turkey	1.6232	0.9853	0.1082
		Chi-Chi, Taiwan	1.9737	1.3569	0.1011
		Iwate, Japan	1.5936	0.7982	0.0644
		Darfield	1.4695	0.8863	0.0946
	Second Floor	Imperial Valley 06	2.2813	1.3836	0.1514
		Coalinga-01	2.3243	1.1988	0.1178
		Kocaeli, Turkey	2.3675	1.4438	0.1616
		Chi-Chi, Taiwan	2.6752	1.6019	0.1657
		Iwate, Japan	1.8618	1.1101	0.1126
		Darfield	2.2310	1.3554	0.1494
	Third Floor	Imperial Valley 06	2.5335	1.5389	0.1695
		Coalinga-01	2.8004	1.6768	0.1734
		Kocaeli, Turkey	2.6348	1.6085	0.1808
		Chi-Chi, Taiwan	2.9913	1.7967	0.1884
		Iwate, Japan	2.7060	1.6301	0.1732
		Darfield	3.5057	2.1406	0.2409
	Fourth Floor	Imperial Valley 06	3.1861	1.9409	0.2163
		Coalinga-01	3.4077	2.0509	0.2170
		Kocaeli, Turkey	3.4232	2.0941	0.2374
		Chi-Chi, Taiwan	3.8551	2.3226	0.2497
		Iwate, Japan	3.0002	1.8113	0.1943
		Darfield	3.5145	2.1460	0.2415

Table V: Base Shear, Overturning Moment and Sloshing Displacement of LST3 (Isolated)

Case	Elevation	Time History	Base Shear (kN)	Overturning Moment (kNm)	Displacement (m)
ISOLATED BASE	Base Floor	Imperial 06	0.3582	0.3816	0.06
		Coalinga-01	0.5499	0.3687	0.0898
		Kocaeli, Turkey	0.2997	0.3355	0.0628
		Chi-Chi, Taiwan	0.4018	0.3820	0.0474
		Iwate, Japan	0.3577	0.3912	0.0580
		Darfield	0.3182	0.3437	0.0599
	First Floor	Imperial Valley 06	0.3722	0.3990	0.0684
		Coalinga-01	0.5406	0.5609	0.0892
		Kocaeli, Turkey	0.3166	0.3565	0.0675
		Chi-Chi, Taiwan	0.4030	0.3836	0.0477
		Iwate, Japan	0.4140	0.4235	0.0650
		Darfield	0.3092	0.3319	0.0571
	Second Floor	Imperial Valley 06	0.4052	0.4398	0.0774
		Coalinga-01	0.6455	0.6521	0.1094
		Kocaeli, Turkey	0.3066	0.3440	0.0647
		Chi-Chi, Taiwan	0.4122	0.3949	0.0502
		Iwate, Japan	0.4500	0.4679	0.0749
		Darfield	0.3135	0.3373	0.0583
	Third Floor	Imperial Valley 06	0.4123	0.4487	0.0794
		Coalinga-01	0.6844	0.7386	0.1286
		Kocaeli, Turkey	0.2857	0.3182	0.0590
		Chi-Chi, Taiwan	0.4253	0.4112	0.0538
		Iwate, Japan	0.4915	0.5193	0.0863
		Darfield	0.3480	0.3780	0.0677
	Fourth Floor	Imperial Valley 06	0.4225	0.4612	0.0822
		Coalinga-01	0.7552	0.8263	0.1479
		Kocaeli, Turkey	0.2997	0.3355	0.0628
		Chi-Chi, Taiwan	0.4225	0.4612	0.0822
		Iwate, Japan	0.5442	0.5845	0.1007
		Darfield	0.3680	0.4049	0.0733

Table VI: Base Shear, Overturning Moment and Sloshing Displacement of LST3 (Fixed)

Case	Elevation	Time History	Base Shear (kN)	Overturning Moment (kNm)	Displacement (m)
FIXED BASE	Base Floor	Imperial 06	0.2415	0.2114	0.0186
		Coalinga-01	0.5802	0.4529	0.0546
		Kocaeli, Turkey	0.1239	0.1094	0.0100
		Chi-Chi, Taiwan	0.4400	0.4000	0.0419
		Iwate, Japan	0.3901	0.4287	0.0310
		Darfield	0.2394	0.2240	0.0263
	First Floor	Imperial Valley 06	0.3927	0.4242	0.0740
		Coalinga-01	0.5076	0.3955	0.0524
		Kocaeli, Turkey	0.3375	0.3825	0.0733
		Chi-Chi, Taiwan	0.5028	0.7080	0.0756
		Iwate, Japan	0.4612	0.4581	0.0506
		Darfield	0.2947	0.3143	0.0533
	Second Floor	Imperial Valley 06	0.5009	0.5581	0.1036
		Coalinga-01	0.5486	0.5709	0.0915
		Kocaeli, Turkey	0.5197	0.6078	0.1231
		Chi-Chi, Taiwan	0.7036	0.7680	0.1328
		Iwate, Japan	0.5691	0.6152	0.1074
		Darfield	0.4800	0.5431	0.1038
	Third Floor	Imperial Valley 06	0.6312	0.7196	0.1394
		Coalinga-01	0.7181	0.7804	0.1378
		Kocaeli, Turkey	0.6400	0.7564	0.1560
		Chi-Chi, Taiwan	0.8376	0.9213	0.1668
		Iwate, Japan	0.7463	0.8349	0.1562
		Darfield	0.7007	0.8166	0.1644
	Fourth Floor	Imperial Valley 06	0.7519	0.8688	0.1724
		Coalinga-01	0.8426	0.9344	0.1719
		Kocaeli, Turkey	0.7744	0.9230	0.1929
		Chi-Chi, Taiwan	1.007	1.131	0.2131
		Iwate, Japan	0.8661	0.9830	0.1889
		Darfield	0.7522	0.8801	0.1785

APPENDIX B

MATLAB code used for the tank analysis.

```
% Simple Procedure for Seismic Analysis of Liquid-Storage Tanks Script

clear

close

% Tank Parameters

htank= 2.5; %Height of the tank (m)

H=2; % Height of the liquid (m)

r=1; % Radius of the tank (m)

rho=1000; % Rho Liquid (kg/m3)

rhosteel= 7800; %(kg/m^3)

Esteel= 2*10^11; % Modulus of elasticity (N/m^2)

h=0.005; %tank wall thickness (m)

ml=pi*r^2*H*rho; %mass of the liquid (kg)

mroof=pi*r^2*h*rhosteel; %mass of the roof (kg)

mwall=2*pi*r*htank*h; %mass of the wall (kg)

% Earthquake Input

acc=load('eqa.txt'); %Read Story Acceleration from the file eqa.txt

dt=0.01; %Time interval

[Spai,Spvi,Sai,Svi,Sdi,T]=ElasticSpec(acc,dt,20,9.807,0.02,2); %Response Spectra
for impulsive component [28]

[Spac,Spvc,Sac,Svc,Sdc,T]=ElasticSpec(acc,dt,20,9.807,0.005,2); %Response
Spectra for convective component [28]
```

```
% Calculation of the mechanical analogue system parameters

HrTable=[0.30 9.28 2.09 0.176 0.824 0.400 0.521 2.640 3.414; 0.500 7.74 1.74 0.3 0.7 0.4 0.543 1.460 1.517; 0.7 6.97 1.60 0.414 0.586 0.401 0.571 1.009 1.011; 1.0 6.36 1.52 0.548 0.452 0.419 0.616 0.721 0.785;1.5 6.06 1.48 0.686 0.314 0.439 0.690 0.555 0.734; 2.0 6.21 1.48 0.763 0.237 0.448 0.751 0.500 0.764; 2.5 6.56 1.48 0.810 0.190 0.452 0.794 0.480 0.796; 3.0 7.03 1.48 0.842 0.158 0.453 0.825 0.472 0.825];

HrRat= H/r; %H/r Ratio

miml=interp1(HrTable(:,1),HrTable(:,4),HrRat,"linear");

mcml=interp1(HrTable(:,1),HrTable(:,5),HrRat,"linear");

mi=miml*ml; %impulsive mass (kg)

mc=mcml*ml; %convective mass (kg)

hiH=interp1(HrTable(:,1),HrTable(:,6),HrRat,"linear");

hcH=interp1(HrTable(:,1),HrTable(:,7),HrRat,"linear");

hi=hiH*H; %Height of the impulsive mass (m)

hc=hcH*H; %Height of the convective mass (m)

Ci=interp1(HrTable(:,1),HrTable(:,2),HrRat,"linear");

Cc=interp1(HrTable(:,1),HrTable(:,3),HrRat,"linear");

Timp=Ci*(H*rho^0.5)/((h/r)^0.5*Esteel^0.5); % Period of the impulsive component (s)

Tcon=Cc*r^0.5; % Period of the convective component (s)

%Seismic Response

STimp=interp1(T,Sai,Timp); %Spectral Accelation for the impulsive component

STcon=interp1(T,Sac,Tcon); %Spectral Accelation for the impulsive component

Q=(mi+mwall+mroof)*STimp+mc*STcon; %Total Base Shear

M=(mi*hi+mwall*htank/2+mroof*htank)*STimp+mc*hc*STcon; %%Total Overturning Moment

d=r*STcon/9.807; %Sloshing Displacement
```